Emerging Trends of Physical Sciences Education & Research

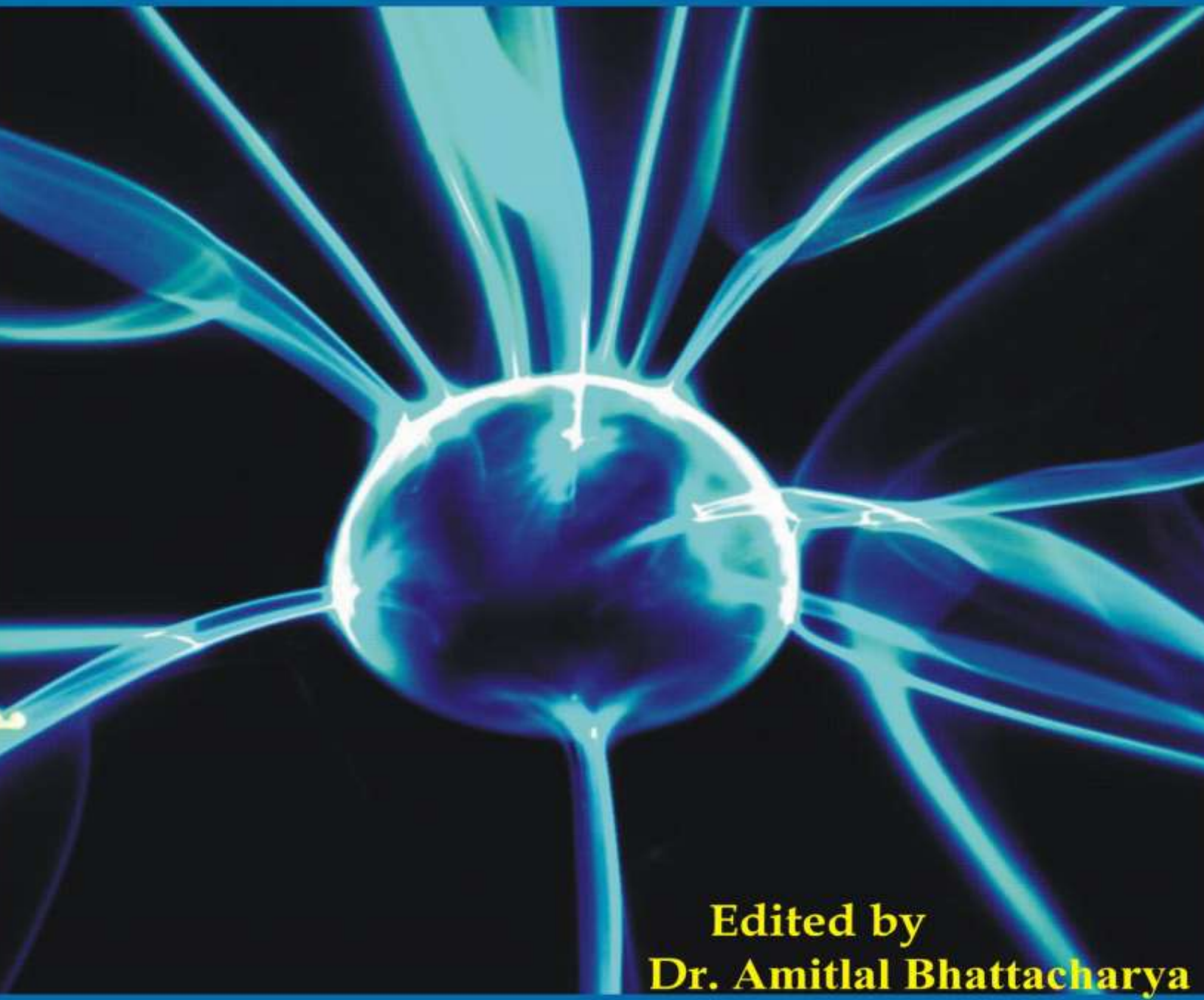

Edited by
Dr. Amitlal Bhattacharya

Ideal International E-Publication Pvt. Ltd.

Emerging Trends of Physical Sciences – Education & Research

Edited by

Dr. Amitlal Bhattacharya

2018

Ideal International E – Publication Pvt. Ltd.

www.isca.co.in

Ideal International E-Publication Pvt. Ltd.

427, Palhar Nagar, RAPTC, VIP-Road, Indore-452005 (MP) INDIA
Phone: +91-731-2616100, Mobile: +91-80570-83382
E-mail: **contact@isca.co.in** , Website: **www.isca.co.in**

Title:	**Emerging Trends of Physical Sciences – Education & Research**
Editor:	**Dr. Amitlal Bhattacharya**
Edition:	First
Volume:	I

DISCLAIMER

The authors are solely responsible for the contents of the papers compiled in this volume. The publisher and editor do not take any responsibility for the same in any manner.

ISBN:978-93-86675-56-9

Dukhulal Nibaran Chandra College
(NAAC ACCREDITED)
Aurangabad, Murshidabad (W.B.)
Pin- 742201 [Nimtita (E. Rly)]
Phone : (03485) 262477
ESTD-1967
Website : www.dnccollege.com
E-mail ID : dnccollege@gmail.com
Telefax - (03485) 262477

From Principal's Desk

I have the pleasure to know that the Department of Physics, Dukhulal Nibaran Chandra College took the responsibility to publish the papers in an edited volume, presented by the learned participants at the International seminar organized on the topic "Emerging Trends of Physical Sciences- Education & Research" and held on 15th March, 2018 jointly with Nathulal Das B.Ed. College, Aurangabad.

Hope, the contents of the publication will definitely act as reference and inspiration to the scholar of the subject at large and the generous labour put by Dr. Amitlal Bhattacharya, Assistant Professor of Physics be accredited by the scholar.

Thanking all the fraternity.

CA Nikhilendu Bikash Das

Preface

This edited volume is the product of International Seminar on "Emerging Trends of Physical Sciences- Education & Research" organized by Department of Physics, Dukhulal Nibaran chandra College in collaboration with Nathulal Das B.Ed. College.

Now-a–days physical science education and research is the backbone of our universal development. So, good academic research and proper education in this field is highly needed. In this context we have tried to make a small step forward by arranging such a conference in our college which is located in a remote part of our country. This will not only be beneficial to the research and academic community but also be very encourageous to the meritorious students of this locality.

All the papers, we received in the seminar, were of excellent quality to be selected for publication in this book, but some of them have been placed in this modest volume. We sincerely apologize to all the scholars whose articles have not been accommodated here.

Now, I want to express my deepest gratitude to the Principal of my college CA Nikhilendu Bikash Das, for his indispensable guidance and encouragement throughout the process of this publication.

I am grateful to all my colleagues for extending their helping hands as and when required.

I would like to place my sincere appreciation to all the delegates and resource persons present in the seminar for their crucial contribution.

I am also grateful to all my family members for giving me inspiration during this work.

Overall, this volume is an attempt to contribute in the field of research and education in Physical Sciences. I hope that this edited book will be very useful to the academicians, researchers and students in this field.

Amitlal Bhattacharya

Table of Contents

Study of composite materials as supercapacitor electrode

Buddhodev Chowdhury and Sudipta Pal*
Department of Physics, University of Kalyani, Kalyani-741235, Nadia
sudipta.pal@rediffmail.com

Abstract

Supercapacitor is an energy storage device. It can store huge amount of energy. They have many properties such as large energy density, high power density, quick charging/discharging, long cycle life and also low maintenance cost. There are three types of supercapacitor based on energy storage mechanism such as electric double layer capacitor (EDLC), pseudocapacitor and hybrid capacitor. Electric double layer capacitor stores energy electrostatically. Carbon materials like activated carbon, graphene etc. are used in EDLC electrodefor their large surface area, good electrical conductivity, low cost, availability and environment friendly. Pseudocapacitor stores energy electrochemically. Metal oxides like Manganese dioxide (MnO_2), Ruthenium dioxide (RuO_2) etc.or conducting polymers like polyaniline are used in pseudocapacitor electrode for its good faradaic redox properties. Hybrid capacitor is built by the combination of both EDLC and pseudocapacitor. It can store energy in both electrostatically and electrochemically. There are three types of hybrid capacitor for their electrode variety such as composite, asymmetric and battery-type. Today composite materials are used in hybrid capacitor electrode because composite electrodes are more effective than pure carbon electrode and pure metal oxide or conducting polymer electrode. Different types of composite are producedsuch as carbon-carbon, carbon-metal oxide and carbon-conducting polymer composite, all are used in a supercapacitor.

Keywords: Energy storage, Supercapacitors, EDLC, Pseudocapacitor, Hybrid Capacitor, AC,Graphene, CNT's, Metal Oxides, Conducting Polymer, Composite materials.

Introduction

The energy demand is increasing with the increasing of population. Also fossil fuels are decreasing day by day[1-4]. Further the environmental pollution is the biggest issue coming from the use of those energy resources[5-7]. So we need clean and green energy sources to solve this problem. Renewable energy sources like solar energy, wind energy are the better options. However in the absence of these sources (i.e. at night or without wind flow) we can't use it. So we need energy storage device that can store huge amount of energy and can be used when needed[8-10]. Electrolytic capacitor and electrochemical battery is used as energy storage but they have many problems. An electrolytic capacitor can store electrostatic energy but its capacity is very poor. A conventional battery store large amount of energy but the power density is lower(< 1kW/kg)[11-13],whereas new technologies require high power density source or storage. Now a day's most of the researchers are trying to invent a large energy storage device. Supercapacitor is one of them. It is an energy storage device with very large capacity and a low internal resistance. So it is capable to store and distribute energy at comparatively high rate compared to electrochemical batteries[14].The energy density of supercapacitor is lying between conventional capacitors and batteries, larger than of conventional capacitors and lower than batteries[14,15]. The energy density of a conventional battery is achieved up to 150 Wh/kg which is almost 10 times with an electrochemical capacitor whereas the power density of a battery is achieved up to 200 W/kg which is almost 20 times less than with an electrochemical capacitor[14,16]. It fills the gap between the electrochemical batteries and electrostatic capacitors[17-20]. Supercapacitors show high specific capacitance than electrostatic capacitors and high power than conventional batteries[21]. They have many conveniences such as long cycle life (>100,000 cycles), quick charging/discharging wide range of working temperature (-40^{0}C to 70^{0}C) and low maintenance cost[14,20,22-30]. Supercapacitor is favorable to use where the power bursts are needed but high energy storage capacity is not necessary[8].

The comparison among the electrolytic capacitors, electrochemical capacitors, batteries and fuel cells according their specific energy versus specific power has shown in Figure-1.

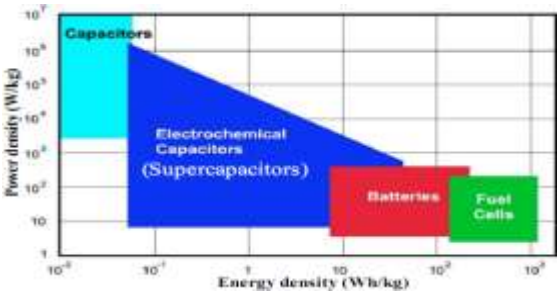

Figure-1: Specific Energy Vs Specific Power plot for various energy storage devices.

Table-1 shows the comparison among the electrolytic capacitor, electrochemical capacitor and battery. In this table we see the supercapacitor is lying between an electrolytic capacitor and a conventional battery in every aspect. So the supercapacitor fills the gap between an electrolytic capacitor and a conventional battery.Table-2 shows the comparison between a conventional and a supercapacitor for their storage mechanism. In this table we see that they are different from each other by the charge storage mechanism.

Table-1: Comparison among the electrolytic capacitor, conventional battery and supercapacitor[8].

Characteristics	Capacitor	Supercapacitor	Battery
Specific energy(W h kg $^{-}$1)	‹ 0.1	1–10	10–100
Specific power(W kg $^{-}$1)	⩾10, 000	500–10,000	‹1000
Discharge time	10^{-6} to 10^{-3}	s to min	0.3–3 h
Charge time	10 $^{-6}$ to 10^{-3}	s to min	1-5 h
Coulombic efficiency (%)	About 100	85–98	70–85
Cycle-life	Almost infinite	› 500, 000	about 1000

Table-2: Comparison between battery and supercapacitor[8].

Comparison parameter	Battery	Supercapacitor
Storage mechanism	Storage mechanism	Physical
Power	Power	Electrolyte conductivity
Energy storage	Energy storage	Limited (surface area)
Charge rate	Charge rate	High, same as discharge
Cycle life limitations	Cycle life limitations	Side reactions

Supercapacitor versus Lithium Ion Battery

There are lots of benefits of the li-ion battery. The energy density of a li-ion battery is very high from any ordinary battery as well as supercapacitor, self-discharging rate is comparatively lower from other rechargeable battery, its maintenance cost is lower etc.[4,31-33]. Though a lots of benefits of li-ion battery, it has many disadvantages such as it require protection from over charge discharge, li-ion battery is suffer from ageing that is one of the major problem, it is costly product from ordinary battery, it has transportation problem (mainly in air) due to its larger size and weight, it is now a developing area[34].New technology require high power storage device, so li-ion battery is a poor solution[4,35,36].

On the other hand Supercapacitor is a unique combination of high power as well as high energy storage device. Supercapacitor has more advantages such as quick charging/discharging, broad range of operating temperature, (-40^{0}C to +70^{0}C), long operating life, less weight and low cost. Only leakage is a main disadvantage of supercapacitor[22,37].

Characteristics of a supercapacitor

- High power density
- High energy density
- High capacitance
- Longer life

Figure-2(a):A typical supercapacitor and its characteristics.

Characteristics of li-ion battery

- High energy density
- Self-discharge much lower
- Low maintenance
- Almost longer life

Figure-2(b): A typical li-ion battery and its characteristics.

Working Principle of a Supercapacitor

A supercapacitorhas two electrodes these are separated by an ion permeable membrane. Both the electrodes are connected by the electrolyte.Carbon like materials is used in the electrode so that surface area of the electrode becomes large. Such type of material is used in an electrolyte that can produce large amount of ions. When external voltage is applied, the charges are accumulates on the outer surface in both electrodes. At the same time opposite ions in the electrolyte are gathered to the interfaceof the electrodes. In this process the electric double layer capacitors (EDLC) are generated in both the electrode- electrolyte interface[38].

The stored electrostatic energy of a supercapacitor is calculated by the equation shows below

$$E = \frac{1}{2} CV^2 \qquad (1)$$

where C and V are the Capacitance and voltage of the supercapacitor respectively. Equation (1) represents the energy density is proportional to capacitance of the supercapacitor. That means if we can increase the capacitance of the capacitor then energy density of the capacitor will be increased[38-41].

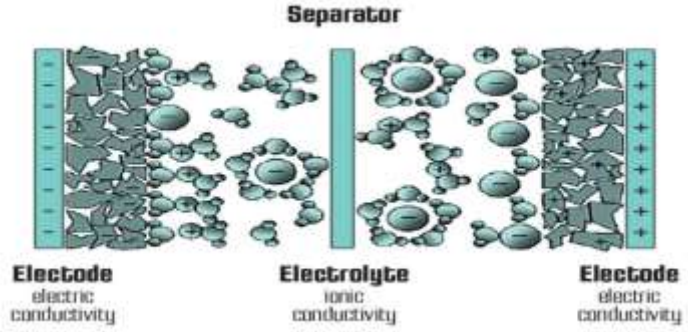

Figure-3: Internal structure of a supercapacitor.

Power density is another important parameter of a supercapacitor. It means how fast store and deliver energy. The maximum power density of a supercapacitor is measured by the equation.

$$P_{max} = \frac{V^2}{4R} \qquad (2)$$

where R is the equivalent series resistance (ESR) in ohms[42]. Equation-2 represent the maximum power is inversely proportional to internal resistance of the supercapacitor. Therefore for high power density of a supercapacitor internal resistance will be lower[38,39,41].

The capacitance of the supercapacitor is represented by the equation

$$C = \frac{\epsilon_0 \epsilon_r A}{d} \qquad (3)$$

Where $\epsilon_0$and ϵ_r are the dielectric constants of the free space and the dielectric material respectively, A is the surface area of the electrode and d is the distance between two electrodes. Equation-3shows that for large capacitance of a supercapacitor the surface area will be large and distance between two electrodes will be lower. So the materials use in electrode whose surface area is large[38,39,41].

Distribution of Capacitance of a Supercapacitor

When external voltage is applied on a supercapacitor, the charges are accumulated onboth the electrodes. At the same time opposite charges are generated near the both electrodes and they are separated by electrolyte molecules. So there are two capacitors are generated in both the electrodes and they are connected by series combination[43]. Therefore the total capacitance of the system (C_{total}) is calculated by given the formula:

$$C_{total} = \frac{C_1 \cdot C_2}{C_1 + C_2} \qquad (4)$$

where C_1 and C_2 are the individual capacitance of the electrodes. C_{total} is the total capacitance of the system. If the supercapacitors electrode is symmetric then $C_1 = C_2$ and equivalent capacitance $C = 0.5 \cdot C_1$ i.e. half of the individual capacitance of the electrodes[43].

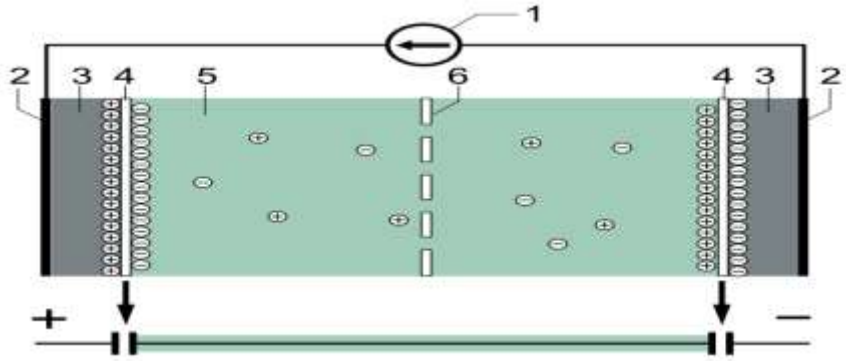

Figure-4: Typical construction of a supercapacitor: 1) power source, 2) collector, 3) polarized electrode, 4) Helmholtz double layer, 5) electrolyte having positive and negative ions, 6) separator.

Energy Storage Mechanism of Supercapacitor

There are three types of supercapacitors based on energy storage mechanism such as electric double layer capacitor, pseudocapacitor and hybrid capacitor[8,14].

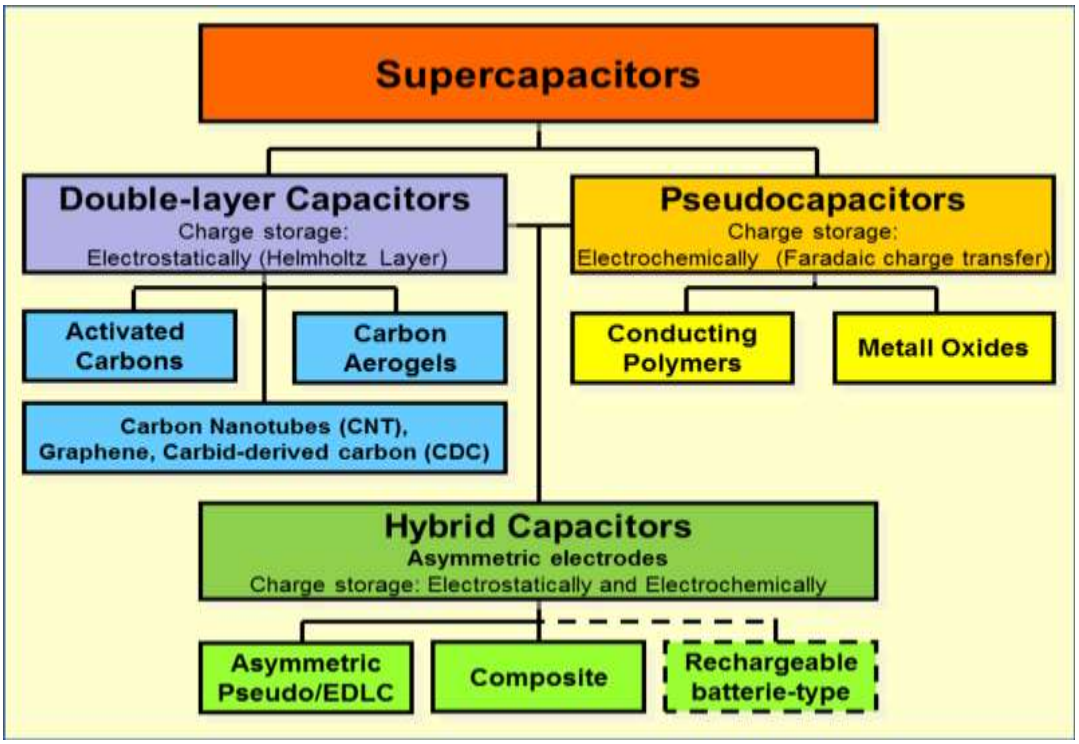

Electric double layer capacitor (EDLC): There are two layers generate on electrode- electrolyte interface i.e. One layer is the surface of the electrode and another opposite layer generates in the electrolyte. These two layers are separated by the solvent molecules which has dielectric properties. So in this region behaves like a capacitor. EDLC stores energy electrostatically. Activated charcoal or graphene are used in this type of electrode for their large surface area[44-51].

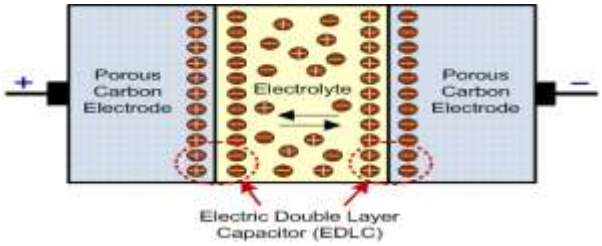

Figure-5: Internal structure of Electric Double Layer Capacitor.

Pseudocapacitor: Pseudocapacitor stores energy electrochemically. There are electron charge transfer between electrolyte and electrode which is coming from dissolved and adsorbed ion. The adsorbed ions do not chemical reaction with the atoms of the electrode. There is only charge transfer by Faradaic redox. In pseudocapacitor use transition metal oxide or conducting polymer electrodes with a high electrochemical pseudocapacitance like Manganese dioxide (MnO_2), Ruthenium dioxide (RuO_2), polyaniline etc.[44-46,48,51].

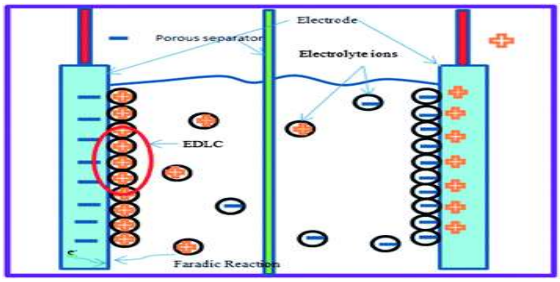

Figure-6: Internal structure of Pseudocapacitor.

Hybrid capacitor: Hybrid capacitor is the combination of both electric double layer capacitor (EDLC) and pseudocapacitor. EDLC shows good cyclic stability and good power performance on the other hand pseudocapacitor shows high specific capacitance. It stores energy by electrostatically electrochemically. At present, researchers have concentrated on three types of hybrid supercapacitors, which are differed by their electrode varieties: Composite, Asymmetric and Battery-type[14, 45].

Composite: This types of electrode is combined with carbon based materials and metal oxides or conducting polymers. So these types of electrodes have both the physical and chemical charge storage mechanisms. Carbon based materials shows capacity due to electric double layer of charge and high specific surface area which is raised the contact between pseudocapacitive materials (stay in electrode) and electrolyte. Metal oxide or conducting polymer materials increases the capacitance due to faradaic redox reaction. There are three types of composites: Binary and ternary composite. In a binary composite use two different types of electrode materials, on the other hand in a ternary composite use three different types of electrode materials in single electrode[14].

Asymmetric: There are two types of electrode (negative and positive) used in asymmetric hybrid supercapacitor. Carbon material is used in a negative electrode on the other metal oxide or conducting polymer is used in a positive electrode. Therefore negative electrode is EDLC type and positive electrode is pseudocapacitor type[14].

Battery type: These types of electrode are the combination of a supercapacitor electrode and a battery electrode. So both the features are present in one cell[14].

Electrode Materials

There are different types of material are used in a supercapacitor electrode such as carbon materials, metal oxide, conducting polymer and composite materials.

Carbon materials: Most of the supercapacitor electrodes carbon materials are used for their large surface area, low cost, availability and environment friendly[52,53]. Carbon material stores energy by the electric double layer mechanism. It is able to accumulate much

charge at the interface of the electrode and electrolyte due to its large surface area and pore shape structure. There are different types of carbon materialare used in a supercapacitor electrode like activated carbon, garphene, carbon nanotubes etc. some of the carbon materials electrodes are discussed below[14].

Activated carbon: Activated carbon is a common material in supercapacitor electrode because of its large surface area, good conductor of electricity, low cost and greater cycle stability. The surface area of the AC is increased up to 3000 m^2/g. previously it was collected from carbon materials such as petroleum coke**,** pitch and coal, but fossil fuels are decreasing day to day**,** now a days it is collected from renewable sources for increasing global energy demand also environment friendly materials. Activated carbon is produced from different types of carbon precursors shown below in Table-3[14,54].

Table-3: BET specific surface are as for different carbon precursors. Data taken from[8].

Carbon precursor	Activation method	S_{bet} (m^2/g)
1. Furfurol	Steam	1040
2. Coconut shell	KOH	1660
3. Eucalyptus wood	KOH	2970
4. Firwood	Steam	1130
5. Bamboo	KOH	1290
6. Cellulose	KOH	2460
7. Potato starch	KOH	2340
8. Starch	KOH	1510
9. Sucrose	CO2	2100
10. Beer lees	KOH	3560
11. Banana fiber	ZnCl2	1100
12. Corn grain	KOH	3200
13. Sugar cane bagasse	ZnCl2	1790
14. Apricot shell	NaOH	2335
15. Sunflower seed shell	KOH	2510
16. Coffee ground	ZnCl2	1020
17. Wheat straw	KOH	2316
18. Fish scale	–	2270
19. Cherry stone	KOH	1300
20. Rice husk	NaOH	1890
21. Rice husk	KOH	1390

Graphene: Graphene is a mono layer, hexagonal lattice structure, sp^2 carbon allotrope[55,56]. One atom is remained in every lattice point. Graphene has many characteristics such as high electric conductivity, high mechanical strength, good thermal conductivity[57], large surface area (around 2630 m^2/g) and high chemical stability. That's why it is used as a supercapacitor electrode material. Graphene is able to reach capacitance of a supercapacitor up to 550 F/g. Graphene is produced from graphite. Recently, there are multiple ways to produce graphene from graphite as like chemical vapour deposition, micromechanical exfoliation electrochemical and chemical method etc.[14].

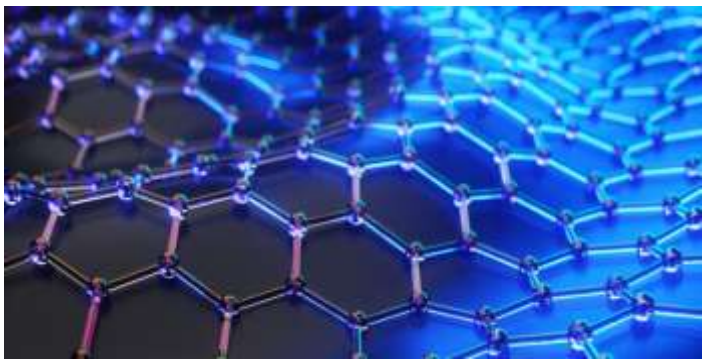

Figure-7: Structure of grapheme.

Carbon nanotubes: Carbon nanotube is an allotrope of carbon. Its structure is cylindrical. It is a good electrode material for their properties such as good electric conductivity, unique pore structure and high stability. There are two types of carbon nanotubes are present these are single-walled carbon nanotubes (SWCNTs) and multi-walled carbon nanotubes (MWCNTs). Both the materials are used in a supercapacitor electrode. It is a high power electrode material due to its good electrical conductivity, but lower energy density for their little surface area[14].

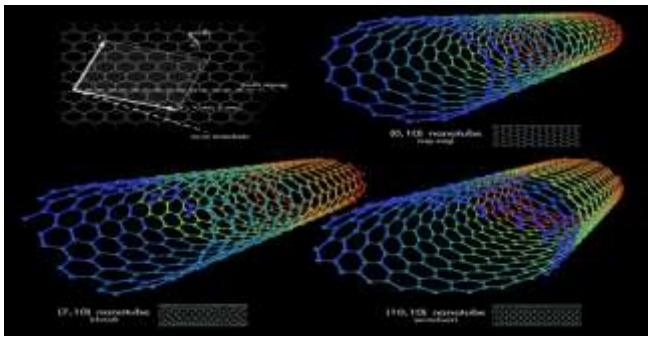

Figure-8: Structure of carbon nanotube.

Metal oxide: Metal oxides are also the substitute material of a supercapacitor electrode for their high specific capacitance and lower resistance. These types of electrodes store energy mainly by pseudocapacitor mechanism. Some of the conventional employed materials are nickel oxide (NiO), ruthenium oxide (RuO_2), manganese oxide (MnO_2), iridium oxide (IrO_2)[14].

Conducting polymers: Recently, conducting polymer is used as an electrode material of the supercapacitor due to its several properties such as good conductivity, high capacitance, simple production and low cost. Conducting polymers store energy by pseudocapacitor mechanism. There are different types of polymer is used in a supercapacitor electrode such as polyaniline (PANI)[14,46].
Composite materials: Composite electrodes are more effective than pure carbon electrode and pure metal oxide or conducting polymer electrode. Composite electrode can store energy by both physical and chemical mechanisms. There are different types of composite such as carbon-carbon, carbon-metal oxide and carbon-conducting polymer composite[14].

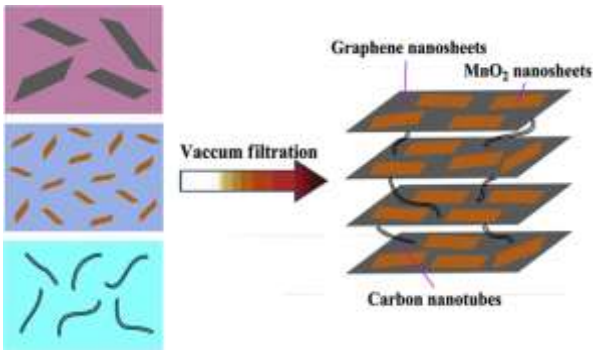

Figure-9: Internal structure of composite material.

Experimental Procedure

Sample preparation: One method has given how to prepare activated carbon to from carbon material. Here coconut shells are used as a carbon material. The outer part of the coconut shell is cleaned by the water and dry. Then it is burned in a muffle furnace at 500^0C for 2hr. After grinded by the mortar and pestle it generates a non-activated carbon. This non activated carbon weighted 1gm is blended with a solution that contains5ml of water and 1.5 gm. KOH as an activated agent. The blend sample is dried an oven at 60^0C for 2 hr. Then the remaining slurry is dried at 110^0C for overnight in the oven. Again the sample is heated from room temperature to 450^0C for 2 hr with the thriving rate temperature at 10^0C/min, then cooling it at a room temperature. This sample is washed repeatedly with a 5 M solution of HCl for removing activated agent. Then it is washed by distilled water until remove the chloride ion. After removing the activated agent, the sample is dried at 110^0C for 12 hr. Finally the sample is converted into activated carbon[14].

Spectroscopic analysis: Fourier Transform Infrared (FTIR) spectroscopy is used to identify the functional groups of the AC samples. Surface area of the AC sample is calculated from the Brunauer- Emmett- Teller (BET) equation through N_2 adsorption– desorption analysis. Before the analysis AC sample is heated at 110^0C for 10 h under vacuum for removing the gas from the sample. The micropore and mesopore volumes are calculated from the t-plot (Harkins-Jura equation) and BJH (Barret-Joyner Halenda) model for

surface analysis respectively. Total number of carbon structures present in the AC sample is measured by Raman spectroscopy with He Ne laser (633nm, 2mW)[58].

Microscopy analysis: Scanning electron microscope (SEM) is used to measure the surface structures of the AC samples. Transmission electron microscope (TEM) is used to investigate the topographical features of the samples[58].

Measurements: One method has given how to measure the performance of AC electrode. At first prepare the mixture of AC, carbon black and PVDF in their mass ratio 90:5:5. This mixture is stirred for 12 h to create homogenous slurry. Then the slurry is brush-coated on nickel foam and dried at 80^0 C for 24 h. This nickel foam is punched into the electrodes of nearly 9 mm thickness. In this process AC electrodes are generated. Glass microfiber is used as the separator and 6M KOH as the electrolyte. After establish the supercapacitor cell, it is connected to an autolabpotentiostat/galvanostat for electrochemical studies such as CV, CDC, EIS etc.[58].

Specific capacitance of a supercapacitor is measured by following cyclic voltammetry (CV) curve. Carbon materials supercapacitor electrode display almost rectangular shape cyclic voltammogram as shown in fig.8 which presents cyclic voltammograms for carbon materials in both, aqueous and organic electrolytes[8].

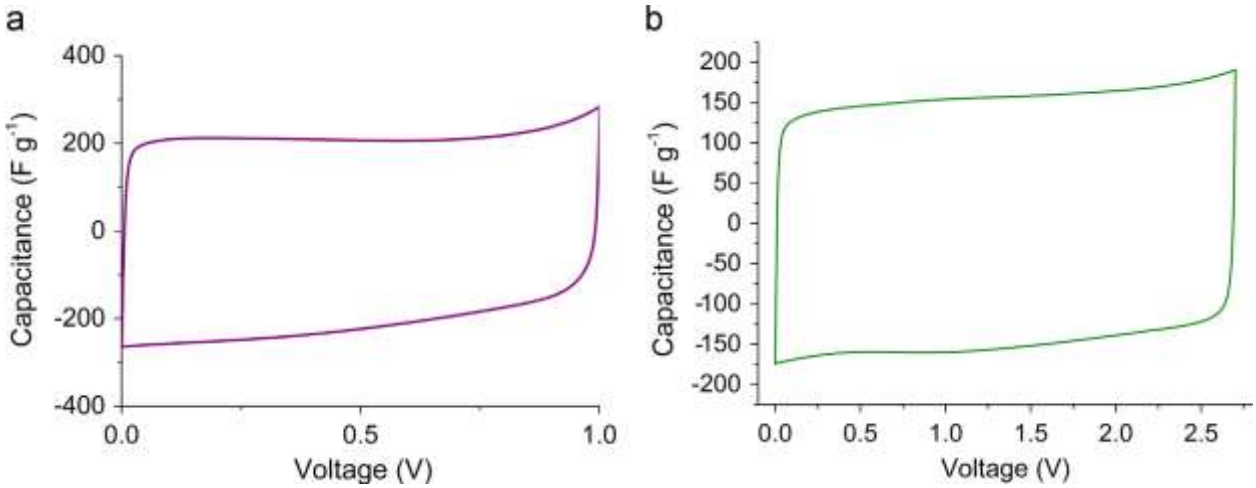

Figure-10: Cyclic voltammogram of an EDLC cell at 5m Vs¯1 in (a) aqueous 6M KOH and (b) organic 1M tetraethyl-ammonium-tetra-fluoro-borate electrolytes.

Conclusion

Supercapacitor is an important alternative energy storage device of batteries. It has many properties such as high electrochemical properties, high power density and good stability, low maintenance cost, high longevity, easy to travel for its light weight. Nowadays researchers are engaged to develop supercapacitor electrode by using different electrode materials like carbon materials, metal oxide and conducting polymers. Although carbon materials has high specific surface area and pore structure, till now their capacitance and energy density are lower. Conducting polymer display high specific capacitance but it has major problem for their swelling and shrinking when charging-discharging. For this reason life time of polymer electrode supercapacitor is very short. Now the scope of research in this field has increased due to discovery of graphene. In future supercapacitor will be an essential storage device for hybrid electric vehicle power systems also for emergency power supplies.

Acknowledgement

Author would like to acknowledge CSIR govt. of India for providing fund through fellowship.

References

1. Jing Xu, Jiaqiang Li, Qiaoling Yang, Yan Xiong, Changguo Chen, ElectrochimicaActa 251 (2017) 672–680

2. Zepeng Bai , Hongji Li , Mingji Li, Cuiping Li , Xufei Wang,ChangqingQu, Baohe Yang, international journal of hydrogen energy xxx (2015) 1 -10

3. Zijiong Li, Weiyang Zhang, Haiyan Wang, Baocheng Yang, ElectrochimicaActa 258 (2017) 561-570

4. Trupti C. Nirmale, Bharat B. Kale, Anjani J. Varma,International Journal of Biological Macromolecules 103 (2017) 1032–1043

5. Prasanna B P, Avadhani D N, Raghu M S, Yogesh Kumar K, S2352-4928 (2017) 30093-4

6. QiufengMeng, KefengCai, Yuanxun Chen, Lidong Chen, Nano EnergyS2211-2855(2017)30242-2

7. Kuo Song, Haifang Ni, Li-Zhen Fan, ElectrochimicaActa 235 (2017) 233–241

8. Ander González, Eider Goikolea, Jon AndoniBarrena, Roman Mysyk, Renewable and Sustainable Energy Reviews 58 (2016)1189–1206

9. Nilesh R. Chodankar, Su-HyeonJi, Do-Heyoung Kim, Journal of the Taiwan Institute of Chemical Engineers 000 (2017) 1–8

10. Rajesh Rajagopal, Kwang-Sun Ryu, ElectrochimicaActa 265 (2018) 532-546

11. Amrita Jain & S. K. Tripathi, Ionics 19 (2013) 549–557

12. KaibingXu,Jianmao Yang, Junqing Hu, Journal of Colloid and Interface Science 511 (2018) 456–462

13. R. Jose, S. G. Krishnan, B. Vidyadharan, I. I. Misnon, M. Harilal, R. A. Aziz, J. Ismail,M. M. Yusoff, Materials Today: Proceedings 3S (2016) S48 – S56

14. Zaharaddeen S. Iro, C. Subramani, S.S. Dash,Int. J. Electrochem. Sci., 11 (2016) 10628 – 10643

15. Ali Olad, HamedGharekhani, Progress in Organic Coatings 81 (2015) 19–26

16. Mahendra Singh Yadav& S. K. Tripathi, Ionics 23 (2017) 2919–2930

17. Soheila Faraji, FaridNasirAni, RenewableandSustainableEnergyReviews42(2015)823–834

18. Tshifhiwa M. Masikhwa, Julien K. Dangbegnon, Abdulhakeem Bello, Moshawe J. Madito, DamilolaMomodu, NcholuManyala, Journal ofPhysicsandChemistryofSolids88(2016)60–67

19. ZuhairAgabElsiddig, HuiXu, Dan Wang, Wei Zhang, XinliGuo, Yao Zhang, Zhengming Sun, Jian Chen, Electrochimica Acta 253 (2017) 422–429

20. Yu Li, Bing Guan, Aimee Maclennan, Yongfeng Hu, Dandan Li, Jing Zhao, Yaqiong Wang, Huaihao Zhang, ElectrochimicaActa 241 (2017) 395–405

21. YachaoXiong, Min Zhou,Hao Chen, Lei Feng, Zhao Wang,Xinzhu Yan and Shiyou Guan, Applied Surface ScienceS0169-4332 (2015)02205-9

22. Jinyang Dong, Ziye Wang, Xiaohong Kang, Colloids and Surfaces A: Physicochem. Eng. Aspects 489 (2016) 282–288

23. Xiaoguang Li, Zhikui Wang, YunfengQiu ,Qinmin Pan, PingAnHua, Journal of Alloys and Compounds 620 (2015) 31–37

24. Fangping Wang, Guifang Li, Qianqian Zhou, JinfengZheng, Caixia Yang, Qizhao Wang, Applied Surface Science 425 (2017) 180–187

25. XiaojuanDuan, Jinxing Deng, Xue Wang, Peng Liu, Materials & DesignS0264-1275(2017)30510-5

26. YachaoXiong, Min Zhou, Hao Chen, Lei Feng, Zhao Wang, Xinzhu Yan and Shiyou Guan, Applied Surface ScienceS0169-4332(2015)02205-9

27. Peipei Liu, Jiang Liu, Shuang Cheng, WeiziCai, Fangyong Yu, Yapeng Zhang,Peng Wu, Meilin Liu, S1385-8947(2017)31101-4

28. Yuhong Bi, AmitNautiyal, Huaiping Zhang, JujieLuo, Xinyu Zhang, ElectrochimicaActa 260 (2018) 952-958

29. Lei Zhang, Tiehu Li, XianglinJi, Zhiyong Zhang, Wenbo Yang, JunjieGao, Hao Li, ChuanyinXiong, Alei Dang, ElectrochimicaActa 252 (2017) 306–314

30. Xi Liu, Guo Du, Jiliang Zhu, ZifanZeng, Xiaohong Zhu, Applied Surface Science 384 (2016) 92–98

31. XueqiangZhang ,Xinbing Cheng , Qiang Zhang, S2095-4956(2016)30309-6

32. LiaKouchachvili, WahibaYaïci, EvgueniyEntchev, Journal of Power Sources 374 (2018) 237–248

33. Ji-Hyun Kim, Min-Jung Jung, Min-Ji Kim, Young-Seak Lee, S1226-086X(17)30698-6

34. V. Ruiz, A. Pfrang, A. Kriston, N. Omar, P. Van den Bossche, L. Boon-Brett, Renewable and Sustainable Energy Reviews 81 (2018) 1427–1452

35. Haegyeom Kim, Kyu-Young Park, Jihyun Hong &Kisuk Kang, Scientific Reports 4 (2014) 5278

36. Reza Younesi, Gabriel M. Veith, Patrik Johansson4, Kristina Edstrom and TejsVegge, *Energy Environ. Sci.* 8 (2015)1905-1922

37. Yu Liu, XinshengPeng, Applied Materials Today 8 (2017) 104–115

38. Qianqiu Tang, Minqiang Sun, Shuangmin Yu, Gengchao Wang, ElectrochimicaActa 125 (2014) 488–496

39. MahirOzanYanik, EkremAkifYigit, YahyaErkanAkansu, ErtugrulSahmetlioglu, S0360-5442 (17) 31197-0

40. A.A. Yadav, A.C. Lokhande, J.H. Kim, C.D. Lokhande, JIEC S1226-086X(2017)30340-4

41. G P Pandey, Yogesh Kumar & S A Hashmi, Indian Journal of Chemistry 49A (2010) 743-751

42. SoheilaFaraji, FaridNasirAni , Renewable and Sustainable Energy Reviews 42 (2015) 823–834

43. Jing Li, Jie Tang, Jinshi Yuan, Kun Zhang, Yige Sun, Han Zhang, Lu-Chang Qin, ElectrochimicaActa 258 (2017) 1053-1058

44. AdekunleMoshoodAbioye, Zulkarnain Ahmad, Noordenc, FaridNasirAni, ElectrochimicaActa 225 (2017) 493–502

45. Ranjit S. Kate, Suraj A. Khalate, Ramesh J. Deokate, Journal of Alloys and Compounds S0925-8388 (2017) 33698-8

46. WANG Qin, LI Jian-ling, GAO Fei, LI Wen-sheng, WU Ke-zhong, WANG Xin-dong, New Carbon Materials 23(3) (2008) 275–280

47. S. Khamlich, T. Mokranid, M.S. Dhlamini, B.M. Mothudi, M. Maaza, Energy Procedia 88 (2016) 614 – 618

48. AbdullahilKafy, AsmaAkther, LindongZhai, Hyun Chan Kim, Jaehwan Kim, Synthetic Metals 223 (2017) 94–100

49. F. Markoulidis, C. Lei, C. Lekakou, D. Duff, S. Khalil, B. Martorana, I. Cannavaro, Carbon 6 8 (2014) 58 –66

50. Kwang Se Lee, Mi So Park, Jong-Duk Kim, Colloids and Surfaces A 533 (2017) 323–329

51. Zhongsheng Sang, Wei Che, Shengbing Yang, Yihui Liu, S0167-577X(18)30039-9

52. PranavBhagwanPawar, ShobhaShukla, SumitSaxena, Journal of Power Sources 321 (2016) 102-105

53. JinggeJu, Huijuan Zhao, Weimin Kang, Nana Tian, Nanping Deng, Bowen Cheng, ElectrochimicaActa 258 (2017) 116-123

54. Lu Wei, GlebYushin, Nano Energy 1 (2012) 552–565

55. Yezeng He, Feng Huang, Hui Li, Yanwei Sui, Fuxiang Wei, QingkunMeng, Weiming Yang, Jiqiu Qi, Physica E 87 (2017) 233–236

56. Dongfei Sun, Xingbin Yan, Junwei Lang, QunjiXue, Journal of Power Sources 222 (2013) 52-58

57. NiyitangaTheophile, Hae Kyung Jeong, Chemical Physics Letters 669 (2017) 125–129

58. Ellie Yi LihTeo, LingeswarranMuniandy, Eng-Poh Ng, Farook Adam, Abdul Rahman Mohamed, Rajan Jose, Kwok Feng Chong, ElectrochimicaActa 192 (2016) 110–119

Simultaneous determination of two fluorescent compounds from their binary mixture using derivative-ratio spectrophotometric method

Soma Mukherjee* and Suparna Dhar
Department of Environmental Science, University of Kalyani, Kalyani, Nadia - 741235, West Bengal, India
somam580@gmail.com; sommukh445@yahoo.co.in

Abstract

*In this method two fluorescent compounds (**1** and **2**) present in their binary mixtures were analyzed using first derivative of the ratio spectra by measurement of the amplitude at zero-crossing wavelengths. Standard solutions of two fluorescent compounds and their binary mixtures were prepared and their absorbance were recorded in methanol within 250-600 nm wavelength range which clearly shows closely overlapping spectral bands of two compounds. In case of compound (**1**), the ratio spectra were obtained by dividing the absorption spectrum (amplitude by amplitude at the appropriate wavelength) of the mixture by the absorption spectrum of a standard solution of compound (**2**). Then first derivative spectra were obtained by using differentiate function of Origin program where ratio spectra were differentiated with respect to wavelength. At specified wavelength, the ratio derivative values of each component were plotted against their concentrations. The statistical analysis of these graphs indicates good linearity. The concentrations of desired component were calculated from their respective calibration curves. The derivative ratio spectra for the determination of compound (**2**) were obtained with the same procedure where a standard spectrum of compound (**1**) used as the divisor. Satisfactory results obtained from derivative-ratio spectrophotometric method (DRM) indicate that the method is effective for determination of the concentration of compounds (**1** and **2**) present in the binary mixture.*

Keywords: Fluorescent compounds, Binary mixture, Absorbance, Derivative ratio spectrophotometry.

Introduction

In recent time industries dealing with dye solutions viz. textile, paint, printing ink industries, etc. are regularly reproduced mixture of colorants by color adjusting or shade adjusting process. There are various analytical methods available for quantitative analysis of dye solutions, using UV-visible absorption spectrophotometry, but the main problem of spectrophotometric multicomponent analysis is determination of two or more compounds in the same sample or in a mixture without any preliminary separation. Sometimes multicomponent analysis using UV-visible absorption spectrophotometry produce incorrect results because of strong overlapping zero-order spectra[1].

The quantitative analysis of such multicomponent preparations is very important and for this, dual wavelength spectrophotometry[2-5], zero crossing of derivative ratio[5], simultaneous equation method (Vierordt's Method)[6-8] absorbance ratio method (Q-Analysis)[9], difference spectrophotometry[10], area under the curve method[11], derivative subtraction[12], ratio subtraction[13],derivative spectrophotometry[14], pH-induced differential spectrophotometry[15], least square method[16], derivative or derivative ratio[17], ratio difference[18-19], multi-wavelength linear regression analysis[20-21], double divisor method[22], ratio subtraction method[23], ratio difference spectrophotometric method[24-27], extended ratio subtraction method[25,29,38], constant center spectrophotometric method[29-31], successive spectrophotometric resolution technique[32], amplitude modulation[33-35] mean centering of ratio spectra[18-19,36-38], second derivative[39] etc. have found wide applications over long periods.

Derivative spectrophotometry (is a spectral technique in which the rate of absorbance change is measured as a function of wavelength) is more reliable in terms of its utility, selectivity and sensitivity than normal spectrophotometry for resolving mixtures of compounds with overlapped spectra by enhancement of the resolution of the overlapping spectra[1,19].

Salinas et al.[40]developed a new spectrophotometric method ratio-derivative spectrophotometry, which is based on the use of the first derivative of the ratio spectra for the simultaneous determination of two compounds in binary mixtures. Furthermore, Berzas Nevado et al.[5]proposed a new method for the simultaneous determination of three compounds in ternary mixtures by ratio derivative spectra zero crossing method.

In the present work, ratio first derivative spectrophotometry method is reported for simultaneous determination of two widely used industrial chemicals, 1-Aminopyrene and 1-Pyrenecarboxaldehyde which are fluorescent compounds, from their binary mixture. 1-Aminopyrene (1-AP) is a metabolic product of the mutagenic environmental pollutants and also have been recognized as chemical carcinogen, mutagen[41-43]. Under UV-A irradiation, 1-AP has been shown to cause light-induced DNA single strand cleavage[44]. 1-Pyrenecarboxaldehyde is an important intermediate used in agrochemical, pharmaceutical and dyestuff field, causes irritation to eyes,

respiratory system and skin. These are ubiquitous organic pollutants of special concern for their carcinogenic, teratogenic and mutagenic properties. Once absorbed in human body, they are oxidized by the cytochrome P450s and then resulting products can form DNA and protein adducts[45]. The aim of this work is to develop a rapid, simple and accurate spectrophotometric method in order to quantify the concentration of 1-AP and 1-PC from their binary mixtures.

Theoretical background

Derivative spectrophotometry (DS) is based on the principle that the absorbance at any wavelength of a mixture is equal to the sum of the absorbance of each component in the mixture at that wavelength. The absorption spectrum of the binary mixture (a mixture of two compounds **a** and **b**) measured in 1 cm cell can be written by the equation

$$A_{M,\lambda 1} = E_{\mathbf{a},\lambda 1}\, C_{\mathbf{a}} + E_{\mathbf{b},\lambda 1}\, C_{\mathbf{b}} \qquad (1)$$

Where, $A_{M,\lambda 1}$ is the absorbance of mixture at wavelength λ_1, $E_{a,\lambda 1}$ and $E_{\mathbf{b},\lambda 1}$ are the molar absorptivity of **a** and **b** at wavelength λ_1, $C_{\mathbf{a}}$ and $C_{\mathbf{b}}$ are the concentrations of **a** and **b** in the mixture.

In Eq. (1), if the absorbance of the mixture at wavelength λ_1 is divided by the absorbance at wavelength λ_1 of a standard solution of **a** whose concentration is $C_{\mathbf{a}}^{0}$ i.e. $E_{\mathbf{a},\lambda 1}\, C_{\mathbf{a}}^{0}$ then Eq. (1) becomes:

$$\frac{A_{M,\lambda 1}}{E_{a,\lambda 1} C_a^0} = \frac{C_a}{C_a^0} + \frac{E_{b,\lambda 1} C_b}{E_{a,\lambda 1} C_a^0} \qquad (2)$$

This can be simplified to:

$$\frac{A_{M,\lambda 1}}{E_{a,\lambda 1}} = C_a + \frac{E_{b,\lambda 1}}{E_{a,\lambda 1}} C_b \qquad (3)$$

Calculation of the first derivative due with respect to λ will remove the constant value,

$$\frac{d}{d\lambda}\left[\frac{A_{M,\lambda 1}}{E_{a,\lambda 1}}\right] = C_b \frac{d}{d\lambda}\left[\frac{E_{b,\lambda 1}}{E_{a,\lambda 1}}\right] \qquad (4)$$

Eq. (4), indicates that the derivative ratio spectrum of the binary mixture is dependent only on the concentration of **b,** and can be easily determined without any interferences of the concentration of compound **a**[46].

Experimental

Apparatus: The UV–Vis spectra (zero order spectra) were measured using Shimadzu UV-1700 double beam UV–visible spectrophotometer and corrected for background due to solvent absorption using 10mm path length quartz cell. Sartorius CP64 balance was used for weighing purpose.

Chemical and Reagents: 1-Aminopyrene (1-AP) and 1-Pyrenecarboxaldehyde (1-PC) were obtained commercially from Sigma Aldrich chemical company and were used without further purification. HPLC grade methanol was used as a solvent for spectroscopic measurements.

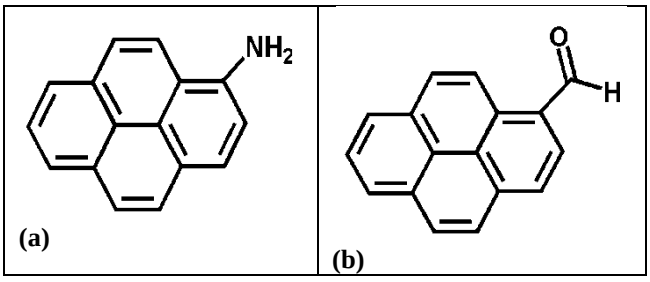

Molecular structure of 1-Aminopyrene (1-AP) (a) and 1-Pyrenecarboxaldehyde (1-PC) (b).

Software: UV Probe used for data recording. Further data treatment were performed by transferring the spectral data to OroginPro 8.5 software and Microsoft Excel 2013 program and processing them with the standard curve fit. ChemDraw Pro 8.0 software used for further work.

Methods

Pure standards: 100 ppm stock standard solutions of 1-Aminopyrene (1-AP) and 1-Pyrenecarboxaldehyde (1-PC) were prepared in methanol.

Working standard solutions: Working standard solutions of different concentrations of 1-Aminopyrene (1-AP) and 1-Pyrenecarboxaldehyde (1-PC) were prepared by appropriate dilution of their respective stock solutions with methanol.

Laboratory prepared mixtures: Synthetic mixtures of 1-Aminopyrene (1-AP) and 1-Pyrenecarboxaldehyde (1-PC) were prepared in methanol by using the stocks solutions.

All the solutions were prepared freshly and protected from light.

Determination of concentration: Zero order absorption spectrum of all standard solutions and their binary mixture were recorded against methanol as a blank over the range of 200–600 nm and then stored. For the determination of 1-AP concentration, the ratio spectra were obtained by dividing the absorption spectrum of the mixture by the absorption spectrum of a standard solution of 1-PC (amplitude by amplitude at the appropriate wavelength) and then differentiated in first order using differentiate function of Origin program. Calibration curve were obtained by plotting the ratio derivative values against their concentration at specified wavelength. The concentration of 1-AP was calculated from their respective regression equation. An analogous procedure was conducted for determination 1-PC concentration[47].

The recovery study was performed on the binary mixture by adding accurately weighed amounts of 1-AP and 1-PC to the excipient mixture and calculating the percentage recovery in each case by comparing measured and expected concentrations[48].

$$\text{Recovery (\%)} = \frac{mg\ measured}{mg\ expected} \text{ X } 100$$

Results and discussion

Zero order absorption spectra of 1-AP and 1-PC and their binary mixture were shown in Figure-1 that illustrates 1-AP and 1-PC have a high overlapping spectra with absorption maxima at the wavelength of 358 nm and 363 nm respectively.

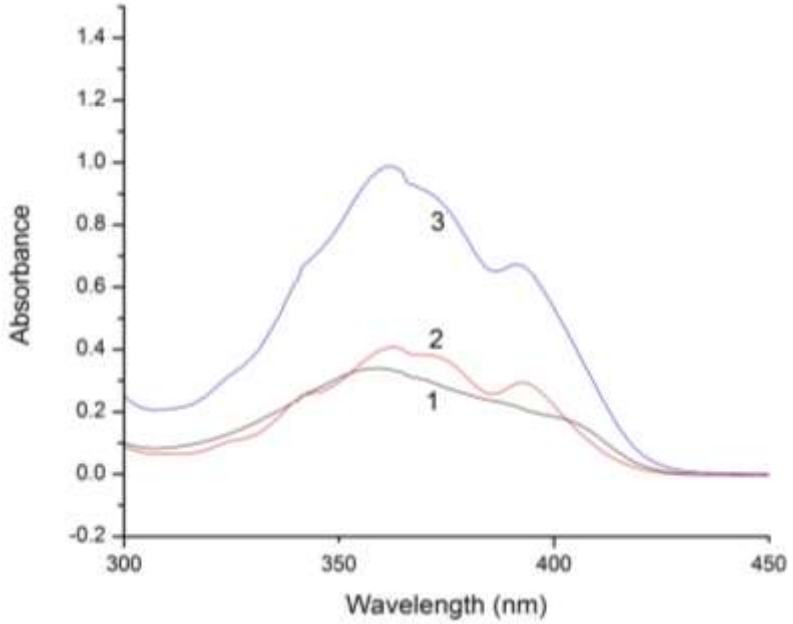

Figure-1: Zero Order Spectra of 1-AP (1), 1-PC (2) and their binary mixture (3).

The ratio spectra were obtained as shown in Figure-2. The first derivative ratio spectra were obtained as shown in Figure-3. For the determination of 1-AP, the spectra of the mixture were firstly divided by the spectrum of 8ppm 1-PC standard solution. The derivative ratio spectra for the determination of 1-PC were obtained with the same procedure but using the spectrum of 8ppm 1-AP standard solution as the divisor.

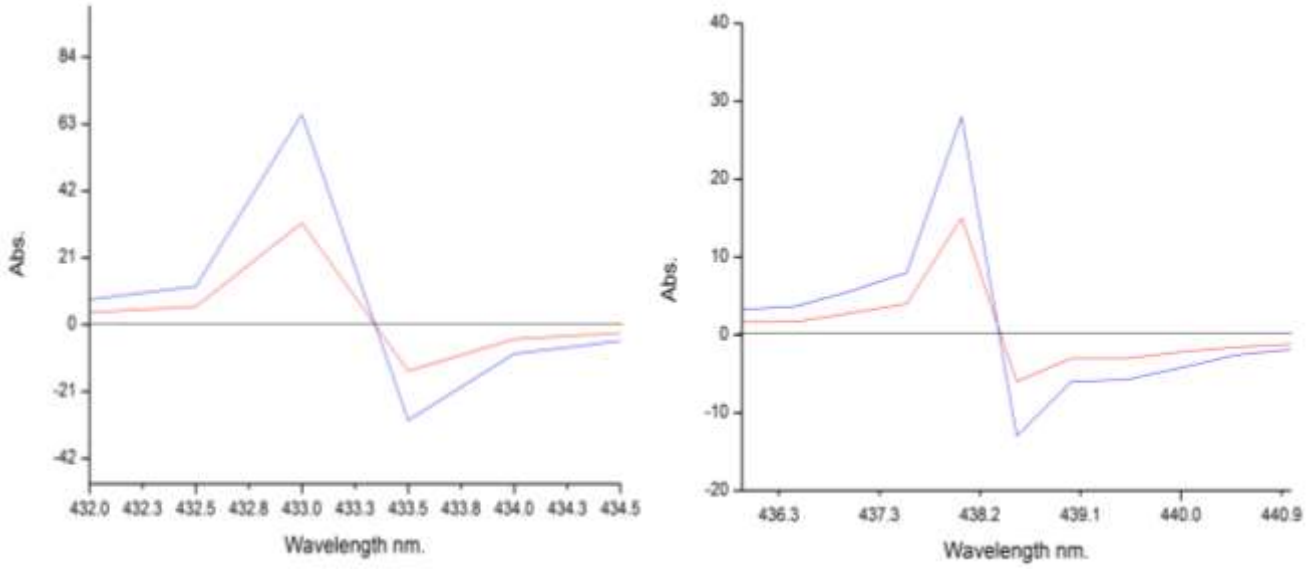

(a) (b)

Figure-2: Ratio spectra of 1-AP (a) and 1-PC (b).

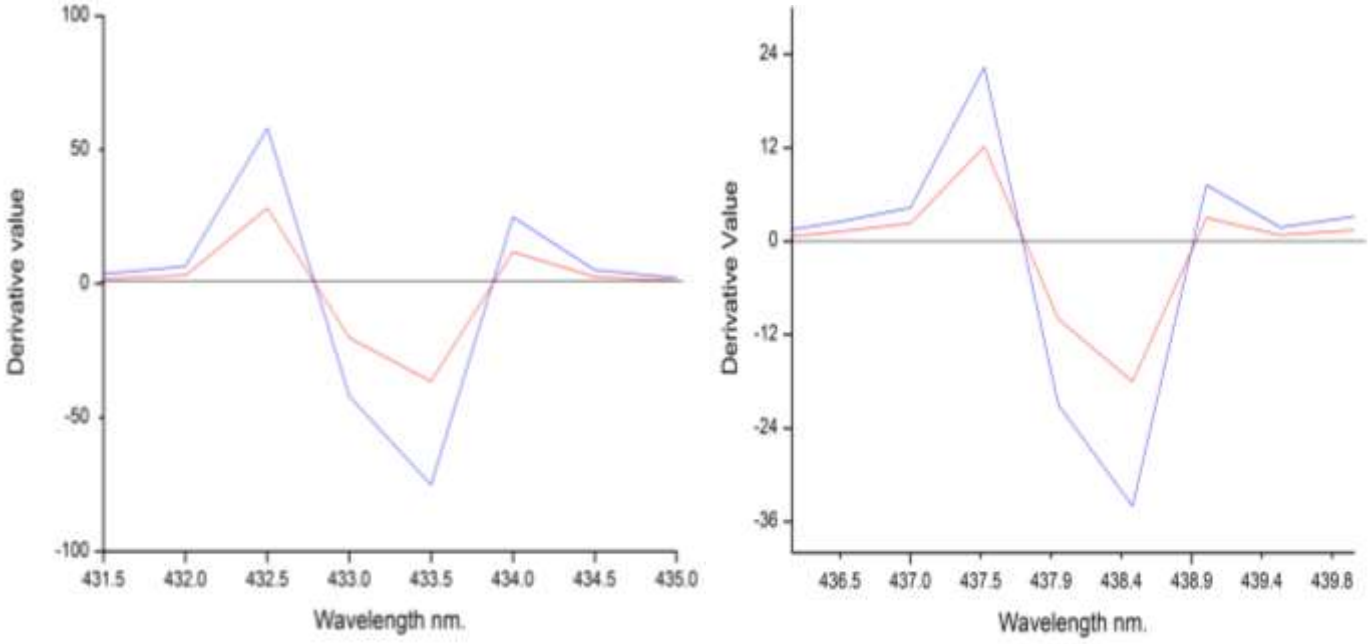

(a) (b)

Figure-3: First Derivative Ratio spectra of 1-AP (a) and 1-PC (b).

Calibration curves as shown in Figure-4 were linear in the concentration range of 2-16 ppm for 1-AC and 2-10 ppm for 1-PC with regression coefficient of 0.981 and 0.987 indicating good linearity.

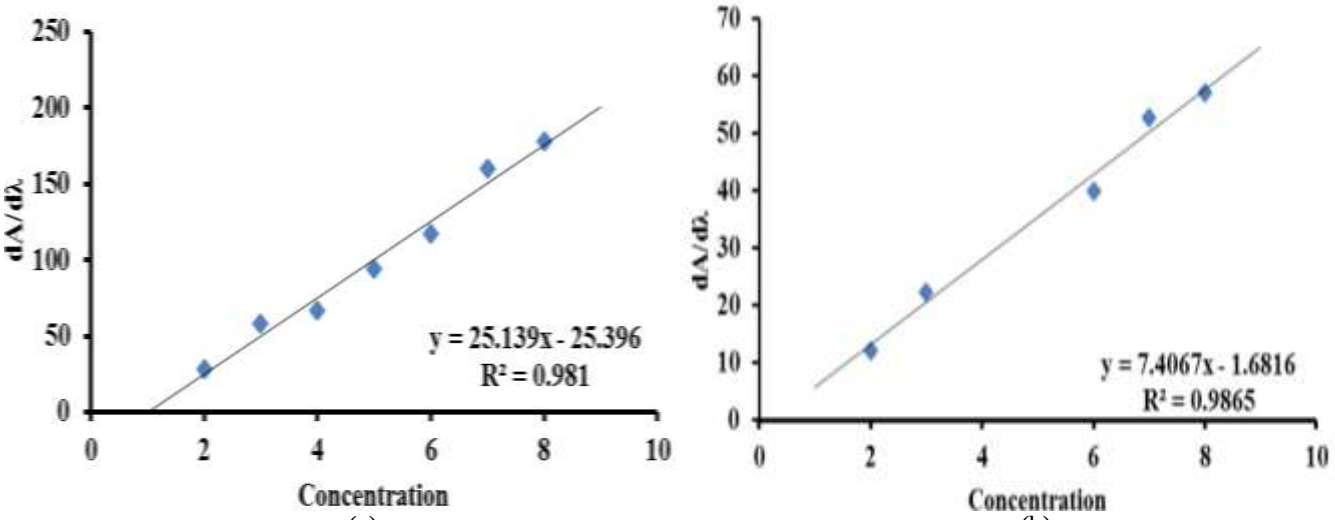

(a) (b)

Figure-4: Calibration graph of 1-AP at 358 nm (a) and 1-PC at 363 nm (b).

Table-1: Calibration data and recovery data of 1-AC and 1-PC in binary mixtures by ratio first derivative spectrophotometry method.

Analyte	Working wavelength (nm)	Linearity range (ppm)	Regression equation	Correlation coefficient	Expected concentration(mg)	Measured concentration(mg)	Recovery (%)
1-AP	432.5	2-16	y=25.139x-25.396	0.981	2.173	2.133	98.2
					4.346	4.32	99.4
1-PC	437.5	2-10	y=7.4067x-1.6816	0.987	2.303	2.1	91.2
					4.606	4.24	92.1

Table-1summarizes the linearity ranges and regression coefficients obtained from the calibration graphs by measuring the signals at specific wavelengths in the first derivative of the ratio spectra for 1-AP and 1-PC. Recovery studies were carried out to study the accuracy of the proposed method which shows that 98.2% and 99.4% recovery for 1-AP and 91.2% and 92.1% recovery for 1-PC respectively from laboratory prepared binary mixtures prepared by adding known amounts of 1-AP and 1-PC.

Conclusion

The ratio first derivative spectrophotometric method is simple and do not require sophisticated technique or instrument and is suitable for the compounds having zero order overlapping spectra. The experimental results of recovery studies were satisfactory. This proposed method is simple, sensitive, selective, rapid and more appropriate for determination of the concentrations of 1-AP and 1-PC from their binary mixture. This method has great promise for the simultaneous determination of two or more compounds present in mixtures and for the analysis of various colorants, cited drugs, without any prior separation, offering a practical potential for multicomponent analysis with its advantages of acceptable sensitivity and high selectivity.

Acknowledgement

We are thankful to the University of Kalyani, Nadia, West Bengal for providing the infrastructural facilities.

References

1. A. S. Nateri, E. Ekrami, Pigment & Resin Technology 38(1) (2009) 43-48.

2. H. W. Darwish, S. A. Hassan, M. Y. Salem, B. A. E. Zeany, Spectrochim. Acta A Mol. Biomol. Spectrosc. 104 (2013) 70-76.

3. N. K. Ramadan, H. M. Mohammed, A. A. Mostafa, J. Appl. Pharm. Sci. 1(9) (2011) 73-80.

4. N. S. Abdelwahab, Arab. J. Chem. (2011).

5. J. J. Berzas Nevado, C. G. Cabanillas, F. Salinas, Talanta 39 (5) (1992) 547-553.
6. P. Giriraj, T. Sivakkumar, Arab. J. Chem. (2013).
7. S. Altınöz, S. Toptan, J. Food Compos. Anal. 16(4) (2003) 517-530.
8. N. Erk, J. Pharm. Biomed. Anal. 20(1-2) (1999) 155-167.
9. K. P. Bhusari, P. B. Khedekar, S. Dhole, V. S. Banode, Indian J. Pharm. Sci. 71(5) (2009) 505-508.
10. H. M. Lotfy, M. A. M. Hagazy, Spectrochim. Acta A Mol. Biomol. Spectrosc. 96 (2012) 259-270.
11. N. A. Bari, S. P. Kela, S. N. Sharma, S. V. Shirse, V. P. Choudhari, Der Pharma Chem. 4(2012) 208-213.
12. H. M. Lotfy, S. M. Tawakkol, N. M. Fahmy, M. A. Shehata, Spectrochim. Acta A 121 (2014) 313-323.
13. M. G. E. Bardicy, H. M. Lotfy, M. A. E. Sayed, M. F. E. Tarras, J. AOAC Int. 91 (2008) 299-310.
14. M. M. Mabrouk, S. F. Hammad, F. R. Mansour, B. Z. E. Khateeb, Der Pharma Chem. 7 (2015) 181-192.
15. A. M. Wahbi, A. M. Faraghaly, J. Pharm. Pharmac. 22 (1970) 848.
16. A. M. Wahbi, H. Abdine, M. A. Korany, F. A. E. Yazbi, J. Pharm. Sci. 67 (1978) 140.
17. A. Afkhami, M. Bahram, Spectrochim. Acta A 61 (2005) 869-877.
18. K. A. M. Attiaa, M. W. I. Nassara, M. B. E. Zeiny, A. Serag, Spectrochim. Acta A 145 (2015) 289-294.
19. K. A. M. Attiaa, M. W. I. Nassara, M. B. E. Zeiny, A. Serag, Spectrochim. Acta A 159 (2016) 219-222.
20. M. Blanco, J. Gene, H. Iturriaga, S. Maspoch, J. Riba, Talanta 34 (1987) 987.
21. E. Dinç, J. Pharm. Biomed. Anal. 33 (2003) 605-615.
22. E. Dinç, F. Onur, Anal. Chim. Acta 359 (1998) 93-106.
23. H. M. Lotfy, M. A. Hegazy, M. R. Rezk, Y. R. Omran, Spectrochim. Acta A Mol. Biomol. Spectrosc. 126 (2014) 197-207.
24. H. M. Lotfy, N. Y. Hassan, S. M. Elgizawy, S. S. Saleh, J. Chil. Chem. Soc. 58 (2013) 1651-1657.
25. H. M. Lotfy, M. A. Hagazy, Spectrochim. Acta A 96 (2012) 259-270.
26. H. M. Lotfy, H. H. Monir, A. E. Abd El-aleem, J. Chil. Chem. Soc. 57 (2012) 1199-1207.
27. H. M. Lotfy, S. S. Saleh, N. Y. Hassan, S. M. Elgizawy, Am. J. Anal. Chem. 3(2012) 761-769.
28. M. Farouk, O. A. Elaziz, S. M. Tawakkol, A. Hemdan, M. A. Shehata, Spectrochim. Acta A 123 (2014) 473-481.
29. H. M. Lotfy, S. S. Saleh, N. Y. Hassan, S. M. Elgizawy, Anal. Chem. Lett. 3 (2013) 70-84.
30. H. M. Lotfy, J. Pharm. Pharm. Sci. 4 (2012) 673-679.
31. A. Samir, H. M. Lotfy, H. Salem, M. Abdelkawy, Spectrochim. Acta A 128 (2014) 127-136.
32. H. A. Merey, N. K. Ramadan, S. S. Diab, A. A. Moustafa, Spectrochim. Acta A 125 (2014) 138-146.
33. H. M. Lotfy, S. S. Saleh, N. Y. Hassan, H. Salem, Spectrochim. Acta A 126 (2014) 112-121.
34. H. M. Lotfy, M. A. Hegazy, M. R. Rezk, Y. R. Omran, Spectrochim. Acta A (2014) 197-207.
35. H. M. Lotfy, Int J Pharm Pharm Sci 6 (2014) 735-741.
36. A. Afkhami, M. Bahram, Talanta 66 (2005) 712-720.
37. A. Afkhami, M. Bahram, Anal. Chim. Acta 526 (2004) 211-218.
38. S. S. Saleh, H. M. Lotfy, N. Y. Hassan, S .M. Elgizawy, Saudi Pharm. J. 21 (2013) 411-421.
39. O. I. Ali, N. S. Ismail, R. M. Elgohary, Spectrochim. Acta A 153 (2016) 605-611.
40. F. Salinas, J. J. B. Nevada, A. E. Mansilla, Talanta 37(3) (1990) 347-351.
41. K. Zeng, H. M. Hwang, S. Dong, X. Shi, K. Wilson, J. Green, Y. Jiao, H. Yu, Environ Toxicol Chem. 23(6) (2004) 1400-1407.
42. K. Fujikawa,F. L. Fort, K. Samejima, Y. Sakamoto, Mutat. Res. 290(2) (1993) 175-182.
43. A. Lafi, J.M. Parry, Mutagenesis 2(1) (1987) 23-26.
44. S. Dong, H.M. Hwang, C. Harrison, L. Holloway, X. Shi, H.B Yu, Environ. Contam. Toxicol. 64 (2000) 467-476.

45. R. H. Kang, Y. S. Wang, H. M. Yang, G. R. Li, X. Tan, J. H. Xue, J. Q. Zhang, Y. K. Yuan, L. F. Shi, X. L. Xiao. Analytica Chimica Acta 658 (2010) 180-186.

46. R. Hajian, N. Shams, I. Kaedi, E-Journal of Chemistry 7(4) (2010) 1530-1538.

47. N. Xiao, J. Deng, K. Huang, S. Ju, C. Hu, J. Liang, Spectrochimica Acta Part A: Molecular and Biomolecular Spectroscopy 128 (2014) 312-318.

48. S. Altınoz, S. Toptan. Journal of Food Composition and Analysis 16 (2003) 517-530.

A Study on groundwater level fluctuation in water scare region of upper catchment area of Kumari river basin in Purulia District, West Bengal

Surajit Modak[1] and Debasish Das[2*]
[1]Research Scholar, Department of Environmental Science, University of Kalyani, Kalyani, West Bengal, India
[2]Professor, Department of Environmental Science, University of Kalyani, Kalyani, West Bengal, India
surajitmodak@hotmail.com, ddas_kly@rediffmail.com

Abstract

The present study was carried out in upper catchment area of Kumari river basin, Purulia, West Bengal. The main aspiration of the study, to mapping the fluctuation of groundwater during pre and post monsoon in third order sub-basin of upper catchment of Kumari river basin. Survey of India topographic map, IRS P6 Satellite image (LISS IV MX), Well inventory data has been used during study and prepared different thematic map to show pre and post monsoon groundwater level fluctuation. Here 64 third order sub basin has been determined. The study revealed that groundwater scenario was drastically changed from pre monsoon to post monsoon. It was recommended that harvest the rainwater and artificially groundwater recharge to reduce the high fluctuation. Groundwater level fluctuation study helps to determine groundwater potential zone and also watershed management.

Keywords: Groundwater, Pre Monsoon, post Monsoon, fluctuation.

Introduction

Groundwater is dynamic and replenishable natural resource, which is present in beneath the earth's surface in soil pore spaces, but the scenario of hard rock environment is different[1].There are occurrences of groundwater is confined in fractured and weathered rock[2]. Beneath the earth surface, upper surface of the saturation zone of water is called water table. Level of groundwater is an indicator of groundwater availability, groundwater flow and physical characteristics of an aquifer of groundwater system[3-4].

Over utilization and over exploitation of groundwater is a common fact in several parts of India[2], consequently water scarcity is common scenario. Purulia is a water scare region of west Bengal[5]. Twenty block of the Purulia district is fall under drought prone region[5]. Our study has been carried out in the upper catchment of Kumari river basin, Purulia District, West Bengal. The study area laying on hard rock terrain[6]. According to Saraf and Choudhury 1998, "In India, 65 per cent of the total geographical area is covered by hard rock formations." In hard rock terrain, occurrence and movement of groundwater in a watershed, mainly controlled by secondary porosity caused by fracturing of underlying rocks [2].In this area as per as laying in hard rock terrain so, groundwater is limited extent and its occurrence is essentially confined to fractured and weathered zones[1].

A number of researcher attempts water table fluctuation study on their delineation of groundwater potential zone[1, 2, 7, 8]or delineation of suitable sites for rainwater harvesting[9-16]. Because they want to ground truth validation of their result that means suitable potential zone.

Here our main aim of this study is to mapping the fluctuation of groundwater during pre and post monsoon in third order sub-basin of upper catchment area Kumari river basin.

If we know about groundwater fluctuation during pre and post monsoon, we will take proper management policies and we will do the work accordingly. This type of study will make simpler watershed management and more effectively. As our study area setting down in hard rock and water scare region, so this study will help the mark of groundwater potential zone or identify suitable sites for rainwater harvesting and rainwater harvesting is the best remedies to resolve the problem of water scarcity.

Study area: The investigated area, upper catchment of Kumari river basin (a sub basin of Kangsabati river) spreading over an area 833 square kilometer and situated in Purulia district, in the extreme western part of West Bengal (Figure-1) and little part in the northern side of East Singhbhum district. And this investigated area has been carried outin an area by longitude 86˚ 9΄42.46΄΄E to 86˚ 31΄΄13.68΄΄E and latitude 22˚52΄ 13.7΄΄N to 23˚14΄7.83΄΄N.

Materials and Methods

For the fulfilment of aforesaid objectives, we have used topographic maps (Detail in table 1) on the scale 1: 50000. Topographic maps were rectified geographically and whole study area was delineated in GIS environment with the help of ArcGIS 10.2.1 software. Third order sub basin demarcated from topographical sheet after that updated from satellite image (LISS IV MX).

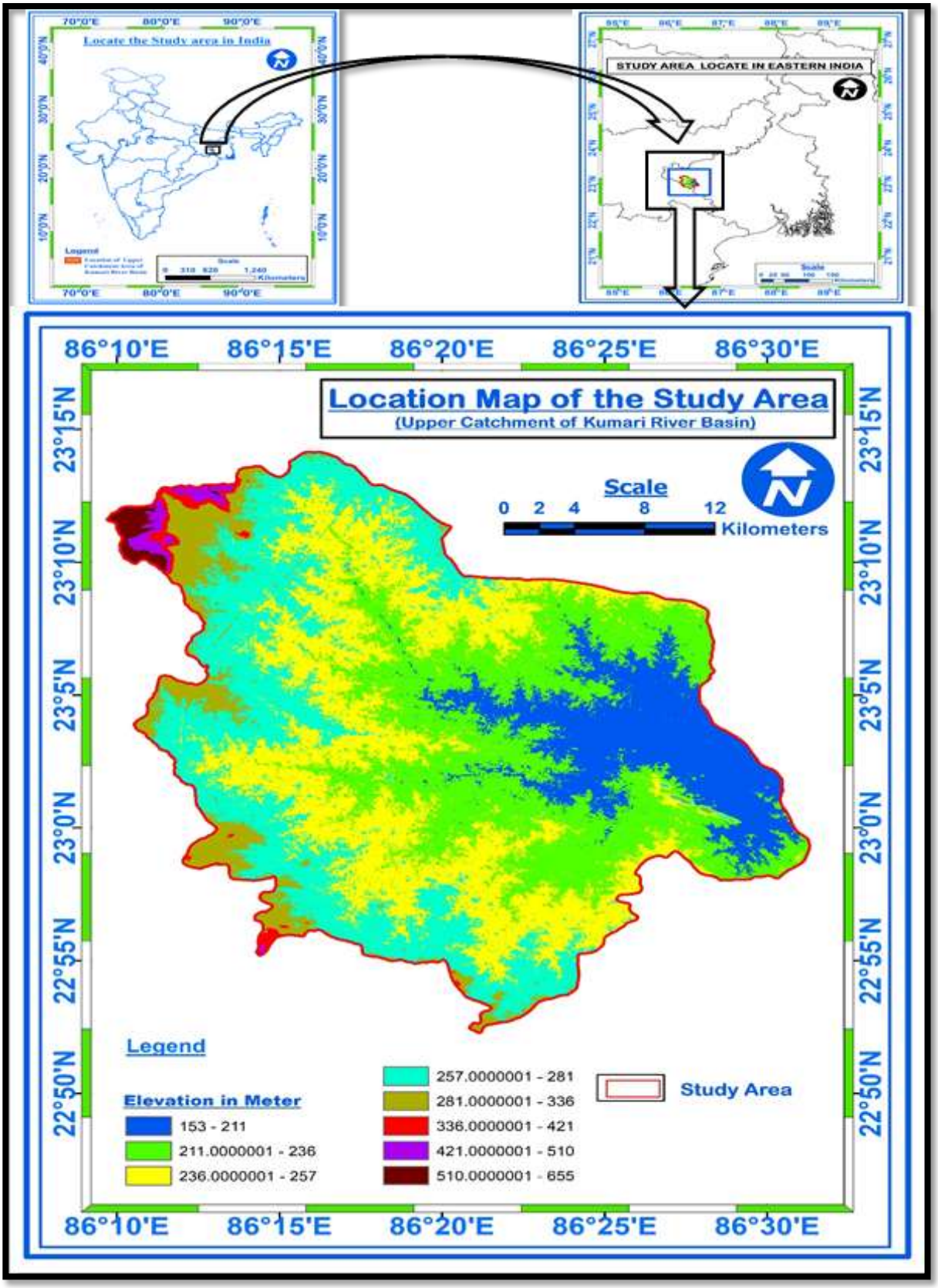

Figure-1: Location map of the study area.

Table-1: Data Source.

Data	Source
Topographical Sheet (73 I/4, I/8, I/12 and 73 J/1, J/5, J/9) scale 1: 50000)	Survey of India, Kolkata
Dug Well Data	Collected from field visit 2017-2018
LISS IV MX	NRSC/ISRO, Hyderabad

To find out the water table fluctuation, we have been used well inventory method[4]. The study periods, we have been divided into two season[1, 17]viz. pre-monsoons (March, April, May) and post-monsoon (November, December, January, February). The fluctuation study was carried out for the period of March 2017 to January 2018. We measured the depth of groundwater level in each well (Figure 3 & 4), after that deducting the length of well height from the total height of the measuring point to the earth surface. We have been observed 80 wells on entire study area during post monsoon and 67 wells during pre-monsoon (see Figure-2 Flow chart).

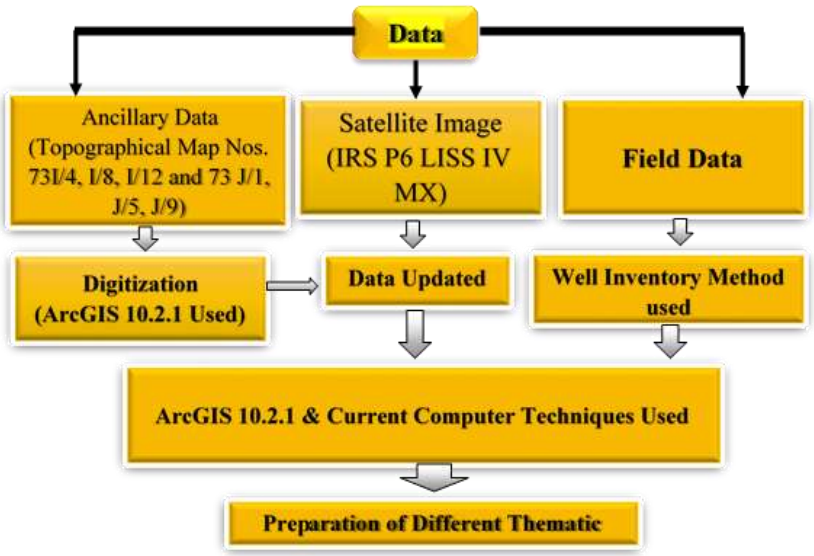

Figure-2: Flow chart of methodology (Modified after Modak and Das, 2018[18]).

Figure-3: Measuring groundwater level depth at well.

Figure-4: Subtract the construction height above the surface.

Results and Discussion

The groundwater level depth data of upper catchment of Kumari river basin was represented in the graphically its variant during pre-monsoon and post-monsoon season are represented in Figures-5 and 6. From the figure it could be seen that all wells have their extreme depth to groundwater level was attained during pre-monsoon season and minimum depth of groundwater level was attained during post-monsoon. From the figure it is revealed that, during pre-monsoon, the depth of groundwater level ranges between 2.2086 meter to 11.2899 meter and during post monsoon it varies between 0.4048 meter to 9.4504 meter. This situation changes due to recharge by rainwater during monsoon time. From Figure-2, it is revealed that, during pre-monsoon, part of 11 & 12 nos. third order sub basins has highest depth, while part of 2, 8, 9, 10, 14, 34, 37 nos. third order sub basins have lowest depth. From the Figure-3, it is revealed that, during post monsoon part of 4, 11, 12, 17, 42, 47, 49 nos. have highest depth, while part of 9, 10, 43, 48, 52, 53 nos. third order basin has lowest depth.

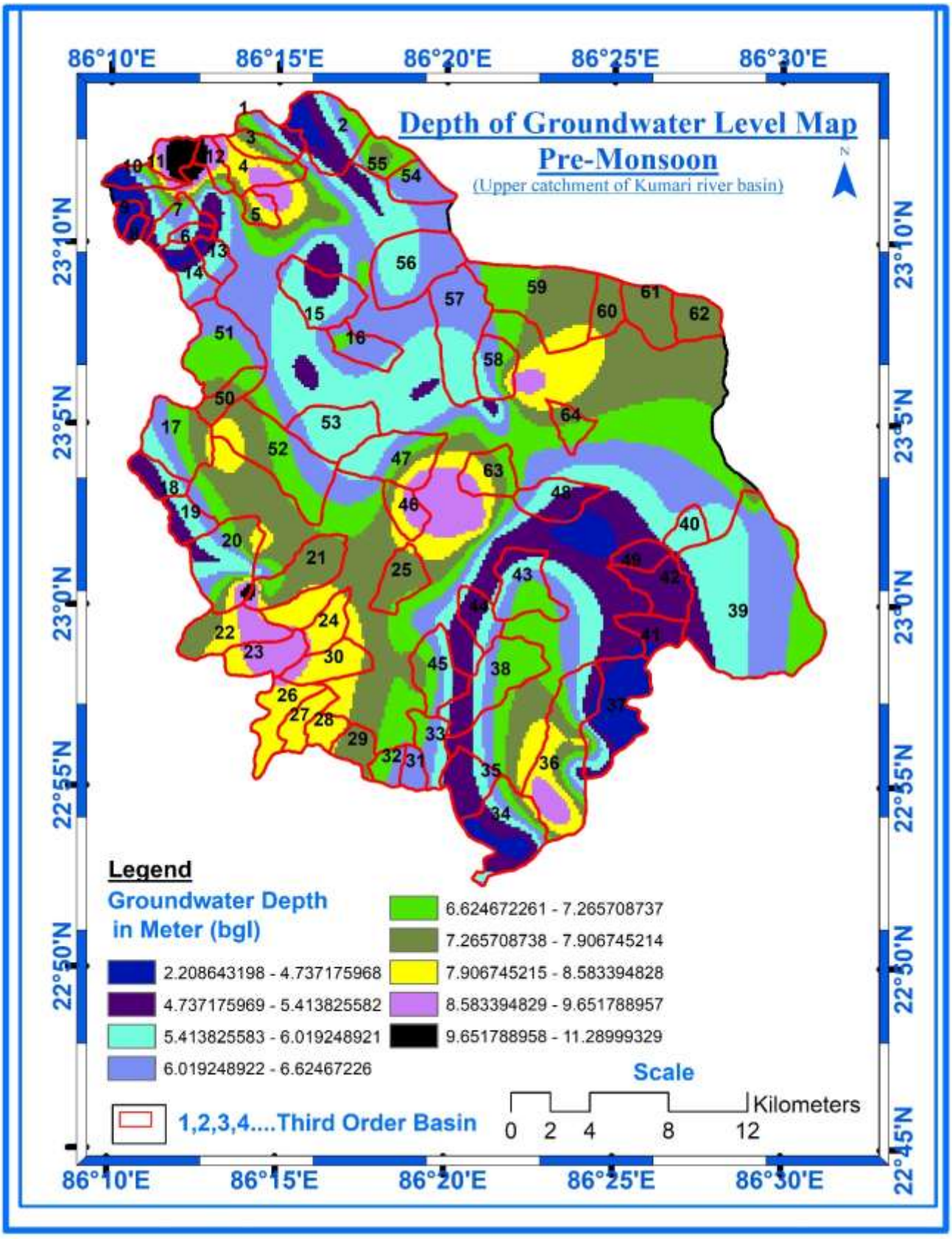

Figure-5: Depth of groundwater level map on pre monsoon, 2017

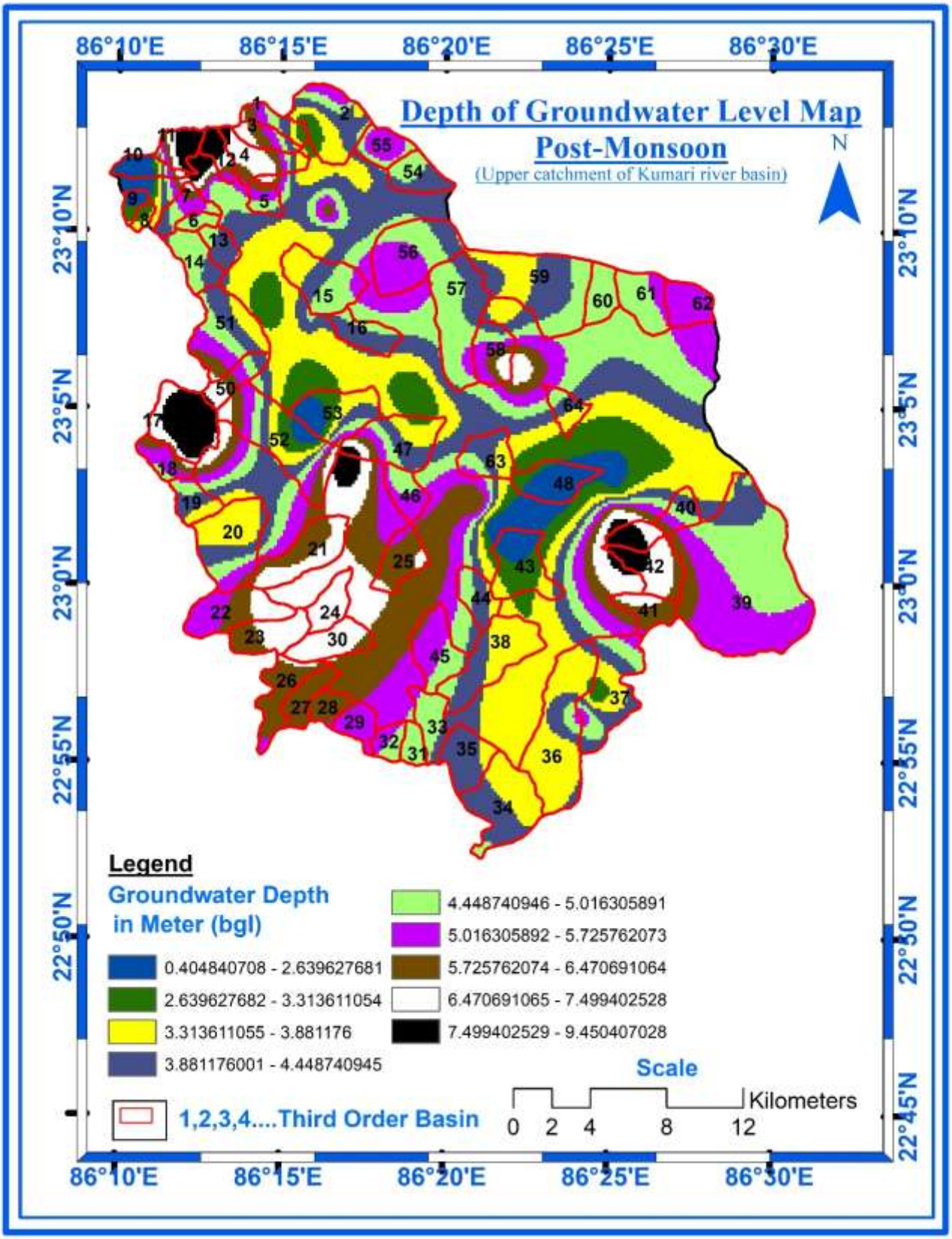

Figure-6: Depth of groundwater level map on post monsoon, 2017-18.

Conclusion

The study result illustrates that; groundwater scenario was drastically changed from pre monsoon to post monsoon. As the study area suffers from water scarcity and high fluctuation of groundwater, the existing water resource such as dug wells, ponds, tanks should be renovated protected for future use as well as artificial recharge should be practiced in large scale along with constructed the structure of rainwater harvesting like check dam, 'nala' bunds, percolation tank, farm ponds. This type of fluctuation study helps to identify the groundwater potential zone and in vast it helps to proper watershed management.

Acknowledgement

From the core of our heart, we are very much thankful to University Grants Commission (UGC) for providing us the required fund.

References

1. Saraf A.K. & Choudhury, P. R. (1998). Integrated remote sensing and GIS for groundwater exploration and identification of artificial recharge sites. International Journal of Remote Sensing, 19(10), 1825-1841.

2. Deepa, S., Venkateswaran, S., Ayyandurai, R., Kannan, M., Prabhu, V., (2016). Groundwater recharge potential zones mapping in upper Manimuktha Sub basin Vellar river Tamil Nadu India using GIS and remote sensing techniques. Model. Earth Syst. Environ, 2, 1-13.

3. Sethi, R. R., Kumar, A., Sharma, S. P. and Verma, H. C. (2010). Prediction of water table depth in a hard rock basin by using artificial neural network. International Journal of Water Resources and Environmental Engineering, 2(4), 95-102.

4. Rekha, V. B. (2013). A comparative study of the hydrological scenario of Peruvanthanam sub-watershed and Valiyathodu sub-watershed of Manimala river basin, Kerala, south India. School of Environmental Sciences, Mahatma Gandhi University, Kottayam, Kerala, India, P 26 (Accessed from http://shodhganga.inflibnet.ac.in/bitstream/10603/25955/14/14_chapter4.pdf).

5. Roy, A. (2014). Availability, Scarcity and Potentiality of Groundwater Resources in Puruliya District of West Bengal: An Appraisal. International Journal of Scientific Footprints. 2(1), 78–93.

6. Modak, S. and Das, D. (2018). Geo-hydrological condition of the upper catchment area of the Kumari river basin using geo-spatial techniques. International Journal of Engineering Sciences & Research Technology. *7*(2), 365-384. DOI: 10.5281/zenodo.1173526.

7. Ghosh, P. K., Bondyopadhyay, S., and Jana, N. C, (2016). Mapping of groundwater potential zones in hard rock terrain using geoinformatics: a case of Kumari watershed in western part of West Bengal. Modeling Earth Systems and Environment. 2(1),1-12.

8. Ramu., Mahalingam, B., and Vinay, M. (2014). Identification of groundwater potential zones using GIS and Remote Sensing Techniques: A case study of Mysore Taluk–Karnataka. International Journal of Geomatics and Geosciences. 5(3), 393- 403.

9. Dhakate, R., Rao, V. V. S. G., Raju, B. A., Mahesh, J., Rao, S. T. M., and Sankaran, S. (2013). Integrated Approach for Identifying Suitable Sites for Rainwater Harvesting Structures for Groundwater Augmentation in Basaltic Terrain. Water Resources Management. 27(5), 1279-1299.

10. Ravikumar A. S., Mohankumar K. C., Punithraj, G., (2016). Identification of potential sites for rain water harvesting structures using RS, GIS and MIF techniques. 4th International conference on Science, Technology and Management. pp 802-811, ISBN :9788193207482.

11. Gogate, N. G. and Rawal, P. M. (2015). Identification of Potential Stormwater Recharge Zonesin Dense Urban Context: A Case Study from Pune city. Int. J. Environ. Res. 9(4), 1259-1268.

12. Nageswara R. K. Identification of suitable sites for rain water harvesting in a hard rock terrain of Eastern Ghats, India using Remote Sensing and GIS.http://a-a-r-s.org/acrs/administrator/components/com_jresearch/files/publications/649.pdf. pp1-10 (Accessed on 06/03/2018).

13. Lakshminarayana, P. and Rao, B. V. (2014). Identification of the Recharge Sites Using Remote Sensing and GIS in Hard Rock Terrain. Indian J. Dryland Agric. Res. & Dev. 29(2), 5-11.

14. Rokade, V. M., Kundal, P., and Joshi, A. K. (2011). Identification of suitable sites for different artificial recharge structures using remote sensing and GIS. Journal of Applied Hydrology. XXIV(3&4), 64-75.

15. Pande, C. B., Khadri, S. F. R., Moharir, K. N. and Patode, R. S. (2017). Assessment of groundwater potential zonation of Mahesh River basin Akola and Buldhana districts, Maharashtra, India using remote sensing and GIS techniques. Sustain Water Resour. Manag. 1-17.

16. Sinha, D. D., Mohapatra, S. N., and Pani p., (2015). Site selection for suitable water harvesting structure using Remote Sensing and GIS. Trans. Inst. Indian Geographers. 37(2), 223-233.

17. Selvam. G, Banukumar, K., Srinivasan. D, Selvakumar. R, Alaguraja, P. (2012). Identification of ground water potential zone in hard rock terrain – A case study from parts of Manapparai block Tamilnadu using Remote Sensing and GIS techniques. Int. Journal of Advances in Remote Sensing and GIS. 1 (1), 8-18.

18. Modak, S. and Das, D. (2017). Application of morphometric analysis of third order basin for geo-hydrological studies using geospatial techniques: A case study of upper catchment of Kumari drainage basin. International Journal of Advanced Research and Development. 2 (6), 294-304.

Adsorption kinetic study of an emerging contaminant in soil sample

Soma Mukherjee[*] and Monami Haque
Department of Environmental Science, University of Kalyani,Kalyani, Nadia – 741235, West Bengal, India
sommukh445@yahoo.co.in; somam580@gmail.com

Abstract

Emerging contaminants include biologically active compounds such as pharmaceuticals, pesticides, personal care and consumer products from domestic, agricultural and industrial origin which have been released in the environment. In current years all the emerging contaminants are of great concern due to their toxicity and chemical persistence in the environment. The extensive use of large number of pesticides have resulted increasing quantities of pesticide residues in soils and aquatic environments. Among them chlorpyrifos is one of the most widely used and frequently detected organophosphorusinsecticides all over the world in agricultural fields. It is highly toxicto freshwater fish, aquatic invertebrates, and estuarine organisms at low concentration and its adsorption in agricultural soils has received considerable attention nowadays. In the present study the adsorption of chlorpyrifos in an agricultural soil sample is investigated. The representative agricultural soil is collected from Murshidabad (24° 10' 5.1234" N, 88° 17' 28.0608" E). The characterization parameters of soil including moisture content, water holding capacity, texture, pH, organic carbon, hardness, chloride, alkalinity, phosphate and nitrate are estimated with the help of standard methods. Pesticide analyses are done by gas chromatography. Adsorption kinetics (time dependent) and correlation study between soil parameter & adsorption percentage are performed.

Keywords: Adsorption, Agricultural soil, Organophosphorus pesticides, Kinetics.

Introduction

Wide application of xenobiotic substances like pharmaceuticals, synthetic fragrances, pesticides, drugs, personal care products etc. leads to the increasing concentrations of these substances in environmental matrices. Thus various newly synthesized and newly introduced compounds into the environment which pose contamination problems are termed as emerging contaminants (ECs).The presence of ECs in environment create immense contamination and serious health problems of animals and human being also[1]. The production and consumption of ECs have been increasing day by day in India[2]. Among these ECs the risks arising from extensive production of pesticides (such as herbicides, insecticides, fungicides, rodenticides etc.)for agricultural applications are a great environmental concern[3]. The pesticide deposits in soil leads to the unexpected uptake through plant roots, leaching to ground water, contamination of surface water during agricultural runoff etc. Many studies have reported that residual pesticides have been found also in organic agricultural products cultivated without pesticide use[4,5].

After phasing out of organochlorine (OCs) pesticides, organophosphorous (OPs) compounds are now widely used for insect control in agricultural practices. These compounds are also used in homes, gardens and veterinary practices for pest control. Several organophosphorous (OPs) pesticides are highly toxic and all can potentially cause acute and sub-acute toxicity[6].

One of the organophosphorous compounds commonly used is chlorpyrifos (O, O-Diethyl O-3, 5, 6-trichloropyridine-2-yl phosphorothioate), which is a broad-spectrum chlorinated organophosphate insecticide, nematicide, and acaricide used for pest control on various crops. It is available in a variety of formulations, under the trade names of dursban and lorsban. It is a degradable compound and despite its high toxicity, it is being increasingly used worldwide. Even after withdrawing chlorpyrifos products from indoor/outdoor domestic, garden, and industrial uses because of toxicity concerns in children, pets, wildlife, and the environment, its production and consumption are drastically increasing every year[7,8].

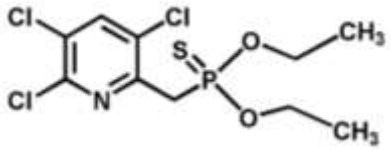

Molecular structure of chlorpyrifos.

Table-1: The physical and chemical properties of chlorpyrifos.

Name of Insecticide	Melting point (°C)	Molecular weight	Vapour pressure (mPa at 25°C)	Water Solubility (ppm at 25°C)	Log K_{ow} (at 25°C)
Chlorpyrifos	41-43	350.6	3.35	2	4.98

Because of its low water solubility and relatively high log K_{ow} (Table-1), the adsorption of chlorpyrifos in agricultural soil will play a crucial role in determining its fate and transport in the environment. This adsorption process may influenced by the soil properties, chemical nature of the insecticide and also climatic factors.

Literatures suggest that adsorption of pesticides to the soil is the most important factor in soil-pesticide interactions that affects their eco-toxicological impact, environmental mobility and the rate of degradation[9,10].Thus, whether an insecticide will contaminate ground water or a nearby stream, become an air pollutant by volatilization into the atmosphere, or control the target pest will depend upon sorption phenomena in the soil. The adsorptionprocess of pesticide is influenced by several factors likeorganic matter content, soil texture, pH, temperature, etc.[9-12].The physiochemical characteristics of soil as well as the chemical characteristics of the insecticide are both important factors of adsorption. The pesticide contamination of surface water and ground water is depends upon the adsorption of pesticides in soil. That's why to protect water from this contamination, extensive knowledge regarding adsorption process in required[12]. Adsorption kinetic study is the major technique for directly measuring adsorption of insecticide in soils. It helps to establish the time required for pesticide adsorption to reach equilibrium in the soil systems[13].

In the present work adsorption kinetic study of chlorpyrifos on agricultural soil has been investigated to get rid of contamination problem. Also an attempt was made to understand the physiochemical properties of soil affecting the adsorption of chlorpyrifos in soil.

Materials and methods

Soil sample: Representative soil samples were collected by composite sampling from agricultural fields of two randomly selected Districts of West Bengal. Sample I is collected from Malda, here the selected agricultural field is situated near Mahananda riverbank. Sample II is collected from Murshidabad, here the selected agricultural field is situated away from Bhagirathi riverbank. The Geological coordinates of sampling sites are given in Table-2.

Table-2: Location of sampling site.

Sample No.	Sampling Site	Latitude	Longitude
Sample I	Malda	24° 59' 48.52" N	88° 8' 45.3289" E
Sample II	Murshidabad	24° 10' 5.1234" N	88° 17' 28.0608" E

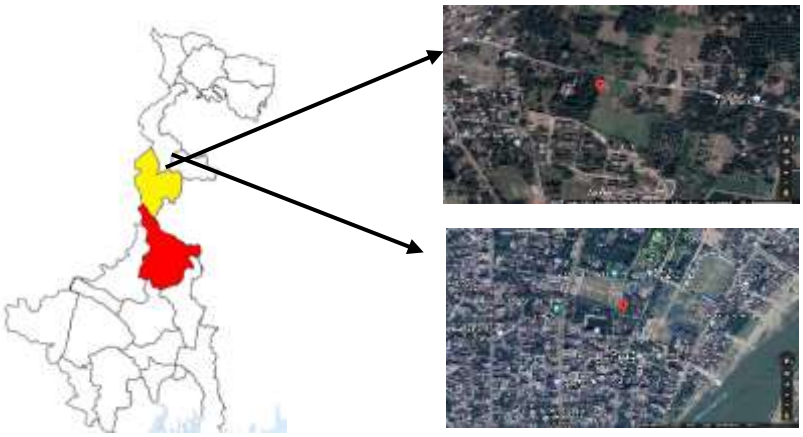

Figure-1: Location of sampling site.

Sample Preparation: Soil sample was collected from the 10-15 cm depth of an agricultural field in air tight plastic bag. The collected sample was air dried, oven dried, grinded and passed through 2 mm sieve and stored in clear plastic bag.

Physiochemical characterization of soil: The physiochemical characteristics of soil includes pH, texture, moisture content, water holding capacity, organic matter, hardness, nitrate and phosphate. Soil pH was determined from soil water suspension in 1:5 ratio with the help ofpH meter. The organic carbon content of soil sample was determined by using Walkley and Black Rapid Titration method i.e. wet combustion method. Soil texture, soil moisture content, water holding capacity, hardness, nitrate and phosphate was estimated using standard methods.

Chemicals: Analytical grade Chlorpyrifos (purity 98%) was purchased from Sigma Aldrich. Other chemical reagents were purchased from Merck and solvents(HPLC grade) were purchased from SRL. The stock Chlorpyrifos solution was prepared in methanol (SRL - HPLC grade) and used for experiments after necessary dilutions with distilled water. All glassware used were supplied by Borosil, India.

Adsorption Kinetic study: The adsorption kinetic study was carried out in batch mode using 250ml conical flask with 5gm soil sample and 100ml 35ppb pesticide solution. The study was conducted in triplicate on a shaker incubator (Thermo-scientific MaxQ 6000) at 150rpm for a period of 24 h at room temperature (28 ± 2 ℃). 5ml of sample is collected at time interval of 1, 2, 4, 8, 16 and 24 h. The collected samples were extracted with n-hexane solution. Then the extracted samples were through anhydrous sodium sulphate to remove moisture content. Finally the extracted samples (Figures-2 and 3) were analyzed by gas chromatography (Thermo-scientific Trace 1310) with electron capture detector (ECD).

Figure-2: Sample I extract after adsorption at time interval of 1, 2, 4, 8, 16 and 24 h.

Figure-3: Sample II extract after adsorption at time interval of 1, 2, 4, 8, 16 and 24 h.

Analysis of chlorpyrifos: The samples were analyzed using gas chromatography (Thermofisher Trace 1310) with electron capture detector (ECD) equipped with split/splitless capillary injection system and analytical capillary column. The operating conditions were as follows: The column was held initially at a temperature of 60℃ for 1min, then at 20 ℃ min^{-1} to 200 ℃, followed by 15 ℃ min^{-1} to 290 ℃ and finally held at 290 ℃ for 3 min. The temperature of injector and detector were maintained at 220 ℃ and 300 ℃ respectively. Nitrogen was used as carrier gas at a flow rate of 1 ml/ min and injections were made in the split mode with a split ratio of 1:10. Total run is 18 min. Under this condition retention time of chlorpyrifos was 12.43 with 0.050 AN window.

Results and discussion

Adsorbent – physiochemical characterization: The physiochemical properties of two soil samples are shown in Table-3.

Table-3: Physiochemical properties of soilsamples I and II.

Parameters			Sample I	Sample II
Physical Parameter	Moisture content (%)		37.89	12.86
	Water holding capacity (%)		67.50	83
	Texture	Course sand	0.95	0.65
		Silt	12.99	18.03
		Clay	69.27	48
		Fine sand	16.20	33.32

	pH	7.47	7.57
Chemical Parameter	Organic Carbon (%)	1.297	0.059
	Organic Matter (%)	2.236	0.878
	Hardness (mg/100g)	14.10	1.603
	Chloride (mg/100g)	184.6	132.06
	Phosphate (mg/100g)	1.590	1.41
	Nitrate (mg/100g)	1.540	0.64

Adsorption Kinetic Study: The adsorption kinetics of chlorpyrifos exhibited in soil samples were characterized by an initial rapid adsorption within 1h. The initial concentration of working aqueous solution of chlorpyrifos was 35 ppb. The amount of chlorpyrifos adsorbed by the soil sample I and sample II was measured at different time intervals of 1, 2, 4, 8, 16 and 24 h (Table-4 and Table-5). Chlorpyrifos adsorbed on to soil surface increases with increasing shaking time and eventually reached at constant at 8hours (Figure-4 and 5) and remain in equilibrium condition upto 24 h.

Table-4: Adsorption of chlorpyrifos in soil sample I at different time interval.

Time (h)	Initial Concentration (ppb)	Final Concentration (ppb)	% Adsorbed
0	35	35	0
1	35	6.848	80.43
2	35	5.625	83.93
4	35	3.707	89.41
8	35	2.688	92.32
16	35	2.688	92.32
24	35	2.688	92.32

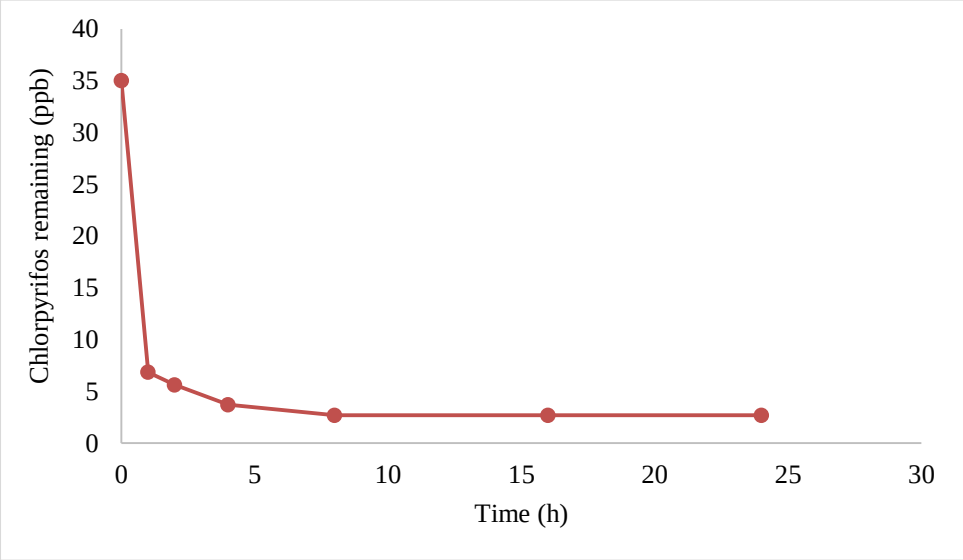

Figure-4: Adsorption kinetics of chlorpyrifos adsorption on soil sample I.

Table-5: Adsorption of chlorpyrifos in soil sample II at different time interval.

Time (h)	Initial Concentration (ppb)	Final Concentration (ppb)	% Adsorbed
0	35	35	0
1	35	5.956	82.98
2	35	4.824	86.217
4	35	3.649	89.574
8	35	2.286	93.469
16	35	2.286	93.469
24	35	2.286	93.469

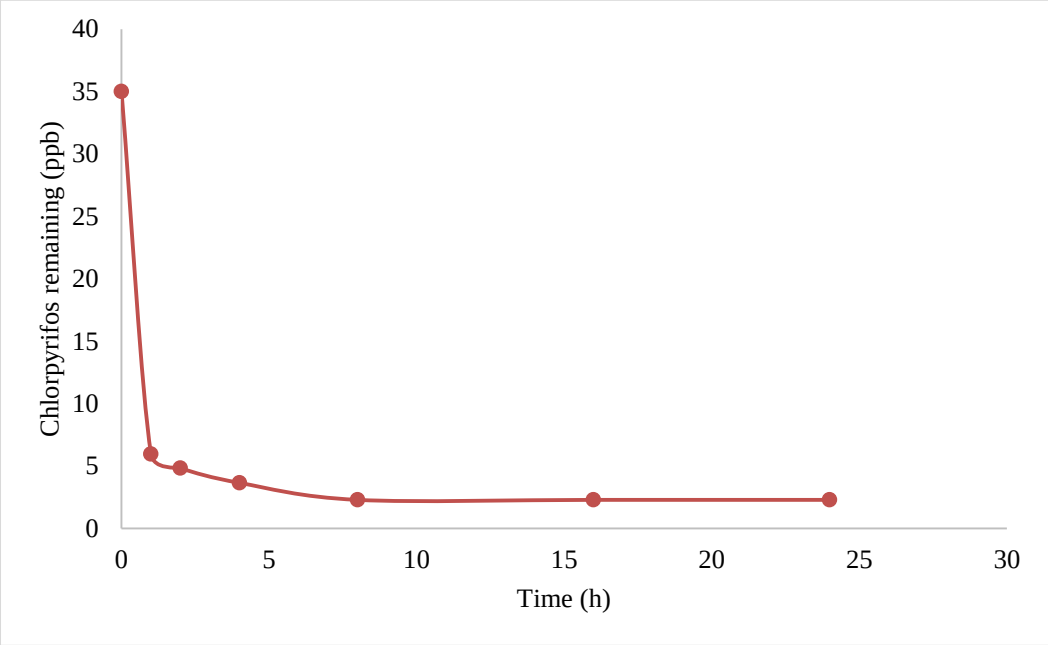

Figure-5: Adsorption kinetics of chlorpyrifos adsorption on soil sample II.

It has been reported that the rate of adsorption of pesticides was insignificant after the short initial phase of rapid sorption. It could be due to limited soil surface for adsorption of the pesticide on to the soil particles. It is known that pesticides are often adsorbed to clay or organic matter constituents of soil at sites that are largely negatively charged[14-16]. Adsorption of chlorpyrifos in sample I and sample II after 8 hours of shaking was found to be 93.47 % and 92.32% respectively. In the present study, a rapid adsorption of chlorpyrifos was observed within 1 hour after onset of kinetic study. Thereafter the rate of adsorption was found to decrease gradually and attained an equilibrium within 8hours. The amount of chlorpyrifos adsorbed on the soil surface after 24 hours of shaking was found also 93.47 % and 92.32 % of the initial solution concentration.

Correlation study: A comparison between adsorption kinetics of these two soils revealed that the adsorption phenomenon in soil depends on physiochemical properties of the soil. It was observed that adsorption of chlorpyrifos on the soil has a positive correlation with moisture, water holding capacity, clay content, pH, organic carbon, organic matter, hardness, chloride, phosphate and nitrate. That means higher the content of moisture, clay, organic matter in the soil higher will be the adsorption of chlorpyrifos. Similarly, abundance of negative ions like chloride, phosphate and nitrate also found to positively influenced adsorption of chlorpyrifos. Correlation between adsorption of chlorpyrifos and soil physiochemical properties are shown in Table-6.

Table-6: Correlation between adsorption of chlorpyrifos and soil physiochemical properties.

	Moisture content (%)	Water holding capacity (%)	Clay content	pH	Organic Matter (%)	Hardness (mg/100g)	Chloride (mg/100g)	Phosphate (mg/100g)	Nitrate (mg/100g)	% Adsorbed
Moisture content (%)	1									
Water holding capacity (%)	-1	1								
Clay content	1	-1	1							
pH	-1	1	-1	1						
Organic Matter (%)	1	-1	1	-1	1					
Hardness (mg/100g)	1	-1	1	-1	1	1				
Chloride (mg/100g)	1	-1	1	-1	1	1	1			
Phosphate (mg/100g)	1	-1	1	-1	1	1	1	1		
Nitrate (mg/100g)	1	-1	1	-1	1	1	1	1	1	
% Adsorbed	1	-1	1	-1	1	1	1	1	1	1

Conclusion

The present work deals with the adsorption kinetics of chlorpyrifos and its correlation study with various physiochemical properties of the soil. From this study it can be concluded that the adsorption kinetics of chlorpyrifos in soil depends upon physiochemical properties of soil. Greater adsorption of chlorpyrifos has been found in soil sample I than sample II as sample I is richer in organic matter and clay content than sample II. The higher adsorption of chlorpyrifos in sample I suggests that adsorption of pesticide molecule in soil increases with increasing clay and organic matter content.

Acknowledgement

Financial support received from DST – INSPIRE programme is gratefully acknowledged. We are thankful to University of Kalyani for providing infrastructural facilities.

References

1. J. M. Philip, U. K. Aravind, C. T. Aravindakumar,Chemosphere 190 (2018) 307-326.

2. M.S.Rehman, N. Rashid, M.Ashfaq, A.Saif, N. Ahmad, J.I. Han, Chemosphere 138 (2015) 1045-1055.

3. C.Robyn, G. K.Huffling, B. Sattler, Journal of Obstetric Gynecologic Neonatal Nursing,39 (1)(2010) 103- 10.

4. M. Tankiewicz, J. Fenik, M.Biziuk,Trends in Analytical Chemistry 29 (9) (2010)1050-1063.

5. D. V.Cepoa, M.Pelajicb, I. V.Vrcekc, A. Krivohlavekd, I.Zuntara,M.Karoglane, Food Chemistry 246 (2018) 394- 403.

6. T.J.Van Emmerik, M.J. Angove, B.B.Johnson& J.D. Wells,Journal of Agricultural Food Chemistry 55 (2007) 7527-7533.

7. S.P. Kale, F.P.Carvalho, K. Raghu, P.D.Sherkhane, G.G.Pandit, A. M. Rao, P.K. Mukherjee & N.B.K. Murthy, Chemosphere 39(6) (1999) 969-976.

8. S. Khalid, I. Hashmi, S. J. Khan, Journal of Environmental Management 168 (2016) 1-9.

9. Y. Liu, Z. Xu, X. Wu, W. Gui, G. Zhu, Journal of Hazardous Materials178 (1–3) (2010) 462-468

10. P. Singh, C.R. Suri, and S. S.Cameotra,Biochemical and Biophysical Research Communications 317 (2004) 697–702.

11. S. Siripattanakul, W. Wirojanagud, J. McEvoy, T. Limpiyakorn, E. Khan,Journal of Applied Microbiology 106 (2009) 986-992.

12. C. Flores, V. Morgante, M. Gonzalez, R. Navia, M. Seeger, Chemosphere 74 (2009) 1544-1549.

13. C. Wu, S. Zhang, G. Nie, Z. Zhang, J. Wang, Journal of Environmental Science (China) 23 (2011) 1524-1532.

14. S.Y.Gebremariam, M.W. Beutel, D.R. Yonge, M. Flury, J.B. Harsh, Springer 215(2012) 123 - 175.DOI: 10.1007/978-1-4614-1463-6_3.

15. Y. Zhao, L. A. Wendling, C. Wang, Y. Pei, Journal of Soils Sediments 17 (2017) 889-900.

16. L.F. Alfonso, G. V. German, P. C. M. del Carmen, G. Hossein, Chemosphere 166 (2017) 292-299.

The Use of Ionizing Radiation in Crop Improvement and its Application in the Field of Agriculture

M. Roy
Directorate of Distance Education, Vidyasagar University, Midnapur-721102, West Bengal, India
misharoy.india@gmail.com

Abstract

A large number of studies have been conducted on the applications of ionizing radiation for the betterment of crop improvement in agriculture. The aim is to provide the agricultural system with a better tool for crop improvement by utilizing the beneficial aspects of radiation stimulation. The use of ionizing radiation to stimulate the growth, germination, survival rates, increased yields, production of desirable mutant varieties and post-harvest storage is considered a safe, well proven process that has found many applications. Depending on the absorbed dose, various effects can be achieved resulting in increased production rates, development of mutant varieties or reducing the loss of post-harvest storage. In this paper we summarize the various application of ionizing radiation treatment on crops for the betterment of agriculture.

Keywords: Ionizing radiation, radiation, stimulation, agriculture, exposure, dose.

Introduction

The ionizing radiation has several impacts on plants, ranging from low dose stimulation to harmful consequences at higher doses. Several works has been done on the effects of ionizing radiation by utilizing different kinds of ionizing radiations. There are a large number of reports in early literature working on the ionizing radiation effects on plants (Gunckel and Sparrow, 1954; Sparrow and Gunckel, 1956a; Gunckel, 1957; Rudolp, 1971). The reports suggest that the low doses have stimulatory effects on plant growth (Sax, 1963). In some cases it has been manifested in early germination, earlier flowering, increased yield or rapid growth (Mei *et al*., 1994). Since then several works has been conducted on the different radiation exposure effects on diverse plants species (Killon and Constantin, 1974; Chauhan and Singh, 1980; Charbaji and Nabulshi, 1999; Chicea and Racuciu, 2007, 2008; Borzouei *et al*., 2010, Roy, 2015; 2016).

The biological effect of ionizing radiation is ionization, which is the generation of ions. These ions can modify DNA, RNA and protein molecules by breaking of covalent bonds. They interact with atoms and molecules in cells to produce free radicals. These free radicals can react with almost all structural and functional organic molecules such as proteins, lipids and nucleic acids. They cause peroxidation of unsaturated fatty acids producing peroxyl and alkoxyl radicals, resulting in metabolic disturbances. These free radicals generated can either damage or modify the cellular compartments in plants and hence induces certain changes in plants. Damage may be caused to the genetic material and can induce chromosomal abnormalities or mutations. Antioxidants, peroxides and super oxides are generally involved in the compensatory mechanism against radiation stress. These changes includes modifications in hormone balance, protein synthesis, enzyme activities, water exchange and active transport, respiration and photosynthesis rate, antioxidant systems (Xiucher, 1994; Stoeva and Bineva, 2001). The diversity in the behavior of these dose response effects can be explained on the basis of different genetical damages and their repairing mechanisms.

Application of radiation has revolutionized the area of research in agriculture and food science. Ionizing radiation is used in modern agricultural practices as a tool to obtain better traits in plants. They have several usages in agriculture. They cause genetic variability that provides plant breeders with new genotypes having improved characteristics, such as increased yield, better quality, higher survival rates, salinity tolerance and disease resistance. The yield of several food crops have been reported to be increased through the radiation treatment. Several desirable traits are obtained in plants through the radiation treatment as physical mutagens. In addition they are also used to increase the period of post harvest storage by delayed germination or by pest eradication. Ionizing radiation is also found to decrease antinutritive substances such as phytic acid (Hania and El-Niely, 2007, Toledo *et al*., 2007; Roy, 2016) and hence enhance digestibility.

The present work summarizes the different applications of ionizing radiation for crop improvement in agriculture.

Different Applications of ionizing radiation in crop improvement

Effects on germination and growth parameters: When the biological materials are exposed to ionizing radiation, it either acts directly on cell or indirectly by generating certain metabolites which then modifies the cell components. Ionizing radiation increases the enzymatic activation and hence affects plant growth. The stimulatory effects of ionizing radiation on germination is reported to be due activation of RNA or protein synthesis (Kuzin *et.al*.., 1975; 1976) or may be due to the elimination of germinating microbial

population (Gruner *et.al..*, 1992). The low dose stimulatory effects are the results of changes in biochemical, physiological and hormonal properties (Rabie *et al*., 1996). These are manifested by accelerated cell proliferation, stimulated germination, higher survival rates, increased yields, earlier flowering, disease resistant and better adapted to different stress (Koepp and Kramer, 1981; Conter et al., 1986; Abo-Hegazi *et.al..*, 1988, Taguchi *et al*,. 1994; Kim *et al*., 1998; Chakravarty and Sen, 2001; Roy, 2015a; Roy 2015b).

The studies were conducted on germination rate and plant growth parameters to determine a suitable dose range which could be advantageous to plants in terms of increased growth, faster germination, higher survival rates, increased yields and other associated growth parameters. In almost all the studies it was found that the higher doses are inhibitory while lower ones were reported to be stimulatory for both angiosperms and gymnosperms (Saric *et al*.,1961; Taylor, 1968; Chauhan, 1978; Chauhan and Singh, 1980; Raghava and Raghava, 1989; Akhaury and Singh, 1993; Bhattacharya *et.al.*, 2010; 2012). Ionizing radiation has also been found to be useful for the effective post harvest storage (Curzio and Croci, 1988; Stewart, 2001). The irradiation treatments are based on delayed sprouting, inhibition of germination or root shoot growth (Kawamura *et al*., 1992a, b; Qiongying et al., 1993; Zhu *et al*., 1993).

Reduction of microbial contamination and effect on nutrient properties: Plant materials usually carry a great number of microbes, which makes them inadequate for use and affects the post harvest storage of food grains. Every year tones of food grains are lost in pathogenic infestations of pests. The chemical methods applied are prone to environmental problems and the toxic effect of chemical treatment affects the food quality. Food irradiation is usually recognized as an effective method for decontaminating microbes, since it can be easily and effectively applied to materials where other methods like exposure to high temperature cannot be applied. Use of ionizing irradiation especially gamma rays to control microbial growth in food crops has long been used. Several studies are conducted to find out the change in the nutritional properties, if any in these irradiated crops. The low dose irradiated crops are generally found to be in similar biochemical contents as the non irradiated ones. However higher dose of gamma irradiation is known to affect the protein by causing conformational changes, or rupturing of covalent bonds (Lee *et al*., 2005). Small loses in amino acid composition is sometimes found due to the formation of peptide bonds. Amino acid profile are affected based on its structure, sulphur containing and aromatic amino acids are most sensitive to radiation (Elias and Cohen, 1997; Matloubi et al, 2004; Wang and von Sonntage, 1991). Gamma rays causes breakage or cleavage of amylopectic chains resulting in decrease in amylase content (Wu, 1986).

In a study conducted by Bagi *et al.* (1988) on pea seedling the height was found shorter, while simultaneously the peroxidase activity was found higher in irradiated plants (15 to 300Gy) compared to control. Similar results are also obtained for glutathione peroxidase activity in corns and triacylglycerol content in nutmeg(Niyas *et al*., 2003). In another work upto 100 Gy irradiation of gamma rays was found to have no affect on linoleic, palmitic, oleic, linolenic and fatty acid contents of garlic bulb (Kwon et al., 1988).

However overall ionizing radiation is also found very useful in sterilization and food preservation without affecting the nutritional properties up to an exposure of 10 kGy (Who, 1994).

Water Stress Management: The plants are exposed to several situations of environmental stresses such as drought, flood, soil salinity *etc*. these induces significant alterations in plant physiology, morphology and biochemistry. The most common symptom of these stress injury is the growth inhibition and reduced yield. Stress either in the form of drought or salinity causes water deficit either by unavailability of water or by restricting the use. It induces generation of reactive oxygen species, causing lipid peroxidation, protein degradation, enzyme inactivation, membrane injury and DNA disruption (Becana *et.al.*, 1998). Water deficit is found to found to inhibit photosynthesis by causing harm to photosynthetic apparatus (Costa *et.al.*, 1997). Water scarcity results stomatal closure and hence reduces carbon dioxide availability. It modifies the enzyme activities, sugar and protein accumulation in plant (Gong *et.al.*, 2005).

Ionizing radiations especially gamma rays have been proven crucial and economical to overcome the water stress response in plants. Low doses of gamma rays induce growth stimulation by increasing the antioxidative capacity of cells to overcome stress factors (Kim *et. al*, 2004). The gamma irradiated plants showed increase in photosynthesis due to improvement of leaf water balance. The accumulation of soluble sugars and free amino acids protects the cell inner condition of water stress by balancing the osmotic potential of cytosol with vacuole (Kerepeu and Galibal, 2000). The gamma irradiation promoted the accumulation of this osmoprotectants such as soluble sugars, protein and proline content and decreases the accumulation of MDA.

An increase in chlorophyll a, b and total chlorophyll content was observed in *Paulowinia tomentosa* plants after gamma irradiation (Abu *et.al.*, 2005). Similar reports were found by Khodary and Moussa, 2003 in dry seeds of Lupin. Positive results were obtained in increasing salinity tolerance in sunflower, banana and rice after treating with gamma rays (Omar *et al*., 1993) Bretaudeau and Traore (1990) found that the stimulation by 200-300 Gy stimulates environmental stress tolerance.

Induction of mutation: In general mutation is defined as a sudden heritable change in the genetic material at the gene or chromosome level and a mutagen is a physical or chemical agent that results in mutation. The natural process of mutation is very slow, laborious and positive results are very scanty. Chemical mutagens are alkylating gents and azides and physical mutagens include electromagnetic radiations (γ, x, uv light) and particle radiation (α, β). Physical mutagens have been successfully used in plant breeding programs to generate desired traits. Radiation stimulation is used as a tool to increase genetic variability and to induce mutations including earlier germination, higher yield, early flowering, higher quality and better resistant to stress and diseases. Radiation treatment increases the mutation rate and specifies the desirable positive aspects. Many cultivars have been induced and officially released in the FAO/IAEAMVD.

Several new mutant varieties are reported by radiation treatment (Mackey, 1954; Nayeem, 1999; Reddy and Viswanathan, 1999; Rehman *et al*., 1987; Javed *et al*., 2000). Gustaffson *et al*. (1971) has developed a mutant barley variety having beneficial characters such as high yielding, early maturity and higher protein content. Eight different mutant varieties have been developed from a single landrace of wheat "SHARBATI" by recurrent irradiation.

Seedless is an important and desirable characteristic of fruit. Mutation induction with gamma rays has been efficient in producing the seedless varieties in several species of citrus. Several new mutant varieties were developed through gamma irradiation treatment in citrus fruits (Wu, 1986; Spiegel–Roy and Padova, 1973; Kukimura, 1976; Spiegel–Roy, 1985). Budwood irradiation in many citrus fruits has lead to production of new varieties (Bermejo *et al*., 2011). Five nearly seedless varieties were developed from 50 Gy gamma irradiated budwood (Micke, 1985). Citrus lemon when irradiated with 50-60 Gy of gamma rays produced a completely new seedless variety (Hearn, 1985).

Conclusion

Various desirable traits are obtained through ionizing radiation treatment and hence are quite efficient for crop improvement. Gamma radiation due to its high penetrating property and RBE is mostly preferred during seed irradiation treatment. This being a cheap, rapid and less laborious method has been successfully applied and achieved success in agricultural improvements. There application must be encouraged in future and further investigations need to be carried out to obtain other improved and desired traits in diverse plants varieties. However considering the overall studies and results it can be assumed that in general the low dose have been reported to be stimulant and higher dose is found to be inhibitory in effect. A low dose irradiation application has been successful in generating useful results without having lethal effects on plants. So it can be recommended that reasonably achievable low dose should be preferred while using ionizing radiation as a tool for obtaining positive response in crops.

References

1. Abo-Hegazi, A. M. T., Ragab, A. I., Moustafa, A. K., 1988. Heritability and Genetic Variabilityfor Some Characters of Sunflower in M3 andM4 Generation after Irradiation. Minufia J Agric.Res. 13,3–15.
2. Abu, J. O., Muller, K., Duodu, K. G., Minnar, A. 2005. Gamma irradiation of cowpea (*Vigna unguiculata* L. Walp) flours and pastes. Food Chem. 95, 138-147
3. Akhaury, K. D. N., Singh, A. K., 1993. Effect of gamma-rays on the seed output of *Viciaspecies.* Neo Botanica. 1, 63-67
4. Bagi, G. P., Bornemisza-Pauspertl, Hidvegi, E. J., 1988 Inverse correlation between growth and degrading enzyme activity of seedlings after gamma and neutron irradiation of pea seeds. Int J Radiat Stud Phys Chem Med. 53, 507-519
5. Becana, M., Moran, J. F., Iturbe-Ormaetxe, I.,1998. Iron dependent oxygen free radical generationin plants subjected to environmental stresses: toxicityand antioxidants. Plant Soil.201,137–147.
6. Bermejo, A., Pardo, J., Cano, A., 2011. Influence of Gamma Irradiation on Seedless Citrus Production: Pollen Germination and Fruit Quality.Food and Nutrition Sciences. 2, 169-180.
7. Bhattacharya, R, Roy, M, Mukherjee, C.2012. Effect of Low Dose Beta Radiation on the Characteristics of Kidney bean (Phaseolus vulgaris) by Proc. International Conference on Engineering Education in the new Century, February 3-4, 135-137.
8. Bhattacharya, R, Barman, P, Roy, M. 2010. Influence of Ionizing and Non ionizing Radiation on Seedling.
9. Borzouei, A., Kafi, M., Khazaei, H., Naseriyan, B., Majdabadi, A., 2010. Effects of gamma radiation on germination and physiological aspects of wheat (*Triticum aestivum* L.) seedlings. Pak J Bot. 42, 2281-2290
10. Bretaudeau, A., Traore, B. M., 1990. Use of mutations breeding in west African Sorghum (Sorghum bicolor L. Moench) improvement. In: International Symposium on the contribution of plant mutation breeding crop improvement, 1990, Vienna. Symposium Viena: IAEA-SM, 1,463-467

11. Chakravarty, B., Sen, S., 2001. Enhancement of regeneration potential and variability by γ-irradiation in cultured cells of *Scilla indica.* Biol Plant. 44,189-193.

12. Charbaji, T., Nabulsi, I., 1999. Effect of low doses of gamma irradiation on *in vitro* growth of grape vine. Plant cell Tiss Org cult. 57, 129-132

13. Chauhan, Y. S., 1978. Gamma rays- induced variation in the development of *S. khasianum* Clarke JIndian Bot Soc.57, 347-352

14. Chauhan, Y. S., Singh, R. P., 1980. Effect of chronic gamma rays on *Chenopodium album* L. J Indian Bot Soc.59, 170-172

15. Chicea, D., Racuciu, M., 2007. On the effects of low doses (0-1.2 Gy) beta radiation Zea *mays* seeds on 12 day plantlets. Rom Journ Phys. 52, 633-640

16. Chicea, D., Racuciu, M., 2008. Results of Zea *mays* seeds β – irradiation in 0–5 Gy range. Rom Journ Phys. 53, 71-176

17. Conter, A., Dupouy, D., Delteil, C., Planel, H., 1986. Influence of very low doses of ionizing radiation on *Synechococcus* lividus metabolism during the initial growth phase. Arch Microbio. 1144, 286-290

18. Costa, L. D., Delle, G., Vedove, G., Gianquinto, R., Giovanardi, A. Peressotti.,1997. Yield, water useefficiency and nitrogen uptake in potato: Influence of drought stress. Potato Res. 40,19–34.

19. Curzio, O. A., Croci, C. A., 1988. Radioinhibition process in Argentinean garlic and onion bulbs. Radiat Phys Chem. 31, 203-206

20. Elias, P., Cohen, A., 1997. Radiation Chemistry of Major Food Components. Elsevier Scientific, Amsterdam, Netherlands. 159-163.

21. Gong, H., Zhu, X., Chen, K., Wang S., Zhang, C.,2005. Silicon alleviates oxidative damage of wheatplants in pots under drought. Plant Sci.169**,** 313–321.

22. Gruner, M.M., Horvatic, D., Kujundzic, Magdalenic, B., 1992. Effect of gamma irradiation on the lipid components of soy protein products. Nahrung. 36, 443-450

23. Gunckel, J. E., 1957. The effect of ionizing radiation: Biochemical, Physiological and Morphological aspects of their effects on plants. In: Encycl. Plant Physiol (ed) W Ruthland XVI: 555-611 Springer- verlag berlin

24. Gunckel, J. E., Sparrow, A. H., 1954 Aberrant growth in plants induced by ionizing radiation. In Abnormal and pathological plant growth Ab Brookhaven Symp Biol. 6, 252-279

25. Gustafsson, A., Hagberg, A., Persson, G., Wikland, K., 1971. Induced mutation and barley improvement. Theo Appl Gene. 41, 239-248

26. Hania, F.G, El-Niely., 2007 Effect of radiation processing on antinutrients, in-vitro protein digestibility and protein efficiency ratio bioassay of legume seeds. Radiat Phys Chem. 76, 1050-1057

27. Hearn, C.J., 1985. Development of seedless grapefruit cultivars through budwood irradiation. Hortscience, 20, 84.

28. Javed, M. A., Khatri, A., Khan, I. A., Ahmad, M., Siddiqui, M. A., Arain, A. G., 2000. Utilization of gamma irradiation for the genetics improvement of oriental mustard (*Brassica juncea* Coss.). Pak J Bot. 32, 77- 83

29. Kawamura, Y., Suzuki, N., Uchiyama, S., Satio, Y., 1992 a. Germination test for identification of gamma irradiated rice. Radiat Phys Chem. 39, 203-207

30. Kawamura, Y., Suzuki, N., Uchiyama, S., Satio, Y., 1992 b. Germination test for identification of gamma irradiated wheat Radiat Phys Chem. 40, 17-22

31. Kerepeu, I., Galibal, G.,2000. Osmotic and salt stress induced alteration in carbohydrate content in wheat seedlings. Crop Sci., 40**,** 482–487.

32. Khodary, S. E. A., Moussa, H. R.,2003. Influence of Gamma Radiation and/or Salinity Stress on Some Physiological Characteristics of Lupine Plants. Egyptian J. Biotechnology.13,29–36.

33. Killion, D. D., Constantin, M. J., 1974.Effects of separate and combined beta and gamma irradiation on the soybean plant.Radiat Bot.14, 91-99

34. Kim, J. H., Beak, M. H., Chung, B. Y., Wi, S. G., Kim, J. S., 2004. Alterations in the photosynthetic pigment and antioxidant machineries of red pepper (*Capsicum annuum* L.) seedlings from gamma irradiated seeds. J Plant Biol. 47, 314-321

35. Kim, J. S., Kim, J. K., Lee, Y. K., Baek, M. W., Kim, J. G., 1998. Effects of low dose gamma radiation on the germination and yield components of Chinese cabbage. Kor J Environ Agr. 17, 274-278

36. Koepp, R., Kramer, M., 1981. Photosynthetic activity and distribution of photoassimilated ^{14}C in seedlings of *Zeamays* grown from gamma-irradiated seeds. Photosynthetica. 15, 484-489

37. Kon, E., Ahmed, O. H., Saamin, S., Majib, N. M. A., 2007. Gamma radiosensitivity study on long bean (*Vigna sesquipedalis*). Am J Applied Sci. 4, 1090-1093

38. Konzak, C. F., 1955. Radiation sensitivity of dormant and germinating barley seeds. Science 122, 197

39. Kukimura, H.F., 1976. Brief description of mutation in vegetatively propagated and tree crops. Gamma Field Symp. 15, 79-82

40. Kuzin, A. M., Vagabova, M. E., Prinak-Mirolyubov, V. N., 1975. Molecular mechanisms of the stimulating effect of ionizing radiation on seed Activation of RNA Synthesis. Radiobiologiia. 15,747-750

41. Kuzin, A. M., Vagobova, M. E., Revin, A. F.,1976. Molecular mechanisms of the stimulating action of ionizing radiation on seeds 2. Activation of protein and high molecular RNA synthesis. Radiobiologiia. 16, 259-261

42. Kwon, J.H., Yoon, H.S., Byun, M.W., Cho, H.O., 1988. Chemical changes in garlic bulbs resulting from ionizing energy treatment at sprout-inhibition dose. J. Kor. Agric. Chem. Soc. 31, 147–153.

43. Lee, S., Lee, M., Song, K., 2005. Effect of gamma-irradiation on the physicochemical properties of gluten films. Food Chem. 92, 621–925.

44. Mackey, J., 1954. Neutron and x rays experiments in wheat and reversion of speltoid problem. Hereditas. 40, 65-180

45. Matloubi, H., Aflaki, F., Hadjiesadegan, M., 2004. Effect of gamma irradiation on amino acids content of baby food proteins. J Food Compos Anal., 17, 133–139.

46. Micke, A., 1985. Plant cultivars derived from mutation induction or the use of induced mutants in crop breeding. Mutation Breeding Rev., 3, 1-92.

47. Mie, M., Deng, H., Lu, Y., Zhuang, C., Liu, Z., Qiu, Q., Qui, Y., Yang, T. C., 1994. Mutagenic effects of heavy ion radiation in plants. Adv Space Res. 14, 363-372

48. Nayeem, K. A., Devkule, S. N., Bhagwat, S. G., 1999. Seed protein variations in radiation induced mutants of wheat. Indian J Genet. 59, 363-369

49. Niyas, Z., Variyar, P. S., Gholap, A. S., Sharma, A., 2003. Effect of gamma irradiation on the lipid profile of nutmeg (*Myristica fragrans* Houtt.). J Agric Food Chem. 22, 6502-6504

50. Oiongying, L., Yanhua, K., Yuemei, Z., 1993. Studies on the method of identification of irradiated food I. Seedling growth test. Radiat Phys Chem., 42,387-389

51. Omar, M. S., Yousif, D. P., Al-Jibouri, A. J. M., Al Rawi, M. S., Hameed, M. K., 1993. Effects of gamma rays and sodium chloride on growth and cellular constituents of sun flower (*Helianthus annuus* L.) callus cultures. Journal of Islamic Academy of Sciences. 6, 69-72Proc. National Seminar on Biodiversity, Water resource and Climate change issues, Kalyani University, 10th March, pp.132-137, 2010.

52. Rabie, K., Shenata, S., Bondok, M., 1996. Analysis of Agric. Science cario 41 Univ Egypt pp. 551-566

53. Raghava,R. P., Raghava, N., 1989. Effect of gamma irradiation on fresh and dry weight of plant parts. Physallis L Geobios. 16, 261-264

54. Reddy, V. R. K., Viswanathan, P., 1999. Induced rust resistant mutants in hexaploid wheat "WH-147".Crop Res. 18, 443-445

55. Rehman, A., Das, M. L., Howlidar, M. A. R., Mansur, M. A., 1987. Promising mutants in *Brassica campestris*. Mut Breed Newsletter. 29, 14-15

56. Roy, M, 2015a. Beta Radiation Effects on The Biochemical and Morphological Properties of Phaseolus vulgaris, International Journal of Multidisciplinary Approach and Studies, 02, (6) 17-24

57. Roy, M, 2015b. Beta Radiation Effects on the Growth Parameters of Phaseolus Vulgaris L. International Journal of Science, Environment and Technology, 4, 1558 – 1565.

58. Roy, M, 2016. A Review on the Stimulatory Effects of Ionizing Radiation Exposure Effects on Plants by Acta Velit, 3,(2) 56-73, 2016

59. Rudolph, T. D., 1971. Gymnosperm seedling sensitivity to gamma radiation: its relation to seed radiosensitivity and nuclear variables. Radiat Bot. 11, 45-51

60. Saric, M. R., Ceric, I., Hadzey, D., 1961. Effect of gamma radiation of some varieties of wheat seed on the morphological characteristics of the seedlings. In: Proc of the symp on theeffects of ionizing radiations on seeds and theirsignificance for crop improvement pp 103-116

61. Sax, K., 1963. The stimulation of plant growth by ionizing radiation. BNL-6900 technical report Brookhaven National Lab Upton NY

62. Spiegel-Roy, P., Padova, R., 1973. Radiosensitivity of Shamouti orange (*Citrus sinensis*) seeds and buds. Radiation Bot., 13, 105-110.

63. Spiegel-Roy, P., 1985. Seedless induced mutant in highly seeded lemon (*Citrus limon*). Mutation Breeding Newslett. 26, 1-2.

64. Stewart, E. M., 2001. Detection methods for irradiated food In: Molins R (ed.) Food irradiation-Principles and Applications Wiley New-York

65. Stoeva, N., Bineva, Z., 2001. Physiological response of beans (*Phaseolus vulgaris* L.) to gamma radiation contamination I. Growth, photosynthesis rate and contents of plastid pigments. J Env Prot Eco. 2, 299-303

66. Taguchi, Y., Tsutsumi, N., Tatara, A., Eguchi, H., Tano, S., 1994. Effects of low-dose γ-irradiation on the root apical meristem of barley. Environ Mut Res Commun. 16, 205-209

67. Taylor, F. G., 1968. Some effect of acute gamma radiation in giant sequoia seedlings. Radiat Bot.8, 67-70

68. Toledo, T. C. F. D., Canniatti-Brazaca, S. G., Arthur, V., Piedade, S. M. S. 2007. Effects of gamma radiation on total phenolics, trypsin and tannin inhibitors in soybean grains. Radiat Phys Chem. 76, 1653-1656

69. Wang, D., von Sonntage, C., 1991. Radiation industrial oxidation of phenylalanine. Leonardi, M., Raffi, J., Belliardo, J. (Eds.), In: Proceedings of the Workshop on Recent Advances on Detection of Irradiated Foods, BRC Information, Chemical Analysis Commission of the European Communities, Brussels, pp. 212–217 (Report EUR 13331 En).

70. WHO. 1994. Safety and Nutritional Adequacy of Irradiated Food. WHO, Geneva. WHO, 1999. High-dose Irradiation: Wholesomeness of Food Irradiated with Doses above 10 kGy. WHO, Geneva (WHO Technical Report Series no: 890). 120-124

71. Wu, S., 1986. Using Gamma-rays to induce mutations for seedlessness in Citrus. Mutat. Breeding Newslett. 27, 14

72. Xiuzher, L., 1994. Effect of irradiation on protein content of wheat crop. J Nuclear Agricul Sci China., 15, 53-55

73. Zhu, S, Kume, T, Ishigaki, I., 1993. Detection of irradiated wheat by germination. Radiat Phys Chem. 42, 21-427.

Impact of Urban Land Use on Land Surface Temperature: A Study on Lucknow City, Uttar Pradesh

Pankaj Barick[1] and Debasish Das[2*]
[1]Department of Environmental Science, University of Kalyani, Nadia, West Bengal, India
[2]Professor, Department of Environmental Science, University of Kalyani, Nadia, West Bengal, India
pankajbarick225@gmail.com; *ddas_kly@rediffmail.com*

Abstract

Urban land use is mainly dominated by concrete buildings, roads etc. Such urban land cover absorbs more solar energy than other natural land cover. Emission of this energy in form of long wave radiation increases atmospheric temperature, and urban area became warmer than its rural surroundings, forming an Island of temperature over the urban area. This study is objective to understand the effect of urban land use on urban land surface temperature. Lucknow city has been taken as the study area. Landsat 8 OLI/TIRS C1 Level-1 data has been used. Various indices, such as, Normalized difference vegetation index (NDVI), Normalized Difference Built-up Index (NDBI), Urban Land use map, has been created to understand the relation between land cover and land surface temperature (LST) variation over Lucknow city and its surrounding rural areas. Surface temperature and concentration of urban built-up land use have found in a positive relation, where NDVI and NDBI have found in a inverse relation. Increase of greenery is recommended as it can shrink the Urban Heat Island effect.

Keyword(s): Urban heat Island, Land Surface Temperature, Lucknow, NDVI, NDBI.

Introduction

Built up area is the only dominating land use type of an urban area, such as, buildings, road etc. These concretes absorbs more solar radiation than natural land cover and traps in form of heat and radiate latter as long wave radiation of infrared[1,2]. Heat form Sun comes through electromagnetic radiation of different wavelength, such as visible light, ultra-violate, infrared, microwave etc[3]. Only 22.5% of incoming solar radiation can come directly on earth's surface, and mostly in form of visible light, consist of three colour,blue (0.4 μm to 0.5 μm), Green (0.5 μm to 0.6 μm) and Red (0.6 μm to 0.7 μm), according to their wavelength. The kinetic energy of electromagnetic wave transferred into heat energy, and makes the surface warm after absorption by surface, and thereafter it radiate in long electromagnetic wave, compared to the incoming solar radiation. All material, above temperature 273.15 K, radiates the absorbed heat in longer wave length called infrared (0.7 μm to 1.0 μm). This is broadly divided into two types, namely Reflected IR and Thermal IR. Within thermal IR, EMR of 8 μm to 14 μm are use to identify the thermal emissivity of an object. In Landsat imagery, band 10 (10.60 μm to 11.19 μm) and band 11 (11.50 μm to 12.51 μm) are used for thermal radiation [4]. Study on the temperature of an area is helpful to understand the weather of an area [5] such microclimatic variation of urban heat island over urban area. Remote sensing is an advance tool that allows us to such analysis, along with observe the land use pattern of an area, and it also allows us to do various analysis of it[6].

Study area: Lucknow is the largest city of the district Lucknow, as well as the capital and headquarter of Uttarpradesh. Lucknow lays at the central part of Uttarpradesh. The city is situated at the bank of river Gomti, a tributary of the Ganga River. From North-Eastern side, the city is bounded by Barabanki district, Raebareli in South-East, Unnao in South and South-West, and hardor and sitapur in North. Geographically the city lays in between 26° 30' N to 27°10' N, and 80°30' E to 81°13' E. Approx elevation is 123 metres from MSL[7]. Geographical area of the city is near to 310 Sq. Km. Connectivity of the city has a great role on its development, as it situate at the junction of three important National Highway, NH-24, NH-27 and NH-30[7]. Road network has developed in a radial form in all directions of the city[8]. The city Lucknow is also connected through a vast connectivity of railway network. Out of fourteen rail station, Lucknow Junction Railway Station at Charbag is the most important one[7]. The station operates by North-Eastern Railway. The city emerged as an urban agglomeration in1981. According to census 2011 provisional data, population density was 1815 per km^2. According to census 2011, it is the eleventh most populous city and twelfth most Urban Agglomeration of the Country[7]. Total population of Lucknow is 4589838, among which, 66.21% people lives in urban area. Decadal growth of population is also higher in urban areas. Urban growth rate is 30.9%, where the growth rate of rural population is only 16.9% in last decade (2001-2011)[9]. The city has a huge importance as it has high GDP among all Indian cities. According to Assocham, the city ranks sixth among ten fastest growing job creating cities of India[7]. High level of connectivity, job opportunity, historical perspective, all have a significant role in the growth of this Urban Agglomeration.

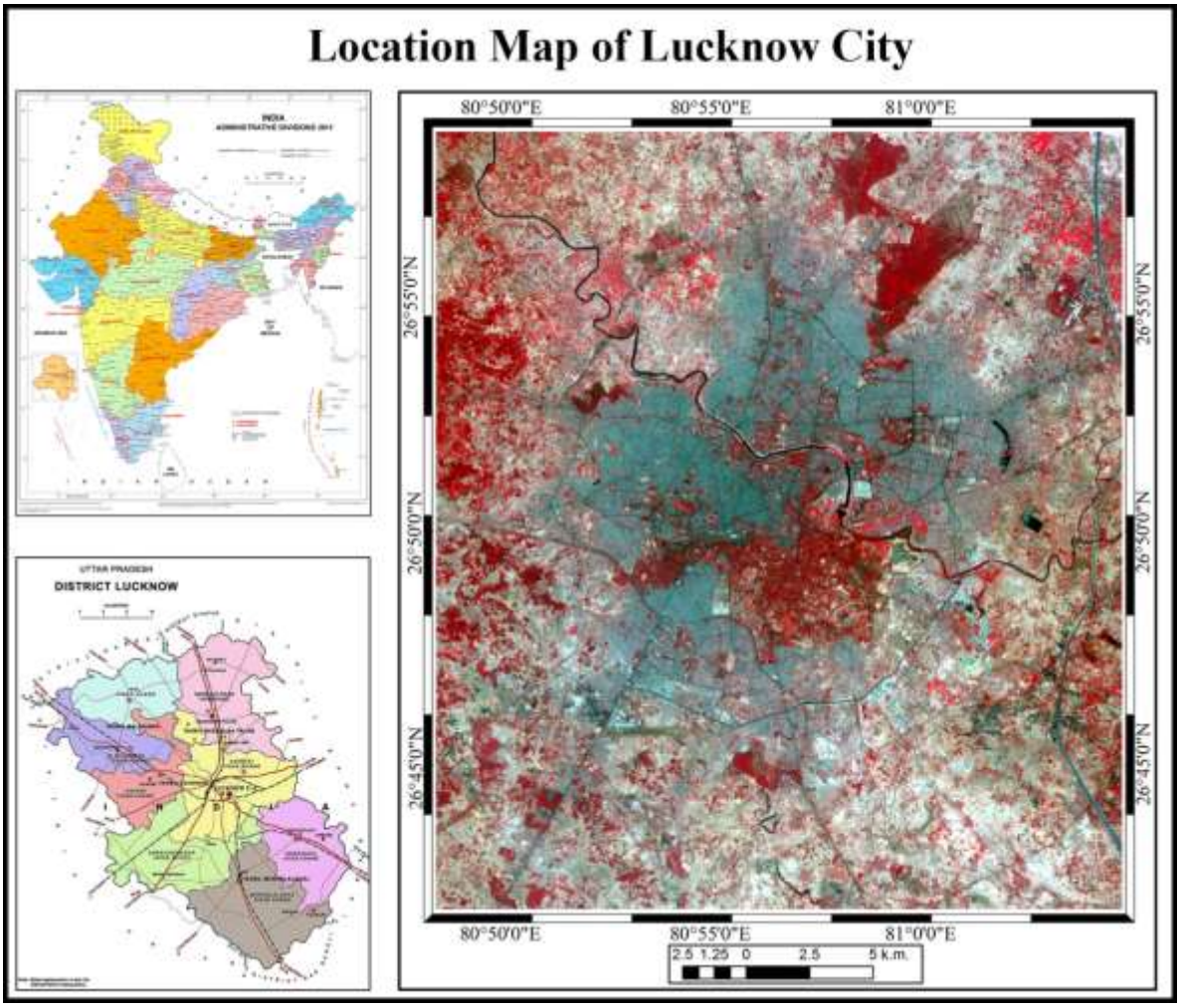

Figure-1: Location of the study area.

Objective: The main objective of the paper is to understand the effect of urban Land Use and vegetation coverage on Land Surface Temperature, in Lucknow city.

Data required: Landsat OLI/TIRS C1 level 1 data of the study area has been downloaded from USGS-Earth explorer. The data acquired on 26th June, 2017. Path no. of the data is 144, row, 41. Total 11 band ware downloaded. Band 2, 3, and 4 are visible bend, blue, green, and red respectively. 5th bend is NIR bend, required to create NDVI. Bend 10 & 11 are the thermal bend, represents the two thermal window, 10.60-11.19 & 11.50-12.51 respectively.

Methodology

According to the objective of the study, Landsat OLI/TIRS C1 level data is the only required data. Various image analysis and indices has been prepared using remote sensing software. False colour composite (FCC) of the study area has been created using band 3, band 4, and band 5 of Landsat OLI/TIRS C1 level 1 data to identify the urban land use. Where, NIR represents Red band, Red band represents Green, and Green represents blue in FCC. Normalized difference vegetation index (NDVI) is computed using Band 4 (Red) and Band 5 (NIR) to identify the condition of vegetation of the city, which is inversely related to urbanisation and Land Surface Temperature (LST) of an area. Normalisation formula has been used to compute NDVI using arc-gis software as follows, NDVI= (Red-NIR) / (Red+NIR). Normalised Difference Built-up Index (NDBI) is derived from Landsat 8 imagery, using NIR (band 5) and SWIR (band 6&7) data to extract the built-up features of the study area. Built-up features have more potential to capture heat from sun light and increases air temperature by radiation. NDBI= (SWIR-NIR) / (SWIR+NIR). A Built-up area extraction map has been prepared. Maximum likelihood classification with a EQUAL priori probability weighting at 0.025 reject function has been computed for extraction of built-up area. In Landsat 8 data, reflected thermal infrared is captured into band 10 (10.60 μm to 11.19 μm) and band 11 (11.50 μm to 12.51 μm). Land surface temperature of the study area has been computed from band 10, 11 and computed NDVI through following steps,

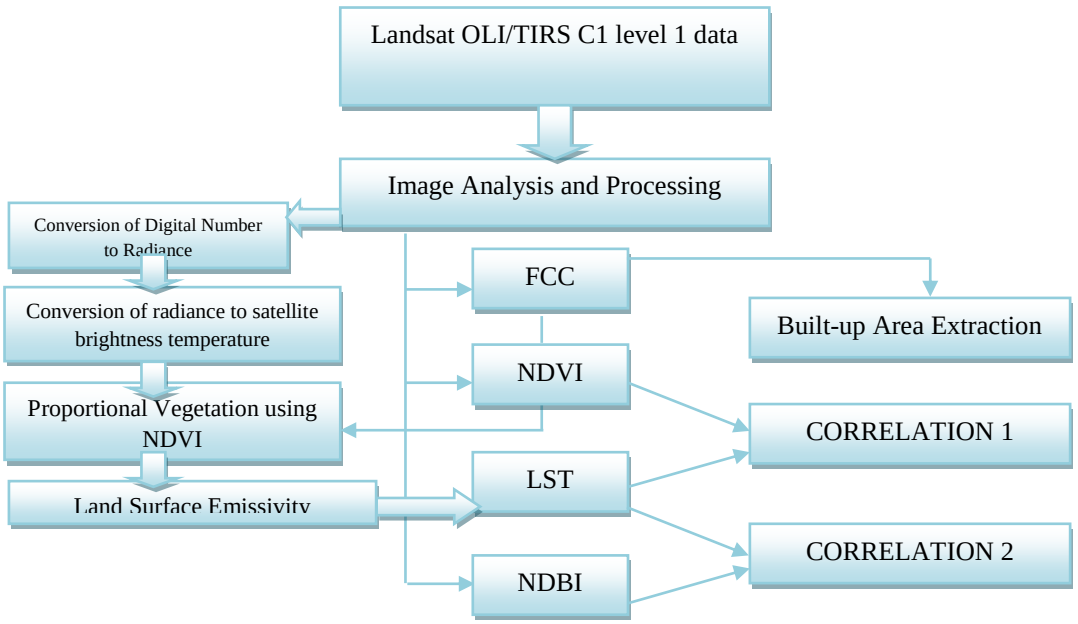

Results and Discussions

Standard False Colour Composite (Figure-2) has been created to identify the urban land cover of the study area. In this image, urban land use of built-up area is showing in bluish-green colour, which is (built-up material) originally recorded in red band of EMR. The central part of the image is under urban land use or consisting of built up area. A water body (River Gomti) is passing through the urban area. Urban density is higher in northern part of the city. Some heritage buildings and sculptures are lies in the central portion of the city, which has a discrete vegetation cover over it.

In Figure-3, built-up area is extracted from the false colour composite (FCC) of the Lucknow city. Built-up area or urban land cover has been extracted using remote sensing tools. Maximum likelihood supervised classification process is used to prepare this map with equal Priori probability weighting at 0.025 reject function. In the image 2, urban built-up area is mainly found in the north-eastern part of the area. 37.75% of the area is under urban built-up area (computed through class-pixel number). Vegetation of an urban area decreases with the increasing urban land use. Thus, there is a strong negative co-relation between urban land use and presence of vegetation and its health. A Normalised Difference Vegetation Index (NDVI) is computed (Figure-4) using Red and NIR band of Landsat 8 data to identify the vegetation health and its coverage. Very low vegetation is observed in urban areas. As the urban land use increases, vegetation coverage and its condition decreases as the results of the urbanisation processes. Thus, NDVI is negatively related with the Land Surface Temperature (LST) of an urban area. To understand the relation between urban land use and its LST, a Normalised Difference Built-up index (NDBI) is computed (Figure-5) from SWIR and NIR. As SWIR is used to compute NDBI, heat reflectance characteristics of built-up area can be identified through it, and a strong positive correlation is observed between them. Reflectance of heat in form of radiation depends on the characteristics of the roof top material that has been used in built-up region. In some situation, there is some other material than concrete which emit more heat radiation than concrete. It results, more heat radiation is observed towards the fringe region of the city. NDBI is also showing very high value at the centre of the city, where lower NDVI is observed. Now it is an area to investigate, that how the urban land use and vegetation is related to Land Surface Temperature (LST) of an urban region. An LST map (Figure-6) has been created using band 10 and 11 of Landsat-8 for the study area. In this LST map, the range of temperature is 27.3021°C to 37.4076°C. Where High LST values are showing in in Red and Lower temperature is projected in Blue colour. Through visualisation it can be identified that there is a strong positive relation Between LST and NDBI of the study area. In the northern part of central urban area, built-up index and LST, both are showing high value, which is absent in the vegetative portion of the city, where both LST and NDBI is observed very low. This positive relation is also found in some other part of the imagery, especially in the fringe region, where rooftop materials of house have more potential to emit heat as SWIR radiation. In the other hand, an inversely proportional relation is observed between LST and NDVI of that same area. A few vegetative patches has been observed in the entire imagery, but the comparatively very low LST values has been observed in place with high NDVI values, which is an indicator of vegetation. Even in the central portion of the imagery, there is vegetative patches consist of urban greenery, observed significant change in LST over it, indicating the inverse relationship between NDVI and LST. To examine the impact of NDVI and NDBI on LST on the study area, correlation between NDVI & LST (Figure: 7), and NDBI & LST (Figure: 8) has been computed to understand the nature of relationship among the variables. The correlation is computed with the break values of the all three indices, classified into 10 classes.

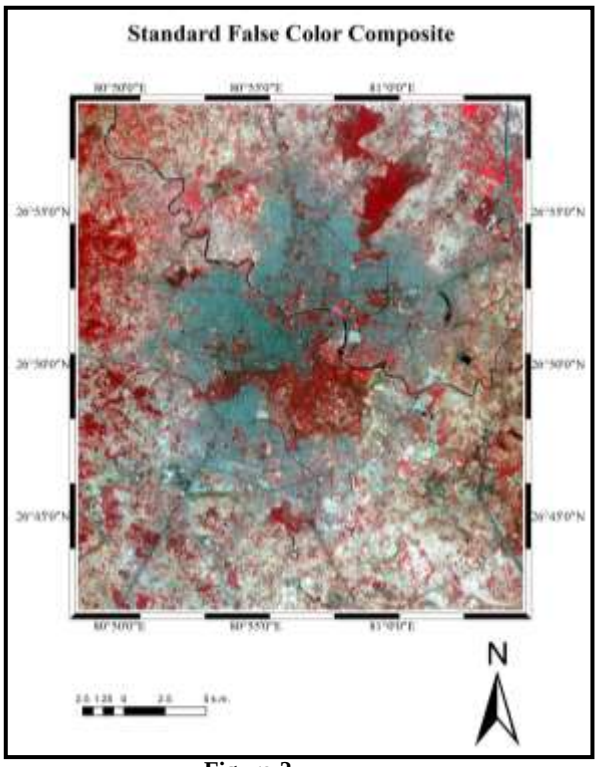

Figure-2

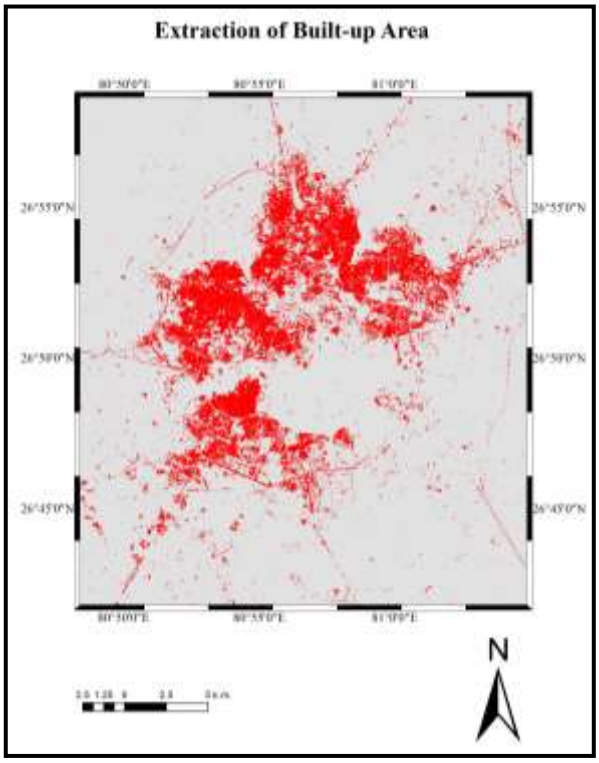

Figure-3

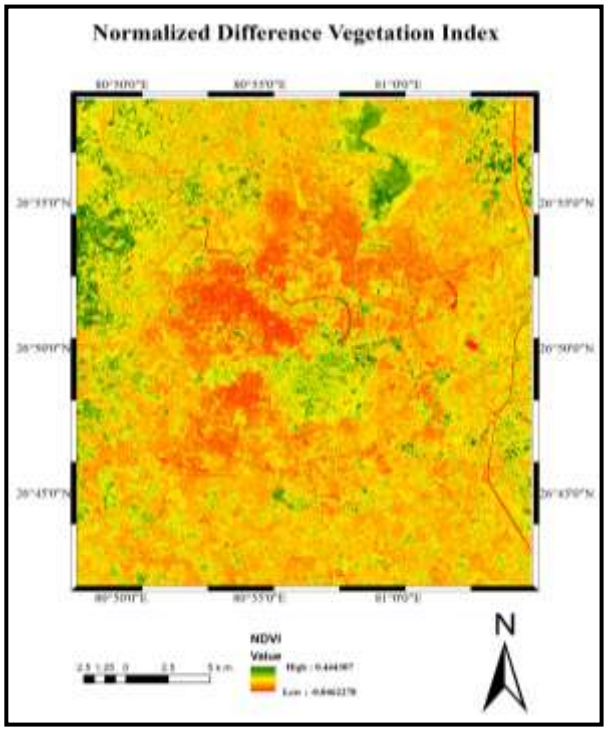

Figure-4

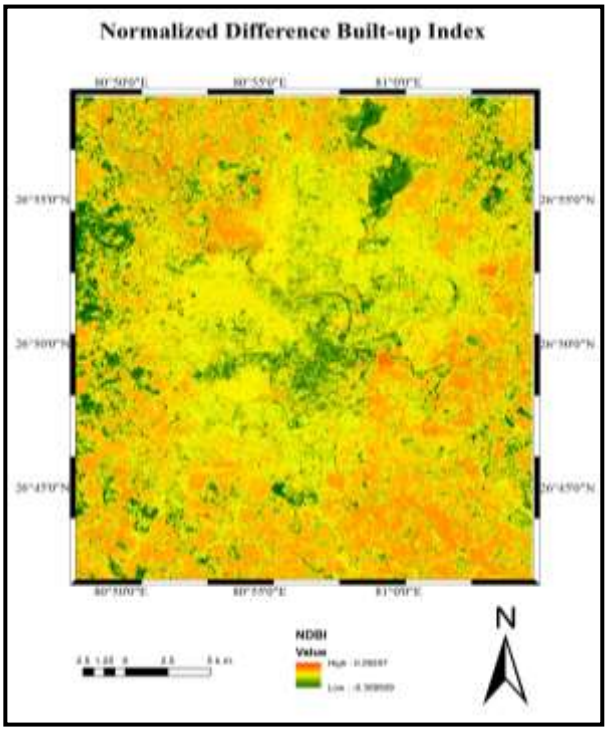

Figure-5

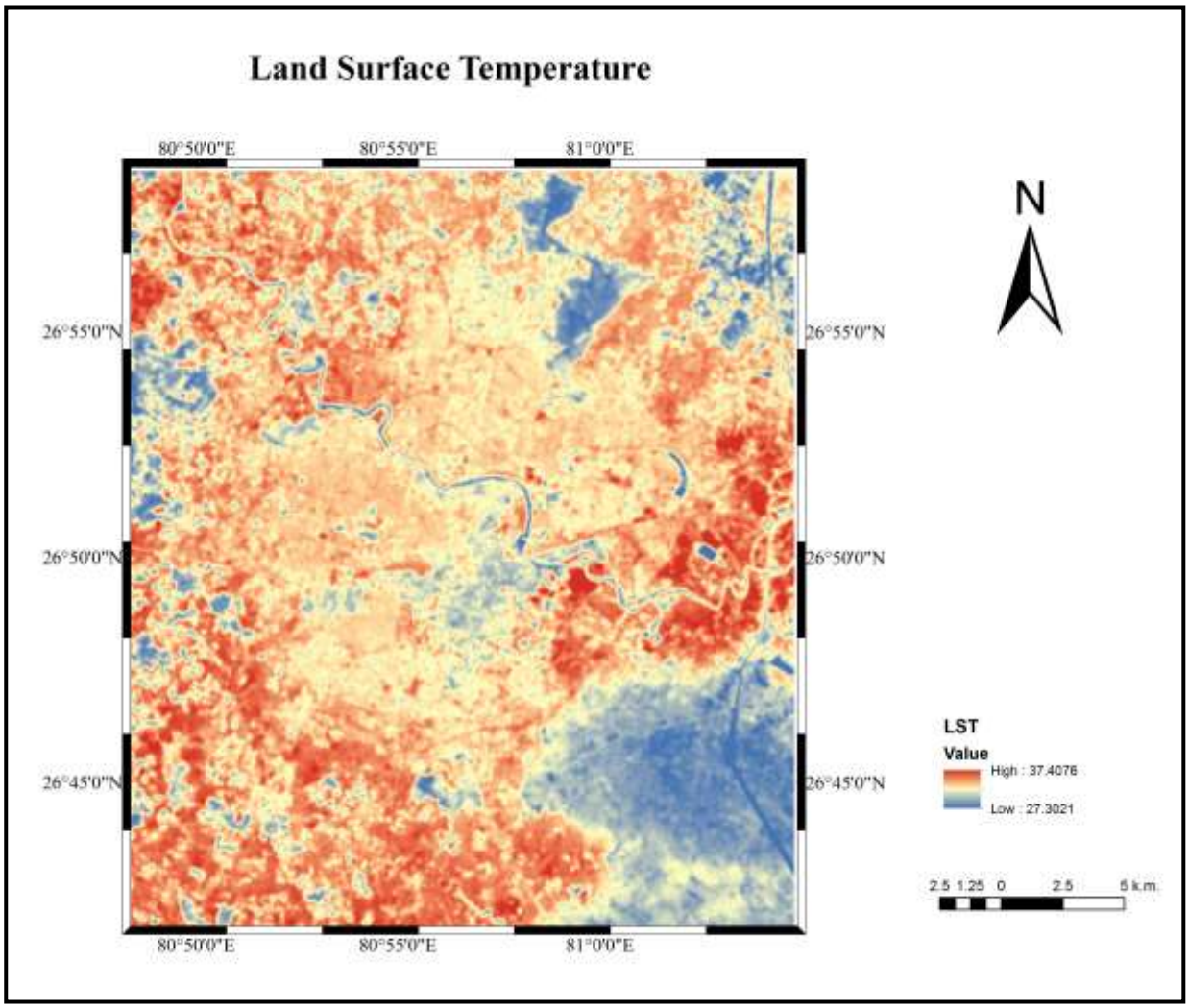

Figure-6

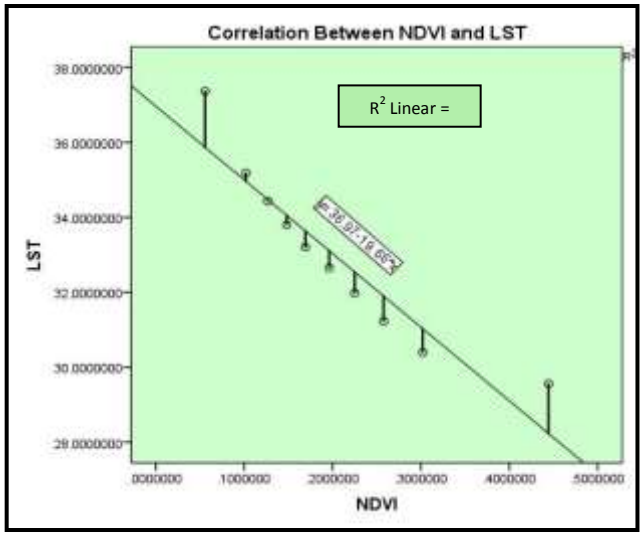

Figure-7

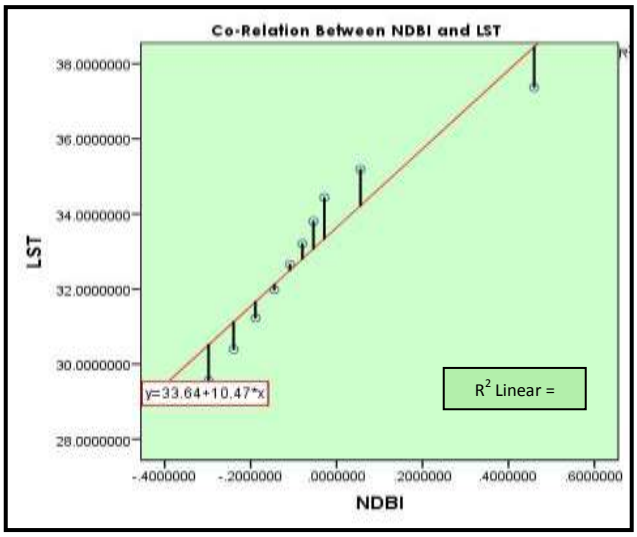

Figure-8

Linear regression is computed using statistical software, where, LST has taken as a dependable variable and NDVI & NDBI as independent variable (Table-1).

Table-1: Variables Entered/Removed[a]

Model	Variables Entered	Variables Removed	Method
1	NDBI[b]	.	Enter
2	NDVI[b]	.	Enter
a. Dependent Variable: LST			
b. All requested variables entered.			

From the model summery, (Table-2), the R square can be obtain, which explain the fitness of the model to the data. R square value for predictor a (NDBI) is 0.885, and for predictor b, which is NDVI, is 0.974. For the both predictors (NDBI & NDVI), a high R square value is observed. This is indicating a high fitness of the model to the data set. Respected Standard Error for predictor a & b is 0.843710564 and 0.4302832458 respectively, is also low.

Table-2: Model Summary.

Model	R	R Square	Adjusted R Square	Std. Error of the Estimate
1	.941[a]	.885	.871	.8437104564
2	.987[b]	.974	.966	.4302832458
a. Predictors: (Constant), NDBI				
b. Predictors: (Constant), NDBI, NDVI				

Table-3: Coefficients[a]

Model		Unstandardized Coefficients		Standardized Coefficients	t	Sig.
		B	Std. Error	Beta		
1	(Constant)	33.637	.280		120.308	.000
	NDBI	10.473	1.334	.941	7.849	.000
2	(Constant)	35.534	.414		85.728	.000
	NDBI	5.764	1.182	.518	4.878	.002
	NDVI	-10.814	2.219	-.517	-4.874	.002
	a. Dependent Variable: LST					

Table 4: Excluded Variables[a]

Model		Beta In	t	Sig.	Partial Correlation	Collinearity Statistics
						Tolerance
1	NDVI	-.517[b]	-4.874	.002	-.879	.332
	a. Dependent Variable: LST b. Predictors in the Model: (Constant), NDBI					

From Table-3 and 4, we can observe the coefficients of the variables in the regression. Standardised coefficient (Beta) for model a, explaining the correlation coefficient for NDBI, is 0.941, showing a very high positive correlation between NDBI and LST. It is indicating, Land Surface Temperature (LST) of this city is highly affected by its built up surface. In table 4, Correlation between LST

and NDVI is described as an excluded variable with tolerance of 0.332. In this model, partial correlation between LST and NDVI is -0.879. It is Indicating a highly negative relation among them.

Conclusion

From the above discussion, it can be say that, vegetation cover reduce the effect of heat radiation coming from sun. From the above discussion, we found NDVI in a negative relation with urban land surface temperature. It helps us to understand the potentiality of vegetation cover to check the temperature increase. In the other hand, it has been found that temperature is higher, where proportion of built up area is higher. And NDBI is also positively related in the statistical analysis. After this observation, it can be concluded that, urban built up land use helps to increase city temperature and vegetation cover helps to reduce this heat effect. Increase of urban greenery is recommended in the Lucknow city to reduce the urban heat island effect over the city.

References

1. Yadav K.N, Santra A, Samanta, K A.,Identification of Urban Heat Islands From Multi Temporal Modis Land Surface Temperature Data in the Southern Part of West Bengal, India Naval. *Int J Eng Sci Res Technolpogy*. 2016;5(5):640-645. doi:10.5281/zenodo.51847.
2. Wikipedia. Outgoing Longwave Radiation (Olr). https://en.wikipedia.org/wiki/Outgoing_longwave_radiation#Atmospheric_energy_radiation. Published 2006. Accessed April 2, 2018.
3. Lillesand TM, Kiefer RW, Chipman JW. *Remote Sensing and Image Interpretation*. Seventh. WILEY; 2015.
4. Department of Geology. Wavelength Regions of Electromagnetic Spectrum used in Remote Sensing. http://geol-amu.org/notes/m1r-1-1.htm. Published 2018. Accessed April 11, 2018.
5. Piratheeparajah N. Spatial and Temporal Variations of Rainfall in the Northern Province of Sri Lanka. 2015;5(15):179-190.
6. Sharma S, Kaur H. Land Use / Land Cover Changes and Urban Expansion in Jammu city , city India and its surroundings. 2016;5(5):32-40.
7. Wikipedia contributors. Lucknow. Wikipedia, The Free Encyclopedia. https://en.wikipedia.org/wiki/Lucknow#Etymology. Published 2018. Accessed April 22, 2018.
8. Kumari K. Urban Sprawl: A Case Study of Lucknow City. *Int J Humanit Soc Sci Invent*. 2015;4(5):11-20. http://www.ijhssi.org/papers/v4(5)/Version-2/B0452011020.pdf.
9. DIRECTORATE OF CENSUS OPERATIONS UTTAR PRADESH. *DISTRICT CENSUS HANDBOOK, lUCKNOW.*; 2011.

Some results on laminar flow in a square cavity

Dr. Pulakesh Sen
Asst. Professor, Sree Chaitanya Mahavidyalaya

Introduction

The phenomenon of Fluid flow separation is associated with a number of Fluid Flow Problems faced in real life situation nowadays. To understand these types of flow problems, even under the assumption of the incompressible viscous flow, is quiet a difficult task. The complexity lies on the wide variety of laminar separated flows depending on the body shape, several low and high Reynolds number, surface roughness, transition, etc. Several attempts have been made to solve the complete unsteady Navier–Stokes equations for low Reynolds number Laminar flow problems using a variety of formulations. Among them, the vorticity-stream function and pressure–velocity formulations are widely used.

In the present investigation, a type of steady–state incompressible laminar flow problem in a lid-driven unit square cavity has been studied, which deals with different low and high Reynolds numbers. For solving this type of problems, attempts have been made to predict the flow characteristics in a uniform laminar cavity of unit square area by solving the full time dependent, two–dimensional Navier–Stokes equations in primitive variable formulations.

In this study, the flow patterns, flow separations (using the upper and lower wall vorticity lines) are observed for different Re. Through the Tables, the comparison of different schemes, mentioned in Peyret and Taylor (1982) with the present scheme is shown ; as well as the effects of Reynolds numbers on the average vorticity, stream-functions, u-velocity at the centerline, points of flow separation on the lower and upper walls, iteration number, etc. are studied here.

Governing equations

In the Cartesian co-ordinate system, the fundamental equations that govern the unsteady two–dimensional incompressible flow of a Newtonian fluid, having no body forces and with some constant properties, in their conservative form are as follows:

The continuity equation: $$\frac{\partial u}{\partial x}+\frac{\partial v}{\partial y}=0 \qquad (1)$$

The u – momentum equation: $$\frac{\partial u}{\partial t}+\frac{\partial u^2}{\partial x}+\frac{\partial uv}{\partial y}=-\frac{1}{\rho}\frac{\partial p}{\partial x}+\frac{\mu}{\rho}\left(\frac{\partial^2 u}{\partial x^2}+\frac{\partial^2 u}{\partial y^2}\right) \qquad (2)$$

and the v – momentum equation: $$\frac{\partial v}{\partial t}+\frac{\partial uv}{\partial x}+\frac{\partial v^2}{\partial y}=-\frac{1}{\rho}\frac{\partial p}{\partial y}+\frac{\mu}{\rho}\left(\frac{\partial^2 v}{\partial x^2}+\frac{\partial^2 v}{\partial y^2}\right), \qquad (3)$$

where, u and v be the velocity components in the x and y – directions, and p be the pressure; ρ = density of the fluid, μ = coefficient of viscosity, respectively.

The above linear quantities can be non–dimensionalised with respect to the height (L) of the cavity; the velocity components are normalized with respect to the velocity of the upper wall boundary (U) and the pressure (p) with respect to $\rho.U^2$ .Thus, the non – dimensional form of the above equations are as follows:

The continuity equation: $$\frac{\partial u}{\partial x}+\frac{\partial v}{\partial y}=0 \qquad (4)$$

The u – momentum equation: $$\frac{\partial u}{\partial t}+\frac{\partial u^2}{\partial x}+\frac{\partial uv}{\partial y}=-\frac{\partial p}{\partial x}+\frac{1}{\mathrm{Re}}\left(\frac{\partial^2 u}{\partial x^2}+\frac{\partial^2 u}{\partial y^2}\right) \qquad (5)$$

and, the v – momentum equation: $$\frac{\partial v}{\partial t}+\frac{\partial uv}{\partial x}+\frac{\partial v^2}{\partial y}=-\frac{\partial p}{\partial y}+\frac{1}{\mathrm{Re}}\left(\frac{\partial^2 v}{\partial x^2}+\frac{\partial^2 v}{\partial y^2}\right), \qquad (6)$$

where, Re = U.L.ρ/μ.

Initial and Boundary Conditions

The initial condition is that there is no flow initially inside the flow domain (unit square cavity), while on the other hand, there is some specified form of velocity at the upper wall boundary of the cavity. This, physically, represents that the flow is initiated by the motion of the upper boundary wall of the unit square cavity.

Because of the elliptic nature of the equations, the boundary conditions surrounding the prescribed domain should be specified. Here, the velocity components (u,v) are specified .The pressure field is obtained from the velocity components at the boundaries. Here, in this study, the velocity components (u,v) are zero on the left, right and bottom walls of the unit square cavity and on the upper wall boundary, the v-velocity is zero and the u-velocity is given by $u(x) = -16.x^2.(1-x)^2,\ 0 \le x \le 1.$

Method of Solution

Mathematical Formulations: The convective terms of the momentum equations are discretised applying the two methods, mentioned earlier, and the diffusive terms are discretised using second order accurate 3–point central difference formulation in both the cases. The time derivative terms are discretised according to the first order accurate 2–level forward time difference formulations.

The difference equations representing the continuity equation in the uniform grid - spacing, for a typical cell (i,j) is given by,

$$\frac{u_{ij}-u_{i-1j}}{\delta x}+\frac{v_{ij}-v_{ij-1}}{\delta y}=0 \qquad (7)$$

The finite difference equations approximating the momentum equations in the finite difference formulation for the uniform grid – spacing, are

$$\frac{u^{n+1}{}_{ij}-u^{n}{}_{ij}}{\delta t}=-\frac{p^{n}{}_{i+1j}-p^{n}{}_{ij}}{\delta x}+uot^{n}{}_{ij},$$

$$uot^{n}{}_{ij}=\frac{1}{\mathrm{Re}}\left[\frac{u^{n}{}_{i+1j}-2u^{n}{}_{ij}+u^{n}{}_{i-1j}}{\delta x^2}+\frac{u^{n}{}_{ij+1}-2u^{n}{}_{ij}+u^{n}{}_{ij-1}}{\delta y^2}\right]$$

where, $$-(1-\alpha)\frac{u^{n}{}_{r}u^{n}{}_{r}-u^{n}{}_{l}u^{n}{}_{l}}{\delta x}-\alpha\frac{u^{n}{}_{r}\phi^{n}{}_{ur}-u^{n}{}_{l}\phi^{n}{}_{ul}}{\delta x} \qquad (8)$$

$$-(1-\alpha)\frac{v^{n}{}_{t}u^{n}{}_{t}-v^{n}{}_{b}u^{n}{}_{b}}{\delta y}-\alpha\frac{v^{n}{}_{t}\phi^{n}{}_{ut}-v^{n}{}_{b}\phi^{n}{}_{ub}}{\delta y}$$

in the x – direction, and

$$\frac{v^{n+1}{}_{ij}-v^{n}{}_{ij}}{\delta t}=-\frac{p^{n}{}_{ij+1}-p^{n}{}_{ij}}{\delta y}+vot^{n}{}_{ij},$$

$$vot^{n}_{ij} = \frac{1}{\mathrm{Re}}\left[\frac{v^{n}_{i+1j} - 2v^{n}_{ij} + v^{n}_{i-1j}}{\delta x^{2}} + \frac{v^{n}_{ij+1} - 2v^{n}_{ij} + v^{n}_{ij-1}}{\delta y^{2}}\right]$$

where,
$$-(1-\alpha)\frac{u^{n}_{r}v^{n}_{r} - u^{n}_{l}v^{n}_{l}}{\delta x} - \alpha\frac{u^{n}_{r}\phi^{n}_{vr} - u^{n}_{l}\phi^{n}_{vl}}{\delta x} \qquad (9)$$
$$-(1-\alpha)\frac{v^{n}_{t}v^{n}_{t} - v^{n}_{b}v^{n}_{b}}{\delta y} - \alpha\frac{v^{n}_{t}\phi^{n}_{vt} - v^{n}_{b}\phi^{n}_{vb}}{\delta y}$$

in the y – direction.

The constant coefficient 'α' in the above expressions gives the desired amount of upstream or donor cell differencing. That is, when α is zero, these difference equations are centered in space and correspond to the original MAC–formulation (Harlow and Welch, 1965). Those centered equations are numerically unstable and normally require some viscosity terms to be stable. When α is equal to unity, the equations reduce to the full upstream or donor cell form, which is conditionally stable.

The present algorithm involves the Poisson equation of pressure in order to model the elliptic nature of the pressure field in a suitable manner. This pressure Poisson equation can be derived either by differentiation and followed by the addition of the momentum equations or by combining the discretised form of the continuity and momentum equations as mentioned previously. The final expression of the pressure Poisson equation in case of uniform grid is given here as follows:

$$\frac{p^{n}_{i+1j} - 2p^{n}_{ij} + p^{n}_{i-1j}}{\delta x^{2}} + \frac{p^{n}_{ij+1} - 2p^{n}_{ij} + p^{n}_{ij-1}}{\delta y^{2}} = \frac{D^{n}_{ij}}{\delta t} + \frac{uot^{n}_{ij} - uot^{n}_{i-1j}}{\delta x} + \frac{vot^{n}_{ij} - vot^{n}_{ij-1}}{\delta y} \qquad (10)$$

Derivation of the pressure Poisson equation: Basic algorithm for the solution of this equation is due to Young (1954), who developed this method by applying the Successive Over Relaxation (S.O.R) method. But, the method which is being used here to solve the equation is a faster one, namely, Bi–CG-Stab method. It is an iterative method and some initial specified values of the parameters are to be provided. This is done by providing the results of the previous time step. Thus, after rearranging the pressure Poisson equation, it becomes

$$(a+b+c+d)p^{n}_{ij} - a.p^{n}_{i+1j} - b.p^{n}_{i-1j} - c.p^{n}_{ij+1} - d.p^{n}_{ij-1} = r.h.s, where$$

$$r.h.s = -\left[\frac{D^{n}_{ij}}{\delta t} + \frac{uot^{n}_{ij} - uot^{n}_{i-1j}}{\delta x_{i}} + \frac{vot^{n}_{ij} - vot^{n}_{ij-1}}{\delta y_{j}}\right]$$

Where,
$$a = \left(\frac{2}{\delta x_{i}(\delta x_{i} + \delta x_{i+1})}\right), b = \left(\frac{2}{\delta x_{i}(\delta x_{i-1} + \delta x_{i})}\right),$$
$$c = \left(\frac{2}{\delta y_{j}(\delta y_{j} + \delta y_{j+1})}\right), d = \left(\frac{2}{\delta y_{j}(\delta y_{j-1} + \delta y_{j})}\right) \qquad (11)$$

and,
$$D^{n}_{ij} = \frac{u^{n}_{ij} - u^{n}_{i-1j}}{\delta x_{i}} + \frac{v^{n}_{ij} - v^{n}_{ij-1}}{\delta y_{j}}, \qquad (12)$$

where D^{n}_{ij} is called the divergence of the velocity–field at the cell (i,j) at nth time level, which is minimized to zero for the convergence of the flow in successive iterations of the method.

Present algorithm: In the derivation of the pressure Poisson equation, the divergence term at n-th time level ($D^{n}_{i,j}$) is retained and evaluated in the pressure Poisson iteration. This is done because due to incompatible specified initial and boundary conditions, this term is not guaranteed to be zero. But, the divergence term at the (n+1)th time level ($D^{n+1}_{i,j}$) is set to be equal to zero. With this incorporation the pressure Poisson equation becomes independent of the (n+1)th time level's velocity field. On the other hand, it may

induce some inaccuracy which may be kept limited to a lower extent by reducing the convergence criteria for the pressure Poisson equation which generally takes more Bi–CG-Stab - iterations to converge.

To reduce the calculation time for each cycle, the number of iterations in the above said scheme has been kept limited to a minimum number of iterations, or the stability criteria (steady-state) has been induced, i.e. the terms $\frac{\partial u}{\partial t} and \frac{\partial v}{\partial t}$ have to be minimized to zero or less than some very small number in absolute sense.

The 2nd stage starts with computing the divergence of velocity field ($\frac{\partial u}{\partial x} + \frac{\partial v}{\partial y}$) for each cell. If it is found to be greater than some prescribing very small limiting value in absolute sense, the velocity components are corrected for each cell using the pressure terms in the flow field for the next time level.

Numerical stability criteria

To make the numerical scheme accurate, effective and at the same time numerically stable, certain restrictions must be followed in defining the mesh–size δx, δy and δt. Moreover, for the present finite difference scheme (FDM), the combination factor α is also limited by restrictions. After discretizing the flow domain depending on the problem on the study, the time step is determined. It is governed by two restrictions.

Firstly, material cannot move through more than one cell in one time step. Therefore, the time – increment must satisfy the following inequality condition: $\delta t_1 \leq \left[\frac{\delta x}{u}, \frac{\delta y}{v}\right]_{\min}$;

And, the momentum must not diffuse more than one cell approximately in a singe time step. From the linear stability analysis, this limitation implies: $\delta t_2 < \frac{\mathrm{Re}}{2} \frac{\delta x^2 \delta y^2}{(\delta x^2 + \delta y^2)}$.

The time step actually used in the computations is determined from the relation:
$\delta t = FCT\,.\,[\,Min\,(\,\delta t_1,\, \delta t_2\,)]$, where the factor FCT takes values from 0.2 to 0.4.

As earlier mentioned, for the present illustrated finite difference formulation, there is another parameter which is very much needed to ensure the stability of the scheme. This parameter is α, the combination factor of two finite difference schemes. The proper choice of this parameter α, is governed by the inequality condition mentioned below:

$1 \geq \alpha > \left[\left|\frac{u\delta t}{\delta x}\right|, \left|\frac{v\delta t}{\delta y}\right|\right]_{\max}$

And, α is taken approximately 1.2 – times larger than what is found from the above inequality condition.

Results and discussion

In this study, numerical results have been obtained for two-dimensional laminar flow in unit square cavity different Reynolds numbers (Re=10, 100, 400, 800, 1200, 2000) which are illustrated through several tables and figures.

Table-1 shows the comparison of the unit square cavity flow predictions of different schemes, as mentioned in Peyret and Taylor (1982), with the present scheme. This includes the comparison of the stream function ψ (max. value), averaged value of the vorticity on the upper wall of the cavity ($\int_0^1 \omega(x,1)dx$) and the maximum u – velocity at x = 0.5). The results obtained in this work agree well with the available results in Peyret and Taylor (1982) as evidenced in Table-1. This shows that the present scheme is correct. Table-2 illustrates the effect of Re on the averaged value of the vorticity on the upper wall of the unit square cavity. We observe that the value

of averaged vorticity increases with Re. Table-3 shows the effect of Re on the stream function ψ. The maximum value of ψ is compared for different Re. The max. of ψ decreases slightly with the Re and the points (x,y) where ψ is maximum, come closer to the middle of the unit square cavity. Table-4 shows the effect of Re on the processing time of the computational program written in FORTRAN-90 programming language and on the number of iterations of the program. It indicates that the higher Re increases the complicacy of the computational process by taking more time and iteration to get the steady-state and divergence criteria satisfied. Table-5 shows the separation of the flow at different Re on the lower wall of the unit square cavity. It indicates that the flow separates at two different points on the lower boundary(y = 0) nearer to the left and the right walls respectively. The points also move towards the middle of the lower boundary. Whereas, in case of the upper wall flow separation, flow separates at two different points for Re = 10,100; but the flow separates only at a single point on the upper wall for Re=400,1200, 2000.

The Schematic diagram is shown in the Figure-1, which illustrates the two-dimensional geometry of the unit square cavity with specified boundary conditions: (u=0, v=0) at the left, right and bottom wall boundaries and ($u(x) = -16x^2(1-x)^2, v = 0$) at the upper wall boundary. The upper wall vorticity lines for different Reynolds numbers are shown in the Figure-2. The point on the upper wall boundary where the vorticity vanishes indicates the points of separations. From this figure, it is observed that the flow separates at one point on the upper wall of the unit square cavity ; whereas, in case of lower wall vorticity lines, we observe that the flow separates at two different points on the lower wall as shown in the Figure-3. From both the figures, it is evident that the points of separations move towards the middle of the upper and lower wall boundaries of the cavity and the length of flow separation decreases with the increase of Re. The Figure-4 illustrates the behavior of the u-velocity at the centerline (x = 0.5). And, it is observed that u-velocity is positive in the right hand side of the centerline (x = 0.5) and gradually becomes negative in the left hand side of the centerline. The points, where u-velocity vanishes, shifts towards the bottom wall of the unit square cavity as Re increases. The behavior of the vertical v-velocity is also investigated at the centerline (y = 0.5), shown in the Figure-5. The patterns of the streamlines and constant vorticity lines are shown in different figures (from Figure-6 to 13) for low and high Reynolds numbers. Figure-6 shows the streamlines corresponding to ψ = 0, 0.01, 0.02, 0.03, 0.04, 0.05, 0.06, 0.07 and 0.08. Those streamlines shift towards the left - upper corner of the unit square cavity as Re increases, shown in Figure-7, 8, 9 respectively. The constant vorticity lines at the Figure-10 indicate that the vorticity expands towards the upper wall of the unit square cavity. Other figures consisting of iso-vorticity lines, as shown in Figure-11, 12 and 13 also agree with the first one and it can be decided that the lines moves towards the left upper corner of the cavity and the density of those iso-vorticity lines increases adjacent to the upper wall.

References

1. Harlow, F. H. and Welch, J. E. (1965). Numerical Solution of Time Dependent Viscous Incompressible Flow of Fluid with Free Surface, Phys. Fluids, vol. 8, pp. 2182-2189.
2. Hirt, C. W. (1968). Heuristic Stability Theory for Finite Difference Equations, J. Comp. Phys., vol. 2, pp. 339-355.
3. Kelley, C. T. (1995). Iterative methods for linear and non–linear equations, Society for Industrial and Applied Mathematics, Philadelphia, chapter.1-3, pp.3-62.
4. Mahapatra, T. R., Layek, G. C. and Maiti, M. K. (2002).Unsteady laminar separated flow through constricted channel, International Journal of Non-Linear Mechanics 37 (2002) 171-186, Pergamon.
5. Peyret, R. and Taylor, T. D. (1982). Computational Methods for Fluid Flow, Springer-Verlag, New York.
6. Young, D. (1954). Iterative Methods for Solving partial Differential Equations of Elliptic Type, Trans. Amer. Math. Soc., vol. 76, pp. 92-111.

Table-1: Comparisonof various schemes for laminar cavity flow predictions(for Re = 400, δx = δy = 1/20)

Sl.no	Scheme	$\underset{x,y}{Max}\Psi(x,y)^a$	$\int_0^1 \omega(x,1)dx$	$\underset{y}{Max}u(0.5,y)$
1.	Run – 1[b]	0.0632	7.62	0.132
2.	Run – 7[b]	0.0718	7.55	0.173
3.	Run – 8[b]	0.0677	7.35	0.141
4.	Present scheme	0.0689	7.23	0.161

[a]Obtained for x = 0.35, y = 0.75 (Run –1); x = 0.35, y = 0.70 (Run – 8); x = 0.40,y = 0.65 (Runs –7); x = 0.40, y = 0.60 (Present scheme).

[b]Peyret and Taylor (1982) , page no. 202.

Table-2: Effect of Reynolds numbers on averaged value of vorticity

Sl. No	Reynolds no.	$\int_0^1 \omega(x,1)dx$ (averaged vorticity)
1.	10	4.2842
2.	100	4.9875
3.	400	7.6846
4.	1200	11.6767
5.	2000	14.2606

Table-3: Effects of Reynolds numbers on the Stream function: $(\Psi)_{max}$

Sl.no	Reynolds no.	Ψmax	x	y
1.	10	0.08295	0.475	0.775
2.	100	0.08217	0.4	0.75
3.	400	0.07900	0.4	0.625
4.	1200	0.07026	0.45	0.55
5.	2000	0.06360	0.45	0.55

Table-4: Effect of Reynolds numbers on the iteration no. and time(for 40×40 grid -points).

Sl.no	Reynolds no.	No. of iterations	Real time	CPU time
1.	10	5337	1: 22.63	1: 24.71
2.	100	5032	1: 08.71	1: 10.51
3.	400	7105	1: 33.76	1: 36.50
4.	1200	11508	2: 08.47	2: 12.25
5.	2000	13749	2: 23.96	2: 28.34

Table-5: Effect of Reynolds number on the flow separation at lower and upper wallsin unit square cavity (for 40×40-grid points)
Flow separation at different points

Sl. No	Re	Lower wall (x)	Upper wall (x)
1.	10	0.08, 0.92	0.06, 0.95
2.	100	0.15. 0.92	0.25, 0.98
3.	400	0.21, 0.89	0.31, [a]X
4.	1200	0.26, 0.79	0.27, [a]X
5.	2000	0.26, 0.75	0.25, [a]X

Note: [a]X – No separation on the upper wall (near the right wall boundary).

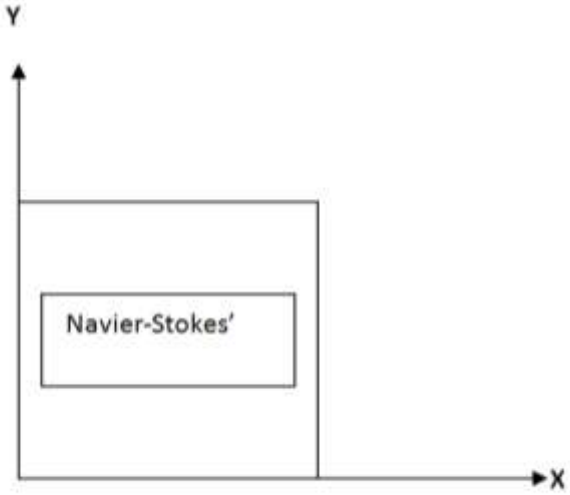

Figure-1:A schematic diagram of the unit square cavity.

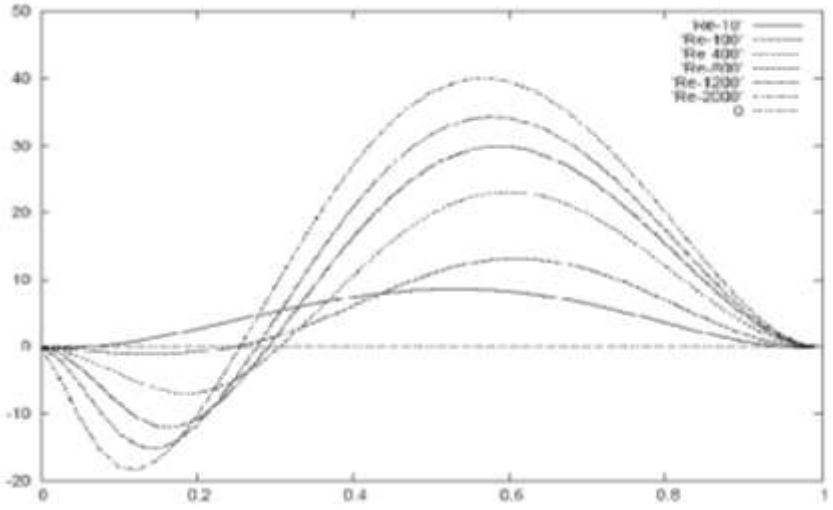

Figure-2: Distribution of upper wall vorticity for Re= 10,100,400,800,1200,2000.

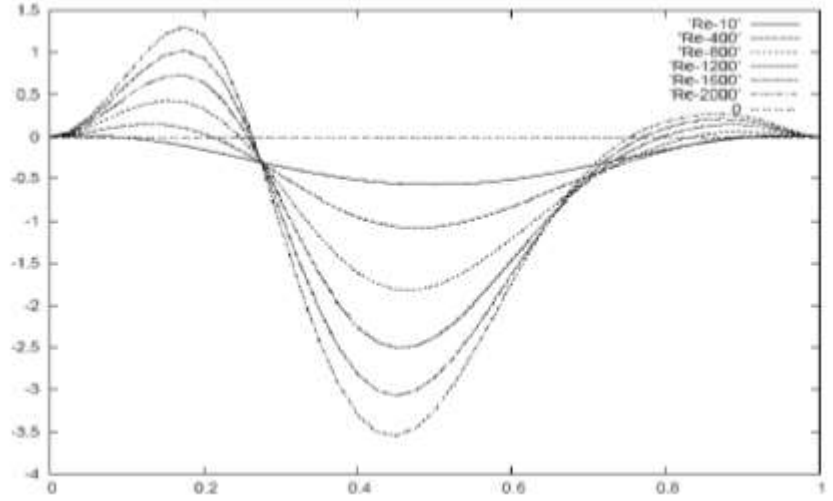

Figure-3: Distribution of lower wall vorticity for Re= 10,100,400,800,1200,2000.

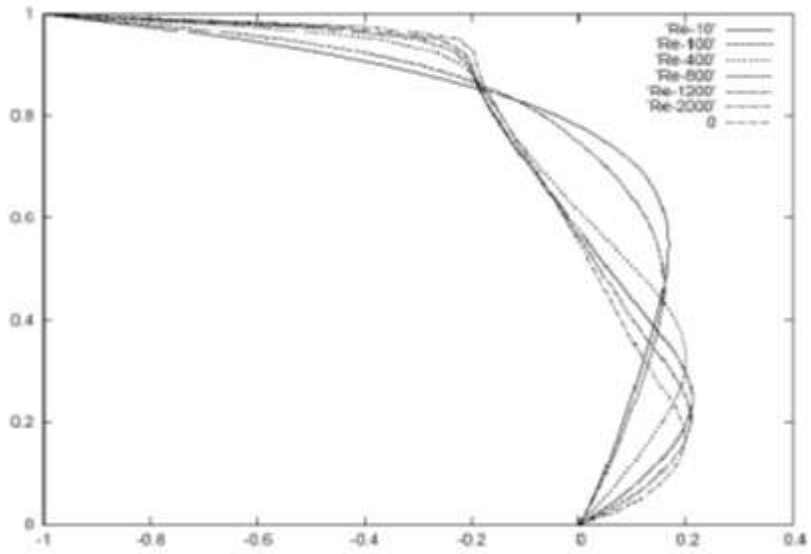

Figure-4:u-velocity on the line x=0.5 for Re= 10,100,400,800,1200,2000.

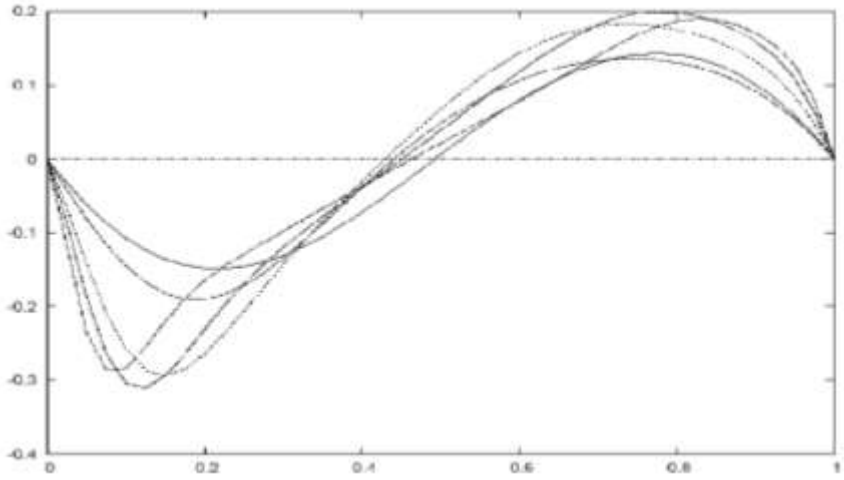

Figure-5:u-velocity on the line x=0.5 for Re= 10,100,400,800,1200,2000.

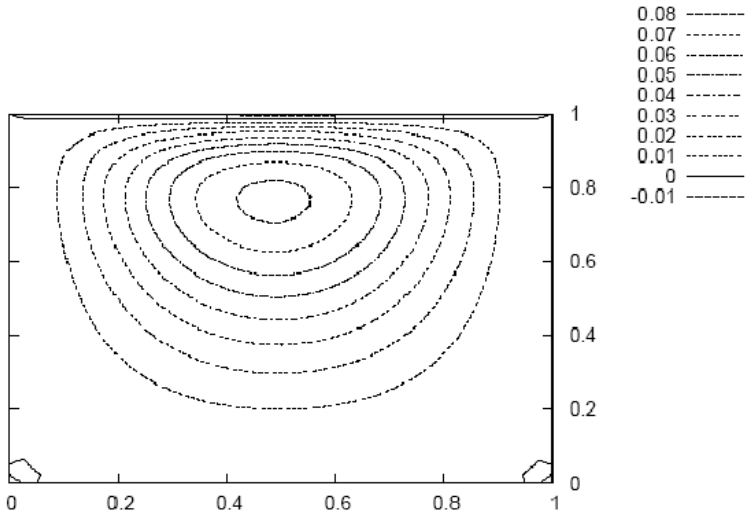

Figure-6: Streamlines for laminar flow in the cavity, Re = 10.

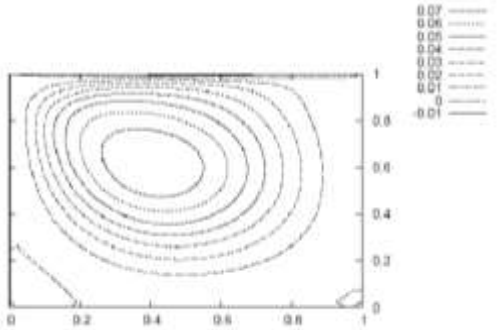

Figure-7: Streamlines for laminar flow in the cavity, Re = 400.

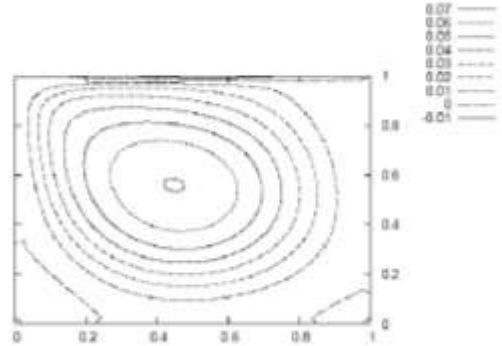

Figure-8: Streamlines for laminar flow in the cavity, Re = 1200.

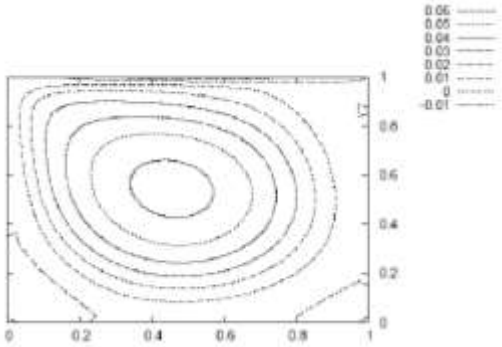

Figure-9: Streamlines for laminar flow in the cavity, Re = 2000.

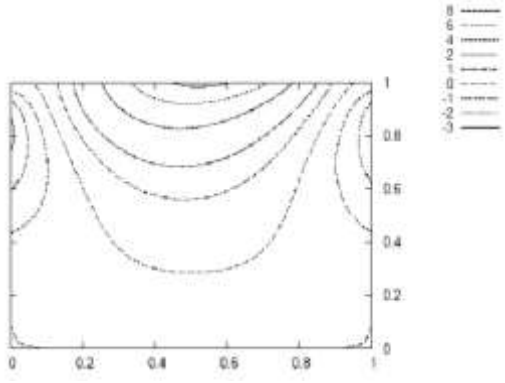

Figure-10: Constant-vorticity lines in the cavity, Re= 10.

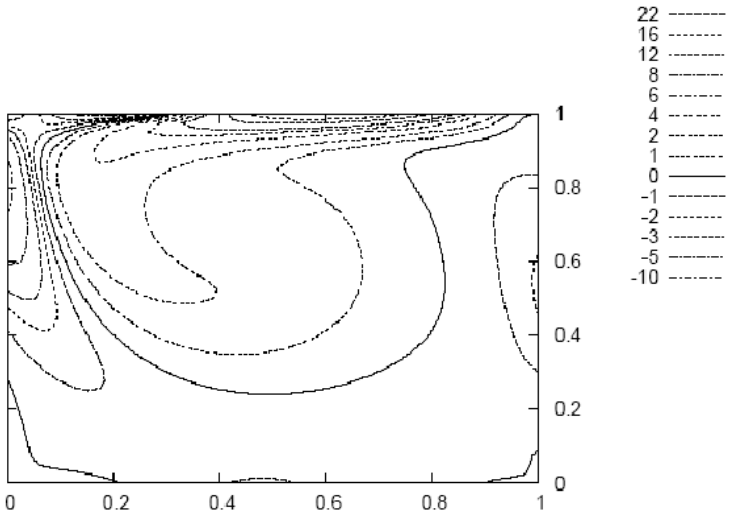

Figure-11: Constant-vorticity lines in the cavity, Re= 400.

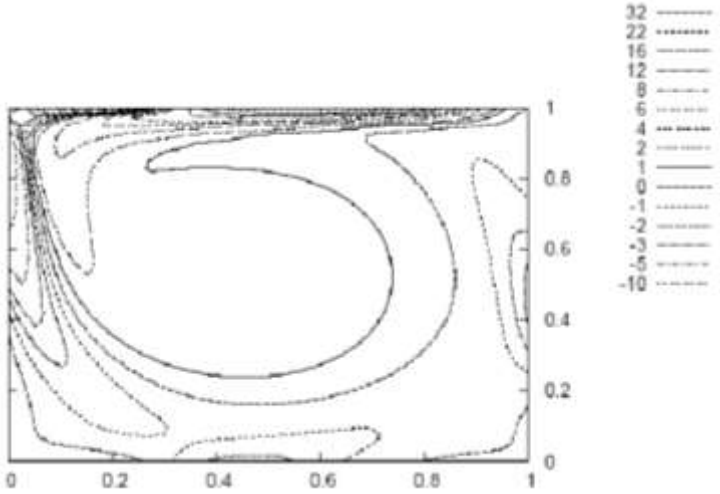

Figure-12: Constant-vorticity lines in the cavity, Re= 1200.

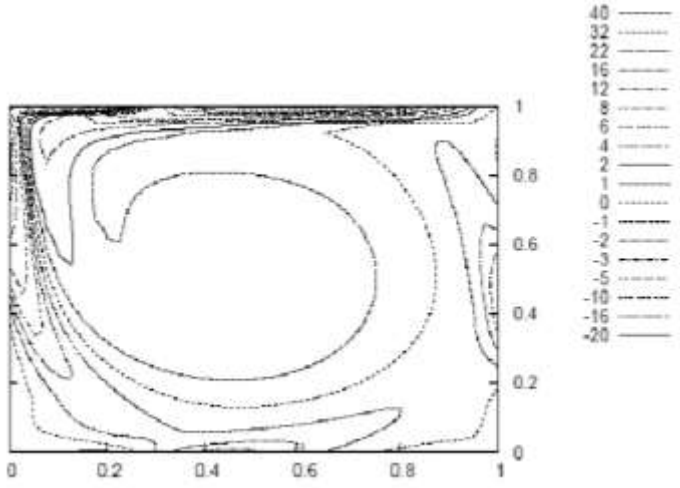

Figure-13: Constant-vorticity lines in the cavity, Re= 2000.

Derivative spectrophotometric study of a binary mixture of dye solution

Soma Mukherjee* and Hemanta Mukherjee
Department of Environmental Science, University of Kalyani, Kalyani, Nadia-741235, West Bengal, India
sommukh445@yahoo.co.in; somam580@gmail.com

Introduction

Derivative technique of spectrophotometry is applied as a powerful tool in the quantitative analysis of multi-component mixtures. Derivatization of a zero order spectrum gives the maxima and minima of the original function into zero values, and the inflections are converted into maxima or minima, respectively. The formed derivative spectrum (DS) is well-organized, enhance the signal and resolve the overlapped peak-signals. Differentiating of a spectrum of closely adjacent peaks and weak peaks in zero order spectra are masked by sharp peaks[1]**.** As per Lambert Beer's law, the absorbance of a mixture at any wavelength is equal to the summation of the absorbance of each component at that wavelength, which depends on the concentration and the extinction co-efficient of each component in multicomponent samples. In the first order DS, the rate of change of absorbance spectra against wavelength is directly proportional to the concentration at each wavelength. This technique with some statistical investigation such as interactive target factor analysis, principal component analysis regression, partial least square, principal component-radial basis function-artificial neutral network, multivariate curve resolution has been applied as a robust and suitable option to resolve the problem[2]. Hence, DS have been successfully applied in the multicomponent analysis, determination of reaction equilibria, calculation of physico-chemical constant, investigation of reaction kinetics; etc.One of the most advantageous applications of DS technique is measurement of unknown concentration of multi-component mixture of dyes in the field of environmental chemistry in connection to the sequestration of dyes from localized polluted environment[3].

Dyes are widely used in several industrial sectors viz. paints, beverages, food and pharmaceutical etc. and research laboratories also. A little information is recorded about the simultaneous removal of multicomponent dyes compared with removal of single component of different dyes in the literature[2,3].Overlapping between spectra of dyes and presence of light scattering particle as impurities as well as solubility of some dyes generate noise in the zero order spectrum. Brilliant green (BG) and eosin (ESN) are very common dyes used in several sectors including medical research field for biological staining cells. Eosin, red acid dyes of the xanthene group, frequently used in textile dyeing and ink manufacturing. It is applied as marker in the paper industry and also used in the cosmetic industry. On the other hand, Brilliant green (BG), a well-known cationic dye, is applied as dermatological agent, veterinary medicine, an additive to poultry feed to inhibit propagation of mold, intestinal parasites and fungus. In textile industries brilliant green is enormously applied for dying of wool and silk fibers[4].From the literature survey it is concluded that several methods (electrocoagulation, adsorption etc.) were applied for simultaneous removal of two dyes[5,6].The prime objective of this work is to develop a simple and accurate spectrophotometric method for simultaneous determination of BG and ESN in a two-component mixture without prior separation.

Background: Derivative spectrophotometry techniques consist of computing and plotting of mathematical derivatives against a normal absorbance spectrum and it measures the rate of absorbance change as a function of wavelength[7]. A mixture of two compounds (X and Y) obeying Beer's law over the whole wavelength range used and if the path length is 1cm, the absorption spectrum of the binary mixture (X and Y) can be written in form of the following equation:

$$A_{m,\lambda i} = \alpha_{X,\lambda i} C_X + \beta_{Y,\lambda i} C_Y \qquad (1)$$

Where, $A_{m,\lambda i}$ is the absorbance of the mixture at wavelength λ_i and $\alpha_{X,\lambda i}$&$\beta_{Y,\lambda i}$ are the absorptivities at λ_i for X and Y, respectively. Then the above equation is divided by $\beta_Y, \lambda i\ C_Y^0$ corresponding to the spectrum of a standard solution of component Y in the binary mixture, the ratio spectrum is obtained

$$\frac{A_{m,\lambda i}}{\beta_{Y,\lambda i} C_Y^0} = \frac{\alpha_{X,\lambda i} C_X}{\beta_{Y,\lambda i} C_Y^0} + \frac{\beta_{Y,\lambda i} C_Y}{\beta_{Y,\lambda i} C_Y^0} \qquad (2)$$

The ratio of $\beta_{Y,\lambda i} C_Y$ to $\beta_{Y,\lambda i} C_Y^0$ is equal to a constant with respect to λ, in a certain region or point of wavelength:

$$\frac{A_{m,\lambda i}}{\beta_{Y,\lambda i} C_Y^0} = \frac{\gamma_{X,\lambda i}}{\beta_{Y,\lambda i} C_Y^0} + \text{Constant} \qquad (3)$$

If the first derivative of Eq. (3) is taken, since the derivative of a constant is zero, Eq. (4) would be obtained and this is mathematical foundation of multi-component analysis:

$$\frac{d}{d\lambda}\left[\frac{A_{m,\lambda i}}{\beta_{Y,\lambda i} C_Y^0}\right] - \frac{d}{d\lambda}\left[\frac{\gamma_{X,\lambda i}}{\beta_{Y,\lambda i} C_Y^0}\right]\frac{C_X}{C_Y^0} \qquad (4)$$

Materials and Methods

The dyes, Brilliant green (BG) and Eosin (ESN) of analytical grade, are purchased from HiMedia Laboratories Pvt. Ltd., Mumbai, India. Both are used without further purification.

Instrumentation: UV-visible zero and first order derivative spectra of the desired concentrations were recorded on double beam UV–visible spectrophotometer of Shimadzu using 10 mm path length quartz cells with fixed slit width and scan range of 250–700 nm.

Preparation of standard and sample solutions: Stock solution of 1000 ppm of brilliant green and eosin were prepared in Millipore water for first order derivative spectrophotometric analysis. The standard solutions were prepared by dilution of the stock solution with millipore water in a concentration range of 1, 2, 3, 4, 5, 6, 7, 8, 9 and 10 ppm with millipore water for first order derivative spectrophotometric methods. The binary mixture of BG and ESN is prepared by mixing of 5 ppm strength of each solution. Millipore water was used as a blank solution. A zero order and first order derivative spectra of an unknown mixed solution of BG and ESN are recorded also.

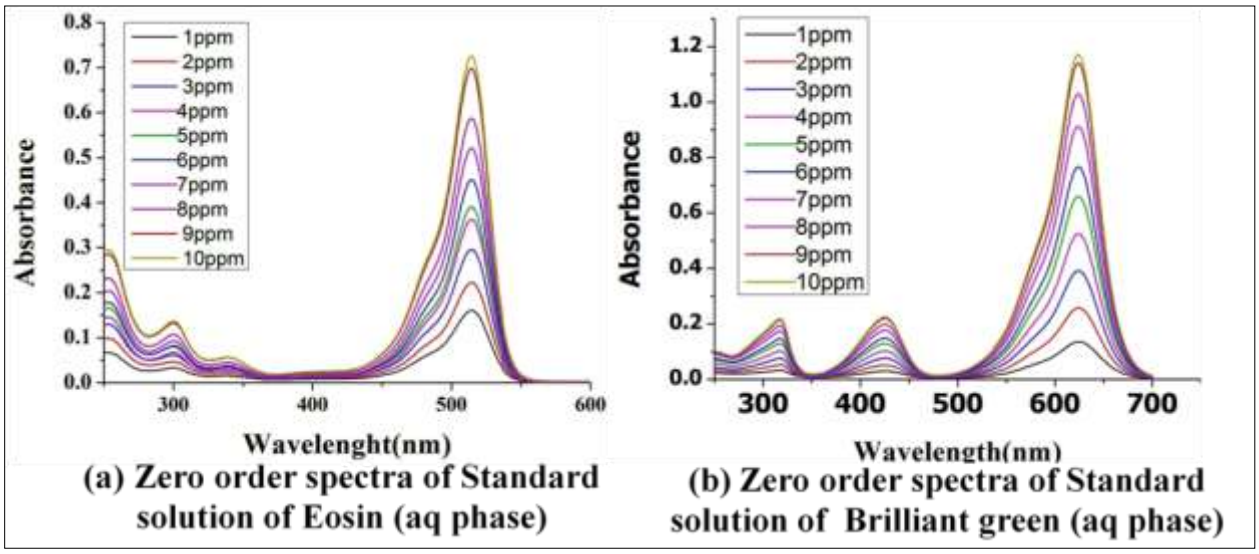

Figure-1: Zero order spectra of eosin and brilliant green.

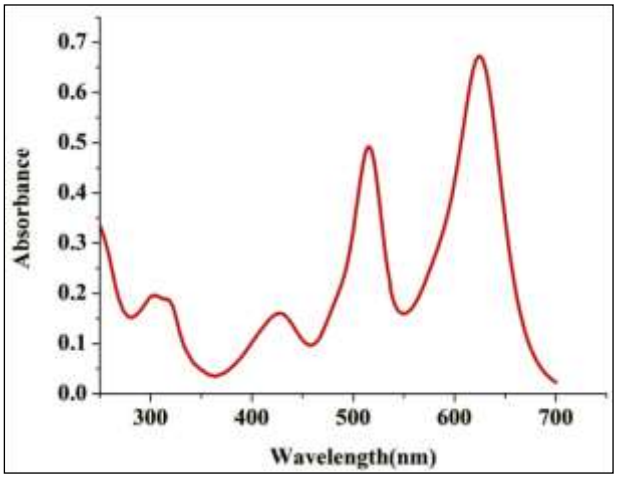

Figure-2: Zero order spectra of mixture of eosin and brilliant green (unknown).

Results and Discussion

The UV-visible spectra of zero order spectra are scanned in the range of 600 nm to 250 nm for eosin and 700 nm to 250 nm for brilliant green respectively. In the derivative ratio spectra method, a standard divisor is selected to minimize experimental error and background noise. For the determination of unknown concentration of ESN, the spectra at increasing concentration in water were divided (amplitude by amplitude at appropriate wavelength) by previously stored absorption spectrum of a well-selected standard solution of BG (5 ppm) to obtain the corresponding ratio spectra.

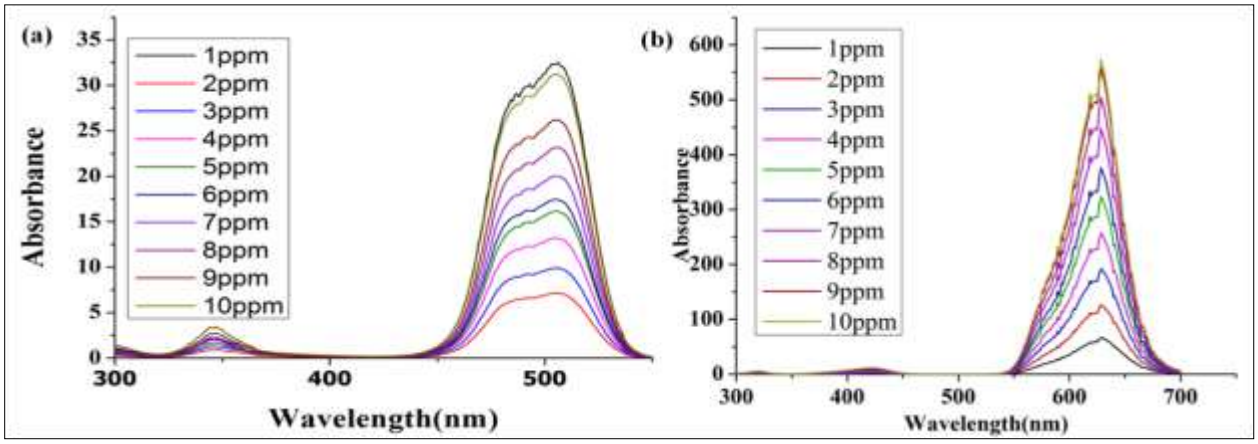

Figure-3: Ratio spectra of (a) Eosin and (b) Brilliant green.

Then the first derivative of the obtained ratio spectra was traced by the Origin Pro software. The same procedure is followed for determination of unknown concentration of BG, selecting eosin (5 ppm) as divisor. The first order derivative spectra for brilliant green were recorded at the wavelength of 616nm (max) and 645nm (min). For eosin first order derivative spectra were taken at the wavelength of 474nm (max) and 521nm (min). Then the absorbance values at the fixed wavelength are plotted against the concentration to get the standard graph. The regression equation of calibration curves is obtained and the regression analysis is done for the slope, intercept and correlation coefficient values. Correlation regression coefficient values lies in between 0.99.The regression equations with the estimated concentration of unknown mixture is furnished in the below Table-1.

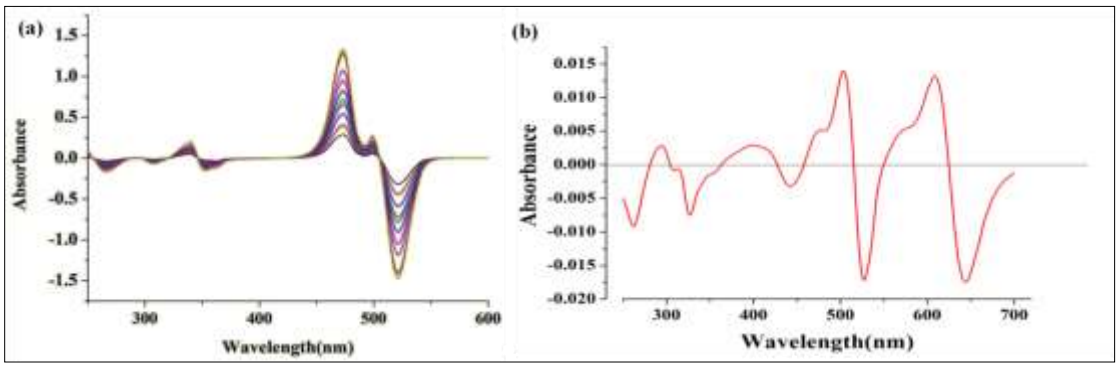

Figure-4: Ratio first order derivative spectra of (a) brilliant green and (b) mixture of brilliant green and eosin of unknown concentration.

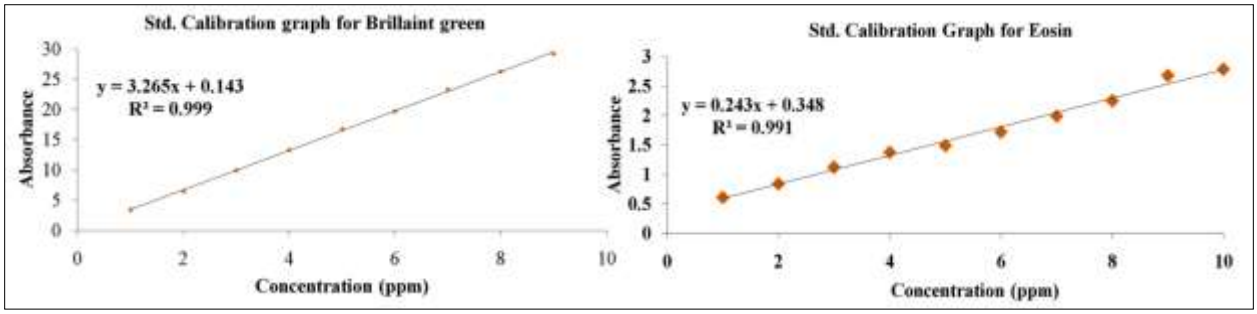

Figure-5: Standard calibration graph of (a) Brilliant green and (b) Eosin.

Table-1: Estimation of unknown concentration of BG and ESN.

Analyte	Linearity Range	Wavelength	Regression Equation	Coorelation coefficent	Expected Concentration	Measured concentration
Brilliant Green	1-9ppm	616(max) 645(min)	y=3.265x+0.143	0.99	5.0 ppm	5.025 ppm
Eosin	1-10ppm	474(max) 521(min)	y= 0.243x+0.348	0.99	5.0 ppm	5.421 ppm

Conclusion

The results obtained from the ratio spectra derivative spectrophotometric method reveal that the proposed method is effective for resolving binary mixtures and suitable for the simultaneous spetrophotmetric determination of brilliant green and eosin in aqueous phase. The developed methods are simple, rapid and selective for the simultaneous determination of binary mixture of two dyes, having the advantages of minimal data processing. Therefore, simple, fast and reliable spectrophotometric methods were developed for the easy and routine determination of concentration of brilliant green and eosin from binary mixture.

Acknowledgement

We are thankful to the University of Kalyani, Nadia, West Bengal for providing the infrastructural facilities.

References

1. C. Bosch Ojeda, F. Sanchez Rojas, Microchemical Journal106 (2013) 1–16.

2. M. S.Tehrani, R.Zare-Dorabei, Spectrochimica Acta Part A: Molecular and Biomolecular Spectroscopy 160 (2016) 8–18.

3. M. M. Issa , R. M. Nejem, A. Abu Shanab, N. D. Hegazy, R. S. Staden, Spectrochimica Acta Part A: Molecular and Biomolecular Spectroscopy 128 (2014) 514–521.

4. A.Singh, A. Tripathi, N.N. Dutta, International Journal of Engineering Science and Computing, April 2017.

5. Md. A. M. Salleh, D. K. Mahmoud, W.Azlina, W. A. Karim, A.Idris, Desalination 280 (2011) 1–13.

6. M.T.Yagub, T.K.Sen, S.Afroze, H.M. Ang, Advances in colloid and Interface Sc 209 (2014) 172-184.

7. Maya S. Eissa, Spectrochimica Acta Part A: Molecular and Biomolecular Spectroscopy 183 (2017) 362–370.

Adverse Impacts of Chemical Fertilizers and Pesticides on Environment and Health of Farmers

M. Roy
Directorate of Distance Education, Vidyasagar University, Midnapur-721102, West Bengal, India
misharoy.india@gmail.com

Abstract

The unbridled use of chemical fertilizers and pesticides in agriculture sector poses severe environmental and health hazards. The use of pesticides and fertilizers helps to considerably decrease crop diseases, reduce crop losses and result in better yield. Nevertheless, their unfavorable effects on environmental quality and human health have frequently been reported and well documented. Pesticides mismanagement starts locally but very soon spreads globally with universal dimensions. The present study is carried out in Egra, Purba Midnapur, W.B, India to ascertain the variety of pesticides that are used in the agriculture sector and their probable impact on the health of farmers. The present study revealed that many farmers use high to extremely hazardous pesticides like Organo chlorides, Organophosphates and Carbamates. Various diseases and physiological disorders were observed among the farmers. The relative risk (RR) is also found to be high. Lack of adoption of adequate protective measures were noticed which increased the declining state of the health of farmers in the region.

Keywords: Pesticides, Fertilizers, Environmental Impacts, relative risk, agriculture.

Introduction

India is an agriculture based country. Despite that every year huge amounts of valued crop is lost due to pathogens and pests attack. Pesticide are applied to increase the crop production and to reduce the crop loss after storage (Gupta, 2004). Proper usage and application of pesticides has resulted in reduction of crop loss and has increased its productivity. However the problem arises when the pesticides are applied indiscriminately. Exposure to pesticides both occupationally and environmentally can result in serious health hazards among the farmers. In addition, inappropriate and excessive applications, lack of proper storage and adopting inadequate protective measures frequently results in harmful health hazards in exposed farmers. Pesticides being non biodegradable enter the food chain and hence affect human health indirectly. There is both direct and indirect relationship between exposure of pesticide use and health hazards (Kishi et.al., 1995; Conway, 1984; Galloway *et. al*., 1987; Leiss and Savitz, 1995; Colborn, 1996; Arbuekal *et al*., 1998).

The farmers are directly exposed to pesticides while application and have both long term chronic and short term acute effects (Forget, 1991; Rola *et.al.*, 1993; Wilson, 2002; Dasgupta, 2005; Roy, 2016). There are very few case studies based on the farmer's self-reported symptoms of pesticides health hazards. The present study is dedicated to understand the direct impact of pesticide applications on the health of farmers.

Methodology

Study area*:* The study is carried out among the agricultural communities of Egra, Purba Midnapur, West Bengal, India.

Data Collection: This study is based on the primary data. The primary data was collected through a personal interview for the agricultural year 2016-2017. Data were collected by interview based on a well prepared questionnaire to find out the details of the time duration, type and nature of pesticides, exposure, protection taken, signs and symptoms of illness, medical history along with the detailed demographic distribution. A total of 500 farmers, engaged in the application of pesticides were interviewed.

Relative Risk: The relative risk is the probability that a member of an exposed group will develop a disease relative to the unexposed group. The relative risk is calculated to observe the probability of developing a disease in exposed group compared to the unexposed ones (Roy, 2016).

Relative Risk (RR) = % (exposed group)/ % (unexposed group).

Results and Discussions

The farmers surveyed in this study area found to have educational qualification mostly below matric (52.5%), secondary and higher secondary levels are found to be 22% and 12%, graduates are found to be very less in number (5%), and around 3% farmers are found to be illiterate. Regarding storage of pesticides most widely used storage is the cowshed while some also stores pesticides in the

kitchen (Table-1). A variety of pesticides under different trade names belonging to different chemical groups were reported to be used, some of which were carcinogenic.

Table-1: Storage of Pesticides.

Type of Storage	Percentage of farmers (%)
Cow shed	57
Store Room	41
Kitchen	2

Application of pesticides requires the use of appropriate protective measures and equipments, like the use of gloves, masks, aprons etc. it was found that most of the farmers in the study area uses masks and aprons, no other protective measure is found to be used by the farmers. They mix the pesticides with bare hands. A great many farmers were seen smoking chewing tobacco during pesticides applications.

The health effect of pesticide application on the farmers is analysed through the questionnaire. They were asked whether they were facing any symptoms and problems during or immediately after the application of pesticides. Several health hazards are reported by the farmer's headache (16.6%), skin diseases (18.8%), Nausea and respiratory problems (5%) and muscle cramps (2%). The relative risk is calculated to determine the probability of determining the risk among the sprayers compared to non sprayers. Among the farmers higher relative risk was observed in headache, skin diseases, respiratory problems, cough, burning/stinging/ itching sensation of eyes (RR = ≥ 1.5) (Table-2).

Table-2: Effect of Pesticide on users Health of Farmers.

Health Hazards	Sprayers	Percentage (%)	Non sprayers	Percentage (%)	Relative Risk (R.R)
Burning sensations	91	18.2	15	3	6.07
Cough	74	14.8	13	2.6	5.69
Headache	83	16.6	22	4.4	3.77
Muscle Cramps	10	2	6	1.2	1.67
Nausea/Vomiting	25	5	22	4.4	1.14
Nervousness	8	1.6	4	0.8	2.0
Respiratory Problems	10	2	2	0.4	5.0
Skin Diseases	94	18.8	21	4.2	4.47

Conclusion

The study indicates that the farmers in the area were affected with different types of problems due to pesticide exposure. Higher relative risk was found among sprayers compared to the non sprayers. Since the prevalence of this disease is computed from the self-reported symptoms there could be some underestimation. In general they lack awareness about the protective measures for application of pesticides. Educating and training the farmers' about proper handling and application of pesticides and awareness about the negative impacts is essential in the area. The use of integrated pest management and creating awareness about the use of bio pesticides is the need of the hour. The availability of bio pesticides should be made wide spread among the farmers.

References

1. Arbuekal TE, Server LE (1998). Pesticides exposures and fetal death: a review of the epidemiologic literature. Crit. Rev. Toxicol. 28:229-270.

2. Colborn T (1996). "Hormonal sabotage. Synthetic chemicals and the endocrine systems. Natural History. 105(3):42-47.

3. Conway G R (1984).Strategic Models, in G R Conway (Ed).Pest and Pathogen Control: Strategic, Tactical and Policy Models, International Series on Applied Systems Analysis, John Wiley and Sons.

4. Dasgupta, S. C. Meisner, D. Wheeler, N. T. Lam and K. Xuyen, (2005). Pesticide poisoning of farmForget G (1991). Pesticides and the Third World

5. Galloway SM, Armstrong MJ, Reuben C, Colman S, Brown B, Cannon C, Bloom AD, Nakamura F, Ahmed M, Duk S, Rimpo J, Margolin BH, Resnick MA, Anderson B, Zeiger E (1987). Chromosome aberrations and sister chromataid exchanges in Chinese hamster ovary cells, evaluation of 108 chemicals. Environ. Mol. Mutagen. 10:1-175.

6. Gupta P K., (2004). Pesticide exposure –Indian scene.Toxicology. 198(1-3): 83-90.

7. Kishi M, Hirschhorn N, Djajadisastra M, Satterlee LN, Strowman S, Dilts R (1995). Relationshipof pesticide spraying to signs and symptoms in Indonesian farmers. Scand. J. Work Environ. Health. 21:124-33

8. Leiss JK, Savitz DA (1995). Home pesticide use and childhood cancer: a case-control study. Am. J. Public Health. 85:249-52.

9. Rola, A. C. and P. L. Pingali, (1993). Pesticides, riceproductivity, and farmers' health: An economicassessment, Philippines: International Rice ResearchInstitute and Washington, DC.

10. Roy, M,Impact of Pesticide Use on the Health of Farmers: a Case Study in Bankura, W.B., India;International Journal of Innovative Research in Science, Engineering and Technology, 5(7), 12370-12374, 2016

11. Wilson C (2002). Private cost and the relationbetween pesticide exposure and health: Evidence fromworkers: Implication of blood test results from Vietnam, Policy Research Working Paper, 3624,

Application of Nonlinear chaos theory in prediction of Atmospheric Systems

Amitlal Bhattacharya[1] and Rishiparna Guha[2]
[1]Assistant Professor, Department of Physics, D.N. College, Murshidabad, West Bengal-742201, India
[2]Assistant Professor, J.D. Birla Institute, Departments of Sciences & Commerce, 11 Lower Rawdon Street, Kolkata -700020, India
amitlal1980@rediffmail.com

Abstract

The dynamical atmospheric systems exhibit nonlinear behaviour. It can be studied by the chaos theory. The fractal fluctuations in space and time are seen in atmospheric flows. The atmospheric instability may be examined by nonlinear chaos theory. The actual physical mechanism of the atmospheric system is still not clear due to its nonlinear complexity. Proper application of nonlinear chaos theory in meteorology is significant and helpful to accurately predict the instability of atmosphere. The application of the chaos theory in the atmospheric systems has been discussed in this paper.

Keywords: Atmospheric instability, fractals, nonlinear chaos theory.

Introduction

The theory of chaos is about deterministic system revolving on the infinitesimal perturbations in the initial conditions. It finds its application in a number of natural processes *viz.* Electronics, chemical kinetics, ecology, hydrodynamics, fluid motion *etc.* Chaos is considered to be an irregular, dissipative, unpredictable and non-linearly dynamic in nature. The terminology of chaos was first introduced by Li and Yorke (1975) in mathematical sciences. The direct relationship chaos and mathematical expression makes it an important tool for explanation of any natural system. Such application was made long back by Hadamard (1898) contributing to the explanation of Geodesic flows. Then Poincare (1908) introduced by studying three body problems of stars and found non periodicity in orbits[1]. He emphasized on the sensitivity of initial conditions of a deterministic system. This in turn explains the science behind the "Butterfly Effect". This theory was firstly applied by Lorentz in 1961 in studying atmospheric systems. Later on the properties of chaotic behaviour are studied together with atmospheric physics as most of the atmospheric motions are directly related with the Navier-Stokes theorem. Thus chaos theory plays a significant role in weather prediction in governing the stochastic fluctuations associated with day to day weather prediction.

Backgrounds

The non linear chaos theory in meteorology has been used in different ways throughout the times and thus summarized in Table-1.

Table-1: Chaos theory in atmospheric systems.

Year	Incidents
1880	Idea of chaos theory by Henry Poincare[1].
1893	Nikola Tesla described the complexity in nature[10].
1898	Jacques Hadamard examined the chaotic motion and put forward the sensitivity of solutions to the initial conditions[11].
1950	The choice of actual physical pattern of atmosphere which depends on some arbitrary and unpredictable factors of the past[2].
1961	Nash and Sutcliffe concluded that the system controls its own faith using cybernetics [12].
1963	Edward Lorentz put forward the non linearity and chaos theory in atmospheric phenomenon [13].
1965	The Butterfly effect explained that the behaviour of dynamic system is highly sensitive to initial conditions[14].
1970	The fractal geometry of unpredictable irregular fluctuations in space and time is identified by Mendelbrot[15,16].
1971	The concept of strange attractor is introduced by Rulle and Takens d[17]
1990	Rulle described strange attractors as finite number of degrees of freedom and infinite number of frequencies[18]
Presently	The progress of chaos theory by use of iteration process with the advancement of computers [19].

Application in Atmospheric Systems

The application of non-linear chaos theory was majorly on natural systems by Mandelbrot (1970) giving the idea of self-similarity pattern without periodicity. Smale (1960) proposed a contradictory theory to Lorentz which later on he himself discarded by

developing the famous Horseshoe counter example to his own conjecture of a dynamic system. Ruelle (1976) emphasized on the importance of Lorentz's work on chaos theory. Guckenheimer and Landford gave a mathematical treatment to the chaos theory of a deterministic approach. In this regard it is to be mentioned that the idea of self-similarity patterns were firstly introduced in the field of meteorology by Richardson (1992) in 1965 together with Kolglomorov, Kandaoff, Monin and Yaglam and many others. Figure-1 summarizes the applications areas of chaos theory and its pathways of manifestation.

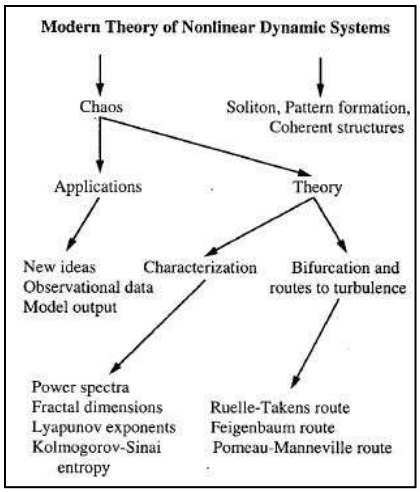

Figure-1: Pathways of non-linear Chaos theory approach (Zheng *et al*, 1993).

Thus irregular space time fluctuations related to branching of geometry are often associated with this self-similarity pattern. This was later identified as fractal. In the field of atmospheric physics these fractals are recognized by long range co-relations in varied space-time. These associations are named as self-organized criticality exhibited by atmospheric flows. One of the most eminent natural examples of fractals is the branching of a lightning occurring in varied scales and sizes. Such geometric patterns are self-similar and demonstrate long range correlations and they are quasi-periodic[25-28].

It is interesting to note that atmospheric turbulent fluid motions may be explained by quasi-periodic 'Penrose tilling' pattern in association with fractal self-similar pattern. These fractal often portray Fibonacci sequence and may be orderly and symmetric in nature but with no periodicity. Thus dynamic system s with large spatial extension is observed to display fractal geometry in varied temporal and spatial scales. Selvam explained such natural occurrences through referring to fractal geometry of cloud cover pattern which have a temporal range between a second and year. Natural bodies have both microscopic and macroscopic scale manifestations of self-similarity developed from apparently turbulent chaotic flows of motion but ultimately end up displaying a coherent structure. Such process flows only encourages one to apply the theory of chaos to predict the formation and life-cycle of atmospheric systems. Consequently it directs to the fact that atmospheric systems show self-organized criticality[29-33].

Discussion

Temporal and Spatial scale –ranges of atmospheric fluid motions vary in a large extent to which standard meteorological theory may never be able to do justice. Here chaos theory comes to play the most significant part in explain the sensitivity to the initial conditions which may present an entirely new portrait of predicted weather. As atmospheric flows are turbulent in nature, it exhibits fractal fluctuations in space and time ranging from millimetre-sec to the scale of kilometre-year[2]. Atmospheric systems highly sensitive to initial conditions, so its dynamics is been studied by chaos theory in different time. Such considerations when applied on initial observational data of tropical cyclone data it successfully demonstrated the trajectories of these storms and showed their dependence on geographical co-ordinates[33-35].

It has been inferred in many researches that chaos theory may serve the purpose of an important tool for weather (short term) prediction as it directly involves with stochastic fluctuations but better results should not be expected for climate prediction. Multidisciplinary approach may help in this scenario to develop statistical and analytical tools for quantification and understanding laws of atmospheric motion governing of long rage observations natural systems. Prediction is done by using observational data and also noise reduction is very important before data assimilation. Chaos theory introduced a new way to deal with the observational data, especially with the data which was earlier ignored due to its erratic behaviour[36,37].

So in the last few years' application of chaos theory in atmosphere was about the evolution of fractal dimensions from the observed data and the existence of low dimensional attractors[3,4,7,20-24,38].

References

1. Poincare, H. (1890) Sur le problème des trois corps et les équations de la dynamique *Acta Mathematica* 13(5)

2. Shaffee, A. and Shaffee, S. (1987) Implications of the spatial finiteness of mesoscale meteorological fields, *Phys. Rev.*, A35, P. 892

3. Yang, P. (1991) On the chaotic behaviour and predictability of the real atmosphere. *Adv. Atmos. Sci.,* 8, pp. 407-420

4. Lorentz, E.N. (1991) Dimension of weather and climate attractors, *Nature*, 353, pp. 241-244

5. Lee, T.Y. and Yorke, J.A. (1975) Period three implies chaos, *Am. Math. Mon.*, 82, pp. 985- 992

6. Cohen, E. G. D. (1997) Lectures given at thr International Meeting "Boltzmann's legacy- 150 years after his birth" Academia Nazionaledei Lincei, 25-28 May, 1994

7. West, B. J. (2004), Comments on the renormalization group, scaling and measures of complexity, Chaos, Solitons and fractals, 20, pp. 33-44

8. Selvam, A.M. (2009) Fractal fluctuations and statistical normal distribution, Fractals, 17(3), pp. 333-349

9. Selvam, A. M. and Fadnavis, S. (1998) Signatures of a universal spectrum for atmospheric interannual variability in some disparate climatic regimes, Meteorology and Atmospheric Physics, 66, pp. 87-112

10. "Tesla Timeline" (http://www.teslauniverse.com/nikola-tesla-timeline-1856-birth-of-tesla#goto-1861). Tesla Universe.16 August 2012

11. Hadamard, J. (1898), Les surfaces à courbures opposées et leurs lignes géodesique, *J. Math. Pures Appl.*, 4, 27-73

12. Nash, J. E. & Sutcliffe, J. V. (1970) River flow forecasting through conceptual models. Part I—A discussion of principles. *J. Hydrol.* 27(3), pp. 282–290

13. Lorenz, E. N. (1963), Deterministic Nonperiodic Flow, *J. Atmos. Sci*., 20, pp. 131–40

14. Lorenz, E. N. (1965), A Study of the Predictability of a 28-Variable Atmospheric Model, *Tellus*, 17, pp. 321–33

15. Mandelbrot, B. B. (1977) Fractals: from, chance and dimension, Freeman Publishers, San Francisco

16. Mandelbrot, B. B. (1983) The Fractal Geometry of Nature, W.H. Freeman publication

17. Rulle, D. And Takens, F. (1971) On the nature of turbulence, *Commun. Math. Phys.*, 20, pp. 167-192

18. Rulle, R. (1990) Deterministic chaos: The Science and the Friction, *Proc. Roy. Soc.* London. 427A, pp. 241-248

19. Boeing, G. (2016). Visual Analysis of Nonlinear Dynamical Systems: Chaos, Fractals, Self-Similarity and the Limits of Prediction. *Systems*. 4 (4) 37. doi:10.3390/systems4040037

20. Poincare, H. (1908) Science of Method, Dover publication, New York, P. 288

21. Li, W. (2010) A bibliography on 1/f noice, http://www.nslij-genetics.org/wli/1fnoise, 5/01/2017

22. Milotti, E.(2001) 1/f noise, a pedagogical review, invited talk to E-GLEA-2, Buenos Aires, Sept. 10-14, 2001

23. Takens, F. (1981) Detecting Strange Attractors in Turbulence, Dynamical Systems and Turbulence, Lecture Notes in Mathematics, 898, Springer-Verlag, New York, pp. 366-381

24. Zeng, X. (1992) Chaos theory and its application in the atmosphere, Ph. D. Dissertation Colorado State University

25. Guckenheimer, J. and Holmes, P. (1983) Nonlinear Oscillations, Dynamical System and Bifurcations of vector fields, Spinger-Verlag, P. 453

26. Hadamard, J. (1898) Les surfaces a courbures opposes et leurs lignes geodesiques, J. Math, Pures. Appl., 4, pp. 27-73

27. Kolmogorov, A. N. (1958)A new metric invariant of transient dynamical systems and automorphisms in Lebesgue Spaces, Dokl. Akad. Nauk. SSR, 119, pp. 861-864

28. Lovejoy, S. and Schertzer, D. (1990) Multifractals, universality classes and satellite and radar measurements of cloud and rain fields, J. Geophysics. Res., 95(D3), pp2021-2034

29. Rulle, R. (1990) Deterministic chaos: The science and fiction, Proc. Roy. Soc. Lond., 427A, pp 241-248

30. Selvam, A.M., J.S. Pethkar and Kulkarni, M. K. (1992) Signatures of universal spectrum for atmospheric interannual variability in rainfall time series over the Indian region, Int. J. Clim., 12, pp137-152

31. D. Schertzer and S. Lovejoy, in Fractals in the Natural and Applied Sciences (A-41), Ed., M. M.Novak, Elsevier Science B. V. (North-Holland) (1994) pp. 325 – 339

32. L. F. Richardson, Weather Prediction by Numerical Process, Dover, Mineola, N. Y (1965)

33. Aubin D., & Dahan Dalmedico A. (2002). Writing the history of dynamical systems and chaos: longue durée and revolution, disciplines and cultures. Historia Math. 29(3), 273-339.

34. Guckenheimer, J., & Williams, R.F. (1979). Structural stability of Lorenz attractors. Inst. Hautes Études Sci. Publ. Math., 50, 59-72.

35. Hadamard, J. (1898). Les surfaces à courbures opposées et leurs lignes géodésiques. Journal de mathématiques pures et appliqués, 5e série 4, 27-74.

36. Maxwell, J.C. (1876). Matter and Motion. New ed. Dover (1952).

37. Ruelle, D. (1976a). The Lorenz attractor and the problem of turbulence. In Turbulence and Navier-Stokes equations (Proc. Conf., Univ. Paris-Sud, Orsay, 1975), 146-158, Lecture Notes inMath., 565, Springer, Berlin, (1976)

38. Smale, S. (1960). On dynamical systems. Bol. Soc. Mat. Mexicana, 5, 195-198

On the Seasonal Variability of Zero Degree Isotherm Height over Eastern Coast of India

Rishiparna Guha[1]* and Amitlal Bhattacharya[2]
[1]Assistant Professor, J. D. Birla Institute, 11, Lower Rawdon Street, Kolkata – 700020
[2]Assistant Professor, Department of Physics, D. N. College, Aurangabad, Murshidabad-742201
rishiparna.guha@gmail.com

Abstract

Zero Degree Isotherm Height (ZDIH) is an important parameter in meteorological science. It has a wide application area in rain-height estimation and radio-communication. Altitudinal occurrences of ZDIH is investigated by observational data of 00Z and 12Z measurements for a period of fourteen years from 2000-2013 for four Balloon Observatories situated along the eastern coastline of India. Variation of ZDIH is studied to find a seasonal standard.

Keywords: Coastal Boundary Layer, Rain height, Vertical Temperature Distribution, ZDIH.

Introduction

Indian coastline receives ~350 cm rainfall on average annually. This amount is three times of the entire country average value. Thus it becomes necessary to have an outlook about the coastal boundary layer structure and also about the altitude of Zero degree Isotherm Height (ZDIH) as it has an important role in deciding the rainfall amount and its distribution[1]. The positioning of the ZDIH is normally altered by thermal advection and radiational and evaporative cooling. This particular parameter determines the vertical staging of stratified layer of mixed phase particles even it decides the type of precipitation that the earth surface will receive. That is reason why Zero Degree Isotherm Height (ZDIH) is also known as Melting Layer Height (MLH) as it represents the height of free atmospheric layer having the temperature of 0º or the freezing point of water[2,3,4]. It is one of the most important isotherms in the science of meteorology. ZDIH also projects the status of Rain Height (RHT) according to Rec. ITU – R P839-3. Figure 1 gives a schematic diagram for the formation of ZDIH. The superiority of Radio-sonde observation on determining ZDIH has already been established by many researchers from Indian sub-continent and other parts of the world. Still it is also estimated from radar and lidar observations where it appears as bright and dark bands in respective profiles of vertical atmosphere[5,6].

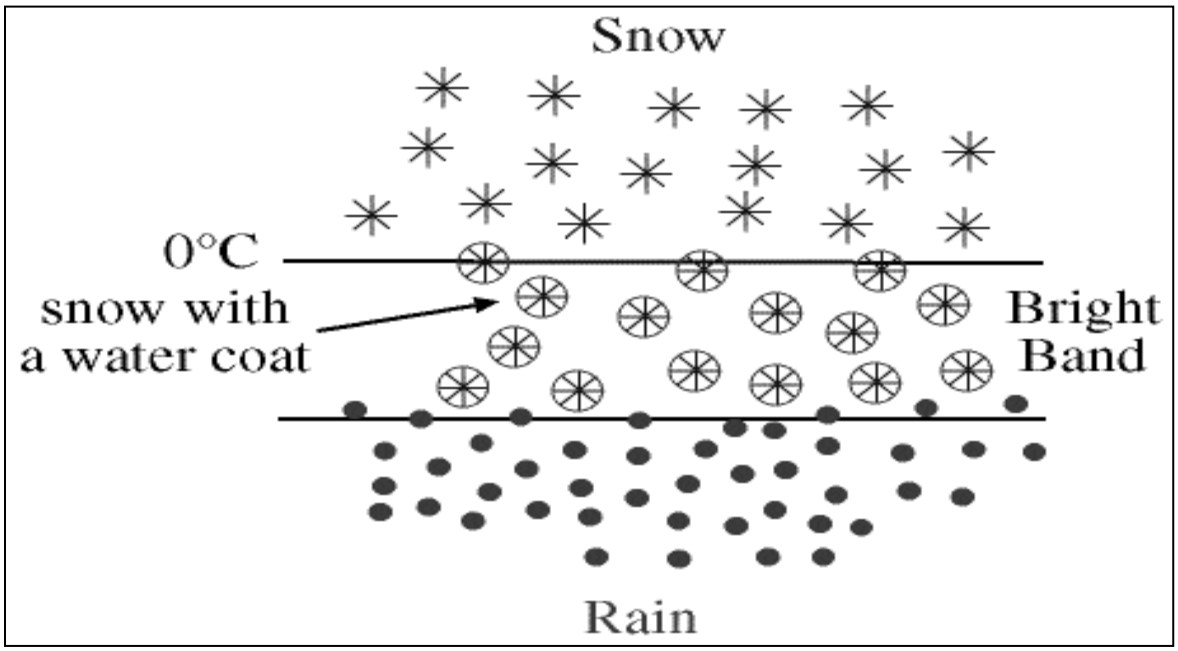

Figure-1: Schematic diagram of ZDIH (Source: COMET-MedED)

Researcher around the world has studied the variation of ZDIH and the average value in the latitudinal area between 40ºN to 40ºS is 2107m according to ITU –R which is 300m less the value given by National Oceanic and Atmospheric Administration (NOAA). Figure-2 gives the global projections of ZDIH as per various sources.

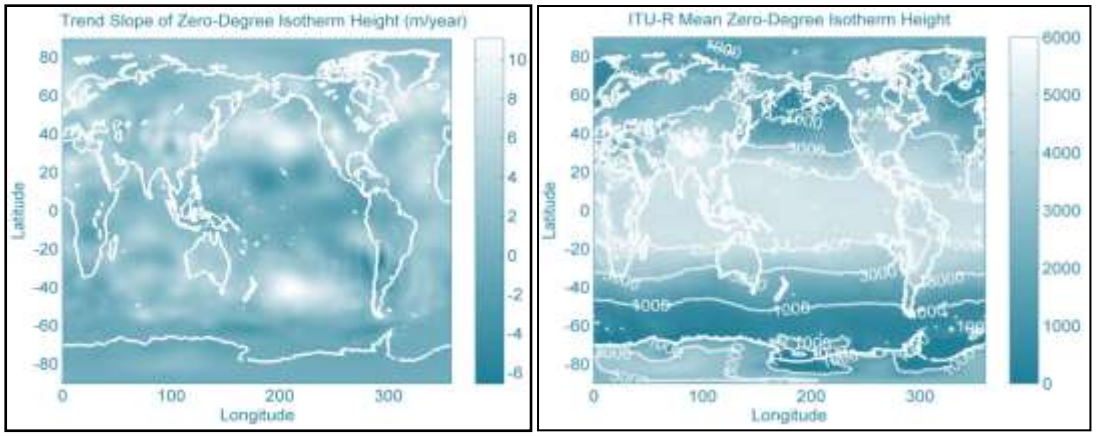

Figure-2: Left-Global annual running average of ZDIH trend (ITU-R 2010);Right - NOAA average global ZDIH (Source: National Snow and Ice Data Centre).

ZDIH is an important parameter in satellite and radio-communication. Thus the variation of its altitudinal position should be studied from time to time and be updated to maintain an uninterrupted LOS link. Present study focusses on this objective only to have an update on the variability of ZDIH in the coastal zones of the Bay of Bengal since it is prone to occurrences of frequent weather systems with huge rainfall activity.

Data and Methodology

Status of ZDIH of tropical costal stations along the Karomandal coast (E) of India are analysed over decadal scale are study in the present approach. Variation of this parameter is studied seasonally for the periods of 2000 -2013 from National Oceanic and Atmospheric Administration (NOAA) RAOB DATA BASE.

Table-1: List of Meteorological stations

Station	*WMO no.*	*Latitude(°N)*	*Longitude (° E)*	*Elevation(m)*
Karaikal (KAKL)	43346	10.92	79.83	7
Kolkata (KOL)	42809	22.65	88.45	7
Chennai (CHE)	43279	13.00	80.18	16
Vishakhapattanam(VSK)	43150	17.70	83.30	66

Attempts are made to reveal the average residence of melting layer in atmospheric levels. Table 1 gives geographical position of the meteorological station along with their elevation from mean sea level.

Data Analysis and Results

The altitude of ZDIH is extracted and their seasonal variation is studied for both morning (00Z) and afternoon (12Z) timings. Their maximum and minimum heights are evaluated to determine the range of variation. Further their temporal variation and most possible occurrence value is observed.

Variation of maximum and minimum values for ZDIH: Table-2 and 3 give maximum and minimum value ZDIH during the study period. Maximum value occurs for Karaikal during winter and minimum value occurs for Kolkata during winter as per morning observations. Afternoon maximum and minimum values are shown in table 3.

Table 2: Seasonal maximum minimum values (00Z)

STATION / **SEASON**	**Kol**		**VSK**		**CHE**		**KAKL**	
	MAX (gpm)	MIN (gpm)	MAX (gpm)	MIN (gpm)	MAX (gpm)	MIN (gpm)	MAX (gpm)	MIN (gpm)
Pre Monsoon	6127	3287	5966	3456	5830	3919	6095	3912
Monsoon	6361	4188	6223	3885	5676	3734	5936	3734
Post Monsoon	6314	2630	7410	3665	5811	3382	5934	3734
Winter	5611	2591	6214	3126	5634	3512	5171	3897

Table-3: Seasonal maximum minimum values (12Z)

STATION / SEASON	KOL		VSK		CHE		KAKL	
	MAX (gpm)	MIN (gpm)	MAX (gpm)	MIN (gpm)	MAX (gpm)	MIN (gpm)	MAX (gpm)	MIN (gpm)
PRE-MONSOON	6217	3232	6151	3754	6044	3966	6666	3931
MONSOON	6577	3990	6196	3162	6615	4130	6685	3491
POST MONSOON	5948	3109	6297	3648	5848	3863	6270	3464
WINTER	5974	2866	5870	3410	5886	3764	5970	3776

Maximum possible occurrences of ZDIH (00Z): ZDIH height determined for 4 seasons *viz.* Pre monsoon, Monsoon, Post Monsoon, Winter over Kolkata, Visakhapattanam, Chennai, Karaikal. Morning observation shows maximum height occurrence during monsoon over Kolkata and Visakhapatnam of value 5290.8 ±323.7 (gpm) and 5096.3 ± 324.3(gpm) respectively. Least value occurs during winter over Kolkata (4036.9 ± 555.8) (gpm).Table 4 gives this overall seasonal status.

Table-4: Average ZDIH from seasonal morning (00Z) observations.

STATION / SEASON	KOL	VSK	CHE	KAKL
	AVG±STDEV (gpm)	AVG±STDEV (gpm)	AVG±STDEV (gpm)	AVG±STDEV (gpm)
PREMONSOON	4413.912± 530.8695	4647.374± 380.2153	4840.001± 320.1543	4780.774± 331.5025
MONSOON	5290.842± 323.7665	5096.332± 324.5308	4868.117± 295.7783	4824.157± 338.7383
POST MONSOON	4721.51± 512.3747	5131.69± 2053.899	4905.246± 288.5403	4768.992± 315.5434
WINTER	4036.974± 555.8136	4655.39± 384.2001	4853.911± 287.1298	4794.427± 505.57

Afternoon observations (12Z) show peak ZDIH(>5 km) during Monsoon for every station. Kolkata shows highest value of 5397.9 ± 349.6 and least value of 4216.2 ± 547.0 during monsoon and winter respectively. Table 5 gives the entire scenario.

Table-5: Average ZDIH from seasonal afternoon (12Z) observations

STATION / SEASON	KOL	VSK	CHE	KAKL
	Avarage±STDEV (gpm)	Avarage±STDEV (gpm)	Avarage±STDEV (gpm)	Avarage±STDEV (gpm)
PREMONSOON	4580.009± 533.4175	4809.935± 459.8961	5048.447± 348.6976	5148.49± 393.3017
MONSOON	5397.91± 349.6145	5173.718± 353.4752	5058.428± 327.3103	5151.802± 381.4222
POST MONSOON	4744.22± 435.8998	5015.664± 371.4538	5021.441± 435.4084	5008.369± 378.3623
WINTER	4216.218± 547.0251	4810.424± 417.5424	5033.859± 329.8807	5034.267± 337.3311

Discussion

ZDIH or MLH is an important parameter in communication pathway design. Developments of convective clouds are very common over tropical region. Thus it is also very important to study the status of ZDIH or the MLH on regional small case basis. Such knowledge helps in having an idea about effective cloud rain height of a particular region. This study reveals current status of this ZDIH parameter over eastern coastal stations India. Earlier studies gave an account of this parameter up to 1990 or ending decade of 19th century. This study carries the approach further and reports the situation. Seasonal variance of this parameter depending on latitude reveals significant difference. However all the values are close to the country average value with a few exemptions.

Acknowledgement

Authors are thankful to NOAA for providing the relevant data. Dr. Rishiparna Guha is thankful to Prof. (Dr.) Deepali Singhee, Principal, J. D. Birla Institute for her constant support and encouragement for research work.

References

1. Yau, M. K.,and Rodgers,R.R.: A Short Course in Cloud Physics,Butterworth-Heinemann.,1989,ISBN 0-75-0632151

2. Diaz, H. F. Eischeid, J. K. Duncan C. and Bradley, R. S., "Variability of freezing levels, melting season indicators, and snow cover for selected High-elevation and continental regions in the last 50 years", Climatic Change, 2003, 59, pp 33–52.

3. Harris JR., G. N., Bowman, K. P. and Dong-Bin Shin**, "**Comparison of Freezing-Level Altitudes from the NCEP Reanalysis with TRMM Precipitation Radar Bright Band Data", Journal of Climate, 2000**,** 13:23, pp 4137-4148

4. Bradley, R.S., Keimig, F. T., Diaz H. F. and Hardy, D. R., "Recent changes in freezing level heights in the Tropics with implications for the deglacierization of high mountain regions", Geophysical Research Letters, 2009, 36, L17701, doi:10.1029/2009GL037712, 2009.

5. Proceeding of the URSI commission F international triennial open symposium on Wave Propagation and Remote Sensing. 22-25 September 1998, Aveiro, Portugal pp. 159-162, ISBN: 972-8021-65-8.

6. V.K.C. Venema[1], H.W.J. Russchenberg, A van Lammeren, A. Apituley and L.P. Ligthart The melting layer:The radar bright band is dark for lidar 1IRCTR, International Research Centre on Telecommunications-transmission and Radar, Department of Information Technology and Systems, Delft University of Technology. Mekelweg 4, 2628 CD Delft, The Netherlands.

About Editor

Dr. Amitlal Bhattacharya is currently working as an Assistant Professor and Head in the Department of Physics, Dukhulal Nibaran Chandra College, Murshidabad, West Bengal, India. He is doing research work on Atmospheric Physics and Radio Wave Propagation. He has special interest in upper atmospheric high energy physics and meteorology. He has worked on Blue Jets, Sprites, Elves, Thunderstorms, Lightning, Solar Eclipses and atmospheric stability. He has presented several papers in National and International conferences and published many papers in reputed journals. He is life member of Indian Science Congress Association, Indian Meteorological Society and Indian Red Cross Society.

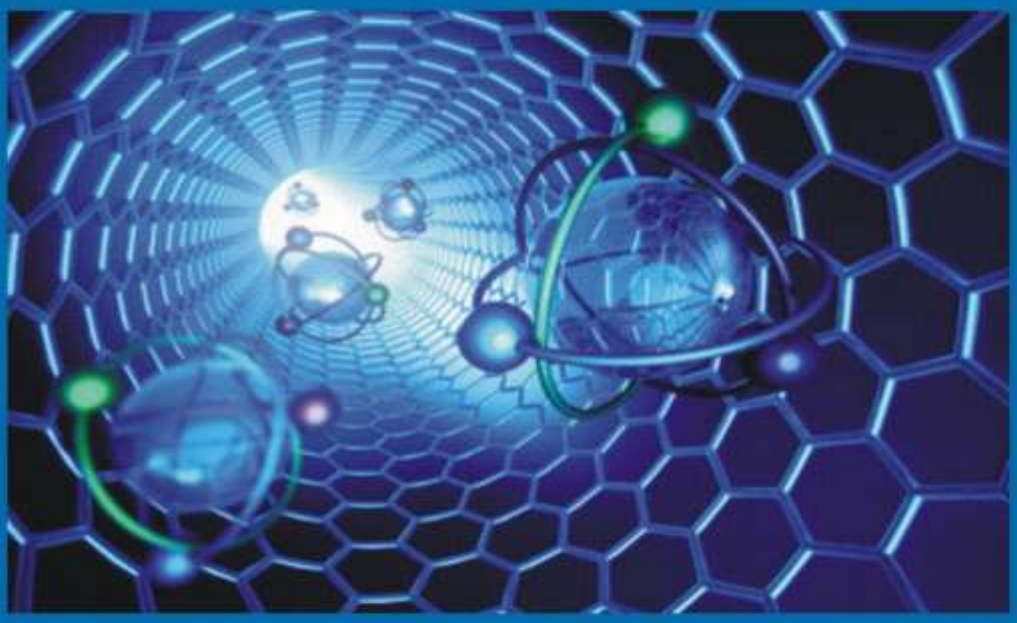

ISBN:978-93-86675-56-9